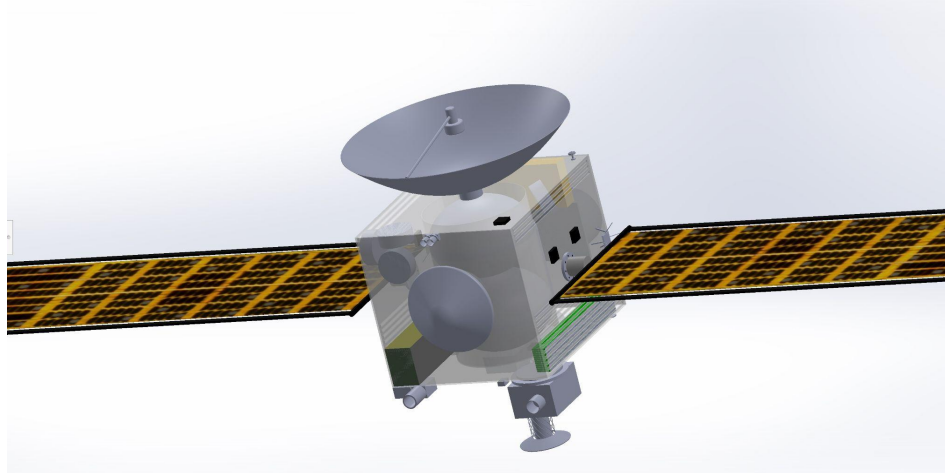


MAYFLY Sample Return Mission



Prepared For

Dr. Dan Goebel - University of California, Los Angeles

Designed By

Spacecraft Systems Engineer: Rebecca Charno

Mission Planning/Trajectory Analysis: Bill Wu

Payload Manager - Instruments: Kyle Brown

Payload Manager - Sample Collection and ERV: Siddarth Harrison

Power Subsystem Engineer: Josh Eggen

Launch Vehicle & Propulsion Subsystem Engineer: Christopher McCormick

Communications Subsystem Engineer: Thomas Leung

Thermal Subsystem Engineer: Jesus Santana

ACS Subsystem Engineer: Jasper Von

Structures Subsystem Engineer: Jimmy Kotecki

Executive Summary

Mission Goals

The goals of this mission are to obtain a sample from the 311P/PANSTARRS comet while prioritizing high-TRL components, minimizing spacecraft mass, and assuming minimal risk. The sample return vehicle will supply scientists with approximately 15 to 30 g of material along with collections from a space dust analyzer. The science instruments will also collect data on the comet. The mission will launch on a Falcon Heavy on 07/06/2034 for a total mission timeline of 7 to 10 years.

Mission Requirements

Due to the Falcon Heavy launch vehicle, the mission will launch from the Kennedy Space Center in Merritt Island, FL. The mission has a total delta v of 14.9 km/s . The dry mass of the spacecraft is 1230 kg and the wet mass is 1900 kg, but should not exceed 2000 kg in order to maintain a 5% launch margin and a C3 of $75 \text{ km}^2/\text{s}^2$. The sample acquisition will occur from 2 AU and the sample return capsule will re-enter the Earth's atmosphere at maximum velocity of 12.9 km/s . The overall cost will be kept under \$1 billion.

Baseline Spacecraft Design

The baseline spacecraft design and vehicle architecture takes inspiration from several heritage missions, including DAWN, Hayabusa, Europa Clipper, OSIRIS-REx, New Horizons, and even the International Space Station. The basic primary structure follows that of a cube-like shape to house all electronic components as well as the propellant for the propulsion and ACS subsystems. Other subsystem components are mounted on all faces to maximum efficiency while

minimizing mass. Scientific instruments are positioned on the front of the spacecraft where the view of the comet can be seen the clearest and for the longest. Redundancy is considered when applicable, including sun sensors and star trackers, and extra precaution has been applied to the xenon propellant tanks through the inclusion of a cylindrical aluminum-carbon fiber housing.

Payload Descriptions

The carefully chosen payload selection of scientific instruments includes the Hayabusa Near-Infrared Spectrometer (NIRS3), Thermal Infrared Camera (TIR), Laser Altimeter (LIDAR), Surface Dust Analyzer (SUDA), and New Horizons Imaging Camera (Ralph). These instruments work together to gather comprehensive data on the comet's surface and composition, map its terrain, and identify sampling sites. Rigorous pre-flight calibrations ensure data accuracy, providing valuable insights into the comet's properties and the early solar system.

Sample Collection and ERV Payload Descriptions

In order to acquire and deliver a sample from the comet 311P/PANSTARRS, three specific payloads have been selected. The first is the Hayabusa Sampler Horn which will directly acquire a sample from the comet using a touch-and-go methodology which has been tested and proven on two previous missions. Second, in order to return the acquired sample to Earth, we have selected the OSIRIS-REx SRC which has successfully delivered both comet and asteroid samples through the Stardust and OSIRIS-REx missions respectively. Finally, we have chosen the xLink robotic arm as the means of transporting the stored sample from the Hayabusa collection capsule to the OSIRIS-REx SRC. This robotic arm was selected in large part due to its

high customizability, which allows for the arm to be curtailed to mission requirements and maximize weight savings.

On-Board Propulsion

The main propulsion system aboard the Mayfly spacecraft is a High-Isp NEXT 9a ion thruster. With the mission only requiring approximately 580 kg of Xenon propellant with 10% contingency, and each thruster having a throughput of 600 kg, only one engine is necessary to complete the mission. However, for redundancy we will bring two thrusters as well as two PPUs. The NEXT 9a ion thruster will be firing with an input power of 3 kW so as to minimize the required solar array size, with an Isp of 4125 s and a thrust of about 95 mN. Throughout the mission, the system will receive a constant 3 kW when firing. Other chemical and SEP systems were considered for this mission, however, they did not fit the mission timeline or they required too much propellant mass.

Power

The Mayfly's power is provided by the Redwire Space Roll Out Solar Array (ROSA), which is a high-power density, lightweight, and stowable design. The solar array's primary power load is directed to the electric propulsion system, which requires a constant 3,000 watts of power while thrusting. Secondary loads include electric heaters, communications equipment, science instruments, attitude control, and the onboard computer. The satellite's solar array area is 83 m², producing 18.67 kilowatts of power at Earth at the beginning of life. The array's output is reduced to 3.56 kilowatts at apogee halfway through the mission. Although the mission expects no substantial eclipse time, a sizable battery has been configured to allow for a safe mode that can sustain the satellite's crucial operations drawing 808 watts for 17 hours without any power generation from the solar arrays. The battery pack consists of 2 modules of lithium-ion cells with

a 12 by 73 configuration for a total of 1,752 cells, with a weight of 77 kilograms and a volume of 0.03 cubic meters.

Communications

The goal of the communication subsystem is to establish a two-way communication link between the spacecraft and Earth to ensure that vital data collected can be downlinked back to Earth and crucial mission instructions can be uplinked to the spacecraft from Earth. During this mission, surface characterization data of the comet will be collected by the payload instruments, which need to be downlinked back to Earth. The mission requirements instruct that all communications between the spacecraft and Earth must be performed through the Deep Space Network (DSN) 34 meter antennas, which are located in California, Spain, and Australia, with a bit error rate (BER) of no more than one in one million. All communications will be performed using the X-band frequency range. During normal operations, data downlink and uplink will be performed through the 2.5 meter high gain antenna with a downlink data rate of 100000 bits per second (bps) and a uplink data rate of 1000 bps. During safe mode operations, data downlink and uplink will be performed through the 0.24 meter low gain antenna with a downlink and uplink data rate of 10 bps. All communications through the high gain and low gain antennas will be below the maximum bit error rate margin.

ACS

The role of the attitude control system is to orient our spacecraft to downlink data to Earth, collect information from the surface of the comet and retrieve a sample from the comet's surface. We have a mission timeline of 10 years which yields 690 slews with an estimated angular

momentum build up of 71000 Nms. We used a Goodrich, Ithaco TW-45C250 reaction wheel which resulted in 1590 dumps with an overall hydrazine propellant mass of 100 kg. Finally we used a star tracker and sun sensor as well as an IMU in order to determine current location and orientation.

Structures

The primary goal of the structures subsystem is to minimize the structural mass and ensure a framework is created to house all payloads, instruments and other spacecraft subsystems that would survive the loads experienced throughout the mission, namely during launch and reentry. By taking influence from past successful missions, such as DAWN and Hayabusa, both primary structures, the cube-like structure to either house subsystem components or allow them to attach to the outside and the cylindrical housing specifically for the two xenon propellant tanks, consist of aluminum-carbon fiber honeycomb with 0.005 m thick aluminum 7075 core and two 0.0025 m thick t800 carbon fiber facesheets. By utilizing the more accurate results from Solidworks, the center of mass as well and moments of inertia about each rotational axis are found. Moreover, using Euler-Bernoulli Beam Theory, the fundamental first order frequencies are approximated for the spacecraft and found to be much larger than those from SpaceX's Falcon User Guide, concluding that our spacecraft will survive launch with several factors of safety above the recommended frequencies.

Thermal

The Thermal subsystem will maintain the temperatures of the Spacecraft MAYFLY. The Spacecraft will be covered in multi-layer insulation (MLI) consisting of a blanket made of

Aluminized Beta Cloth. A set of louvers will be used as well as heaters capable of outputting 265W of heat in order to maintain the bus within a temperature range of- 10°C and 40°C for when we are at the Comet and the highest temperature of 40°C when we are at 1AU. This will allow our equipment to be operational along its journey from earth to the Comet.

Table of Contents

| | |
|---|-----------|
| 1 - Mission Description..... | 14 |
| 2 - Mission Requirements..... | 16 |
| 3 - Technical Approach..... | 18 |
| 3.1 - Design Methodology..... | 18 |
| 3.2 - Assumptions..... | 19 |
| 3.3 - Acceptable TRLs and Risk..... | 20 |
| 4 - Mission Timeline and Trajectory Analysis..... | 22 |
| 4.1 - Mission Timeline..... | 22 |
| 4.2 - Interplanetary Trajectory Analysis..... | 24 |
| 4.2.1 - Orbital Elements..... | 24 |
| 4.2.2 - Chemical Trajectory..... | 25 |
| 4.2.3 - Solar Electric Propulsion (SEP) Trajectory..... | 26 |
| 4.2.3.1 - David Oh Model..... | 26 |
| 4.2.3.2 - Delta v for Inclination Change..... | 28 |
| 4.2.3.3 - Mars Gravity Assist..... | 28 |
| 4.2.3.4 - Rendezvous..... | 29 |
| 4.2.3.5 - Patched Conics..... | 30 |
| 4.2.3.6 - Hyperbolic Trajectory for Sample Return..... | 31 |
| 5 - Design Models..... | 34 |
| 5.1 - GMAT vs. David Oh Model..... | 34 |
| 6 - Baseline Design and Vehicle Structure..... | 35 |
| 7 - Subsystem Design..... | 39 |
| 7.1 - Payload Description..... | 39 |
| 7.1.1.1 Hayabusa Spectrometer (NIRS3)..... | 40 |
| 7.1.1.2 Hayabusa Thermal Infrared Camera (TIR)..... | 41 |
| 7.1.1.3 Hayabusa Laser Altimeter (LIDAR)..... | 43 |
| 7.1.1.4 - Surface Dust Analyzer (SUDA)..... | 45 |
| 7.1.1.5 - New Horizon Imaging Camera (Ralph)..... | 47 |
| 7.1.2 - Sample Collection and ERV Payload..... | 49 |
| 7.1.2.1 - Hayabusa Sampler Horn..... | 49 |
| 7.1.2.2 - OSIRIS-REx SRC..... | 52 |
| 7.1.2.3 - xLink Space-Rated Modular Robotic Arm System..... | 55 |
| 7.2 - Launch Vehicle..... | 57 |
| 7.2.1 - Launch Vehicle Trade Study..... | 58 |
| 7.3 - On-Board Propulsion..... | 60 |

| | |
|---|------------|
| 7.3.1 - Chemical Propulsion Trade Study..... | 61 |
| 7.3.2 - Solar Electric Propulsion Trade Study..... | 63 |
| 7.3.3 - High-Isp NEXT 9a Ion Thruster Analysis..... | 69 |
| 7.3.4 - Risk Assessment..... | 72 |
| 7.4 - Power..... | 72 |
| 7.4.1 - Power Summary..... | 72 |
| 7.4.2 - Power Trade Study..... | 73 |
| 7.4.3 - Solar Array..... | 74 |
| 7.4.4 - Battery..... | 76 |
| 7.4.5 – Power Distribution and Conditioning Unit..... | 78 |
| 7.5 - Communications..... | 79 |
| 7.5.1 Communications Overview..... | 79 |
| 7.5.2 Hardware..... | 80 |
| 7.5.3 Band Choice..... | 83 |
| 7.5.4 Simplified Block Diagram..... | 85 |
| 7.5.5 Noise Figures..... | 86 |
| 7.5.6 Link Performance..... | 86 |
| 7.6 - Attitude Control System (ACS)..... | 88 |
| 7.7 - Structures..... | 98 |
| 7.7.1 - Structures Summary..... | 98 |
| 7.7.2 - Spacecraft Bus Design..... | 98 |
| 7.7.3 - Spacecraft Structural Properties..... | 107 |
| 7.8 - Thermal..... | 111 |
| 7.8.1 - Temperature Requirements..... | 111 |
| 7.8.2 - Iterative Thermal Design Process..... | 112 |
| 7.8.3 - Thermal balance at Earth..... | 113 |
| 7.8.4 - Thermal balance at Comet..... | 116 |
| 7.8.5 - Thermal Controls..... | 118 |
| 7.8.6 - Surface Property Controls..... | 119 |
| 7.8.7 - Heaters..... | 119 |
| 8 - Mass, Power, TRL, and Summary Tables..... | 120 |

List of Figures

- 1.1: Hubble Space Telescope Image of Comet 311P/PANSTARRS
- 6.1: Global coordinate system for Mayfly
- 6.2: Iso front view of Mayfly with labeled components
- 6.3: Iso back view of Mayfly with labeled components
- 7.1.1.1: NIRS3
- 7.1.1.2: TIR
- 7.1.1.3: LIDAR
- 7.1.1.4: SUDA
- 7.1.1.5: Ralph
- 7.1.2.1: Hayabusa Sampler Horn
- 7.1.2.2: Hayabusa Sample Horn Acquisition Sequence
- 7.1.2.3: OSIRIS-REx SRC
- 7.1.2.4: OSIRIS REx Parachute Recovery System
- 7.1.2.5: xLink Robotic Arm
- 7.1.2.6: Sample Transfer Mock-Up
- 7.2.1: Launch Vehicle C3 at Varying S/C Masses
- 7.2.2: Falcon Heavy & Delta IV Heavy at Launch
- 7.3.1: Chemical and Electric Propulsion System Propellant Masses
- 7.3.2: SEP Thrusts at Varying Power
- 7.3.3: SEP Specific Impulse at Varying Power
- 7.3.4: SEP Engine Efficiency at Varying Power
- 7.3.5: Engine Deliverable Masses
- 7.3.6: Engine Trip Times
- 7.3.7: NEXT 9a Ion Thruster, PPU, and Xe Propellant Tank
- 7.3.8: Proposed Propulsion System Configuration
- 7.4.1: Mission Phase Power Requirements
- 7.4.2: Power Budget Timeline
- 7.4.3: Power Generation Trade Study
- 7.4.4: Rosa Array
- 7.4.5: LG MJ1 cells
- 7.4.6: MJ1 Specifications
- 7.4.7: 18650 Battery Pack
- 7.4.9: Airbus PSR 100V MkII
- 7.5.1: Juno 2.5 meter High Gain Antenna (Source: IEEE)
- 7.5.2: Juno Low Gain Antenna (Source: NASA)
- 7.5.3: Juno Small Deep Space Transponder (SDST)
- 7.5.4: L3 X-band Traveling Wave Tube Amplifier
- 7.5.5: Simplified Communication Block Diagram
- 7.7.1: Aluminum honeycomb core
- 7.7.2: Complete honeycomb structure
- 7.7.3: DAWN spacecraft's core graphite cylinder
- 7.7.4: CAD model displaying Cartesian coordinates
- 8.1: MAYFLY Mission MEL

8.2: MAYFLY Mission PEL

8.3: TRL Summary

8.4: MAYFLY List of Science Instruments

8.5: Structures Mass Calculations

List of Tables

- 3.1: Details of Critical Events of the MAYFLY Mission
- 7.1.1: NIRS3 Specs
- 7.1.2: TIR Specs
- 7.1.3: LIDAR Specs
- 7.1.4: SUDA Specs
- 7.1.5: Ralph Specs
- 7.3: On-Board Propulsion
 - 7.3.1: Chemical Thruster Trade Study
 - 7.3.2: SEP Input Power, Thrust, Specific Impulse, and Mass Comparison
 - 7.3.3: NEXT 9a System Component Masses
- 7.4.8: Component Specifications
- 7.5.1: Communication Performance
- 7.6.1: Physical Constant
- 7.6.2: Disturbance Torques
- 7.6.3: Angular momentum of the disturbance
- 7.6.4: Angular Momentum build up
- 7.6.5: Number of Dumps and Momentum Accumulation Time
- 7.6.6: Propellant Mass Values
- 7.7.1: Comparison of Common Aluminum Alloy Densities
- 7.7.2: Results summary from Solidworks
- 7.7.3: Primary frequencies produced by Falcon Heavy
- 7.7.4: First order frequencies along primary structure dimensions modeled as beams
- 7.8.1: Operational Temperature Ranges for Mayfly Components

Nomenclature

ACS - Attitude Control System

ADCH - Attitude Determination Control and Handling

AU - Astronomical Unit

BER - Bit Error Rate

ERV - Earth Re-Entry Vehicle

GA - Gravity Assist

IMU - Inertial Measurement Unit

LIDAR - Hayabusa Laser Altimeter

NIRS3 - Hayabusa Spectrometer

PD - Power Distribution

Ralph - New Horizon Imaging Camera

ROSA - Roll-Out Solar Arrays

SA - Solar Array

SEP - Solar Electric Propulsion

S/C - Spacecraft

SRC - Sample Retrieval Capsule

SUDA - Space Dust Analyzer

TRL - Technology Readiness Level

TIR - Hayabusa Thermal Infrared Camera

1 - Mission Description

In 2004, the Stardust spacecraft became the first mission to successfully return an extraterrestrial sample from the Wild 2 comet to Earth. Now—two decades later—we are designing a mission to retrieve a sample from 311P/PANSTARRS and return it to the very same test site in Utah. Since this novel mission, the technology to execute sample return missions has improved and gained significant heritage. Generally speaking, comets are collections of frozen dust, particles, and ice that contain information on the origins of planets, and our universe at large. Similar to the Wild 2 sample, the return specimen from the MAYFLY mission will help us continue to develop an understanding of the origins of our universe. The main belt comet being examined by MAYFLY is shown in Figure 1.1.

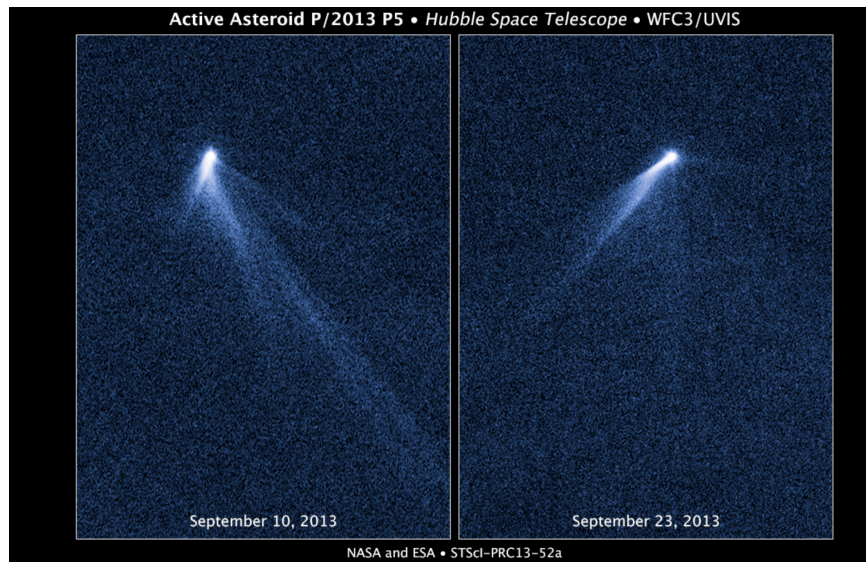


Figure 1.1: Hubble Space Telescope Image of Comet 311P/PANSTARRS

The 311P/PANSTARRS comet is located between Mars and Jupiter in the main asteroid belt and was discovered by the Pan-STARRS telescope in 2013. In a study performed by D. Jewitt at the University of California, Los Angeles, it was determined that the comet has at least

six dust tails. This makes the comet particularly interesting, because we can perform a dust analysis of the tail as well as take a sample of the nucleus. While the Surface Dust Analyzer (SUDA) takes periodic samples of the dust tails, the NIR3 Spectrometer from the Hayabusa mission, TIR Thermal Infrared Camera from the Hayabusa Mission, LIDAR Laser Altimeter from the Hayabusa mission, and the Ralph Imaging Camera from the New Horizon mission will collect data on the comet. These instruments allow us to gather data on infrared readings, heat compositions, mineral compositions, and chemical compositions of the comet. We can also determine if there is a presence of organic chemicals and visualize the topography of the comet. Ultimately, this will help us determine where to make periodic contact and perform a sample return with the Sampler Horn used on the Hayabusa mission to obtain around 15-30 grams of comet material. The sample will be transferred to the Sample Return Capsule (SRC) using an xLink Robotic Arm. The SRC is capable of withstanding temperatures up to 2900 °C and can enter the atmosphere at 12.9 km/s . There is a drogue and parachute system to achieve this entrance velocity.

The mission will launch on a Falcon Heavy on 07/06/2034 with a C3 of $75 km^2/s^2$ with a total timeline of 10 years. The S/C will perform a Mars gravity assist before rendezvous with the comet on 10/09/2037. After spending 6 months at the comet, the S/C will journey back to Earth on 04/09/2038 for a 1640 day burn. Finally, the Earth Re-Entry Vehicle (ERV) will detach and begin its descent towards Earth on 10/05/2042. The mission has a total delta v of $14.9 km/s$. The dry mass of the S/C is 1230 kg and the wet mass is 1900 kg, but should not exceed 2000 kg in order to maintain a 5% launch margin. Every subsystem component of the system has a mass contingency of 30%, with the science instruments having a mass contingency of 21.9%. The spacecraft is carrying 100 kg of Hydrazine for Attitude Control Systems (ACS) and 580 kg of

Xenon for Solar Electric Propulsion (SEP), which use a High-Isp NEXT 9a ion thruster. To orient the spacecraft in order to collect data and downlink with the Earth, the ACS system uses a Goodrich Itacho TW-45C250 Reaction Wheel, sun sensors on each face of the cube-like spacecraft, and an Inertial Measurement Unit (IMU). The thermal system will keep the bus temperature within a range of -10°C and 40°C using the following components: multi-layer insulation (MLI), louvers, and radiators. The temperature reaches the cold limit at the comet and the hot limit at Earth.

Like any long-distance space mission, there are risks on the MAYFLY mission. There is one component given a Technology Readiness Level (TRL) of 8 on the mission since it has not flown yet. There are also single-fault susceptible systems in the power and sample collection subsystems. These risks are deemed acceptable, and mitigation is detailed throughout the report to ensure mission success. Overall, this mission prioritized high-TRL, low risk, and low mass designs throughout the entire design realization process.

2 - Mission Requirements

Level 1 Requirements

1. Return a sample from Main Belt Comet 311P/PANSTARRS.
2. Visualize and perform measurements of the comet's surface characteristics before sample acquisition and return to Earth.

Level 2 Requirements

1. Launch spacecraft between 2030-2034.
2. The mission duration is estimated to be between 7 to 10 years.
3. Return 1g - 1 kg sample to Utah Test Site.

4. Perform a hyperbolic flyby of Earth upon return and drop sample return capsule at less than 12 km/s.
5. Sample acquisition and comet surface surveillance performed from 2 Astronomical Units (AU).
6. Due to launch vehicle limitations, the spacecraft dry mass must not exceed 1230 kg and the spacecraft wet mass must not exceed 3000 kg.
7. Communications executed through the DSN Network on 34 meter antennas.
8. Cost will be kept under \$1 billion.

Level 3 Requirements

1. In order to characterize and visualize the surface, the payload inventory includes a camera and spectrometer.
2. Utilizing the Hayabusa horn and projectile technique for the sample acquisition.
3. The sample return system includes a return capsule with a heat shield, drogue deployment, and main parachutes in order to meet the required 12 km/s re-entry velocity.
4. Using gridded-ion thrusters for the Solar Electric Propulsion (SEP) system.
5. The entire mission maintains a factor of safety above 1.5 for systems and components; the uplink, downlink, safemode up, and safemode down telecommunication components maintain a Bit Error Rate (BER) of less than $1 \cdot 10^{-6}$; overall mass margin and contingency of 20% or more.
6. Using monopropellant hydrazine thrusters and 45 Nms reaction wheels used for Attitude Determination Control and Handling (ADCH).

In addition to the Level 1, 2, and 3 Requirements of this mission, there are additional

constraints on the system. Using the SpaceX Falcon Heavy as our launch vehicle, we are required to launch from the Kennedy Space Center in Merritt Island, Florida. The Falcon Heavy provides the necessary C3 for our spacecraft (S/C) within a total wet mass limit: we assume a wet mass of 2000 kg. With these mass constraints, the Falcon Heavy provides sufficient thrust to bring our S/C to the required orbit. While the S/C travels and orbits 311P/PANSTARRS, the Solar Array (SA) system provides sufficient power for the SEP system and the mission's necessary payloads. Due to the high cost of the mission, high number of critical events, and distance to Earth, we prioritized high Technology Readiness Level (TRL) components and designs when applicable. Since we cannot land or make a secure attachment to the comet, it is necessary to use a lower heritage projectile-horn system for sample acquisition. Despite this being the lowest heritage item, it is still a TRL 9 since it was used successfully on the Hayabusa mission.

3 - Technical Approach

3.1 - Design Methodology

The MAYFLY was designed with the goals of minimizing S/C mass, prioritizing high-TRL components, minimizing risk, and successfully obtaining the comet sample. After performing a trade study which compared SEP and chemical propulsion systems, it was obvious that an on-board chemical propulsion system was not feasible because it required a wet mass that far exceeded the C3 capabilities of a Falcon Heavy. Each subsystem in this mission was designed to prioritize high-TRL and high heritage components, drawing inspiration from a number of successful missions, such as the Psyche, Hayabusa, the International Space Station, and Dawn

missions. The structures subsystem was designed with these missions in mind, and componentry layout placed critical components, such as propellant tanks, in more secure locations in the event of S/C disturbances. Additionally, the components were organized such that the center of mass would be as close as possible to the center of the spacecraft. The cameras and telecommunication devices are all towards the front of the S/C. The telecommunication systems were designed to have enough power to send signals with minimum error, each with a BER of less than $1 \cdot 10^{-6}$.

Ultimately, the mission was simplified to prioritize the retrieval of the sample. We limited the number of payload instruments, adopted a roll-out SA design, and enhanced the Earth Re-Entry Vehicle (ERV) with drogues and parachutes in order to reach the Earth re-entry velocity requirements.

3.2 - Assumptions

The design of this S/C makes four significant assumptions to simplify design. The first assumption pertains to the Mars Gravity Assist (GA), which is not given a strict timeline in the trajectory plan. This is because we are assuming that the exact date of the GA will not have an overall impact on the timeline of the trip. Secondly, we used the David Oh Model under the assumption that the thrusters are operating at a constant power, which is valid because the comet is within a close enough proximity. Also related to the trajectory, we assumed that during the duration of the mission there is no eclipse time, which would affect the SEP system. Finally, the emissivity of the radiator and the thermal louvers were deemed to be the same since they operate simultaneously in the thermal management system.

3.3 - Acceptable TRLs and Risk

Every component of this mission has a maturity of TRL 9, except for the xLink Robotic Arm which is a TRL 8 system. This arm was designed and tested by the NASA engineers that designed the Mars 2020 Perseverance Rover. While the xLink system specifically was never flown, it was placed on the OSAM-2 Mission and received all necessary flight certifications. Additionally, the xLink arm can be tested while the spacecraft is in flight due to the sufficient power supply on this mission. Therefore, the xLink arm could reach TRL 9 before the actual sample transfer occurs which reduces the risk significantly. MAYFLY is also bringing a Space Dust Analyzer to collect data on the comet's dust trails. For all of these reasons, the risk will be assumed for now and a full Verification and Validation Plan will be advised before launch. Regardless, every other component meets the necessary high-TRL requirement for this mission. The details of each critical event is provided in table 3.1. The Earth Re-Entry event occurs when the Sample Retrieval Capsule (SRC) separates from the main S/C.

| Critical Event | Date of Event | Elapsed Time | Location |
|--------------------------|-----------------------|--------------|---|
| Launch | 07/06/2034 | – | Kennedy Space Center in Merritt Island, Florida |
| Mars GA | TBD | + TBD | Mars, (depends on location of Mars at time of assist) |
| Rendezvous | 10/09/2037 | + 1190 Days | 311P/PANSTARRS, 2.2 AU |
| Sample Collection | 10/09/2037-04/09/2038 | + 182 Days | 311P/PANSTARRS, 2.2 AU |

| | | | |
|--|-----------------------|-------------|--|
| Sample Transfer | TBD | - | 311P/PANSTARRS, 2.2 AU |
| Return Burn | 04/09/2038-08/04/2042 | + 1640 Days | - |
| Earth Re-Entry and ERV Deployment | 08/04/2042 | - | Periapsis of the hyperbolic return orbit |

Table 3.1: Details of Critical Events of the MAYFLY Mission

The S/C will be in close proximity to the comet for 6 months to collect data and retrieve samples of the comet. This provides ample time to take the necessary surveillance and spectrometer measurements to determine where to make periodic contact with the comet. This entire process reduces risk because there is no crucial connection or attachment with the surface of the comet in order to obtain the sample. Additionally, there is extra time to perform surveillance and make multiple sample collections. When the projectile-horn system was used on Hayabusa, there was malfunction because the horn tended to tip. This is because the sample capture system was not properly aligned with the center of mass. On our S/C, however, we intentionally aligned the projectile-horn system with the center of mass in order to avoid the tipping that occurred during the Hayabusa mission.

There are some systems on the spacecraft which are single-fault susceptible. The SA and power distribution (PD) unit are single-fault susceptible. However, these two components have such significant heritage—ROSA is used on the International Space Station, and the PD unit has 30 years of heritage—so the risk is assumed. There are a total of two SA ROSA systems on the S/C, and if one fails the other cannot provide sufficient power for the mission. Therefore, there are backup batteries which provide double the necessary capacity. These batteries are also

single-fault susceptible. However, considering the reliability and combined heritage of the entire power supply design, this risk is acceptable. Finally, the aforementioned xLink Robotic Arm is also single-fault susceptible, but this risk is acceptable due to the Verification and Validation Plan that will be executed prior to flight.

Because the S/C is traveling through the Main Belt, there is risk of micrometeorites and collisions with the S/C. This risk is managed by the componentry layout, which places the most crucial components in the central, cylindrical hub. This provides extra protection for the Xenon Tank in the event that the S/C travels through an area that is densely populated with space debris. Similarly, there is an unlikely risk of solar flares which is managed by the roll-out design of the arrays. In the event of a catastrophic solar flare, we place the entire SA on standby and operate the S/C on the backup battery, which provides up to 17 hours of power. All risks will also be managed by the architecture of the flight software.

4 - Mission Timeline and Trajectory Analysis

4.1 - Mission Timeline

1. Launch: 7/6/2034
 - a. Mayfly will launch from Cape Canaveral on a Falcon Heavy launch vehicle. The Falcon Heavy will supply a C3 of $75 \text{ km}^2/\text{s}^2$ to reduce the mean acceleration required from the electric thruster.
2. Mars Flyby
 - a. A Mars gravity assist flyby will occur during the spiral orbit from Earth to 311P. It will produce a Δv to counter the Δv required for inclination change. For

simplicity, we assume that the flyby will not affect trip time and the trajectory significantly.

3. Rendezvous with 311P: 10/9/2037

- a. After 1191 days of travel, of which 1109 days require the thruster firing and the rest consists of coasting, Mayfly arrives at Comet 311P with essentially the same orbital parameters as the comet.

4. Sample Acquisition

- a. A 6-month window allows for surface measurements of 311P and sample acquisition.

5. Back to Earth: 4/9/2038

- a. After the 6-month window, Mayfly starts to accelerate towards the inner orbit of Earth from the comet's orbit. The cruise will take 1640 days with 1512 days of thruster firing, arriving at Earth with a hyperbolic orbit and C3 of $21.3 \text{ km}^2/\text{s}^2$.

6. Entry, Descent, Landing: 10/5/2042

- a. At the hyperbolic orbit's periapsis of about 120 km, the sample return capsule will be ejected from the spacecraft and slowed down by the Earth's atmosphere. It will follow a ballistic reentry to land at the Utah test site.

| Mission Phase | Length (days) | $\Delta v (\text{km/s})$ | $C3 (\text{km}^2/\text{s}^2)$ |
|----------------------------|---------------|--------------------------|-------------------------------|
| Launch | / | / | 75 |
| Inclination Change | / | (+2) | / |
| Mars Gravity Assist | / | (-2) | / |

| | | | |
|---------------------------|------|------------------|------|
| Cruise to 311P | 1191 | 4.82 | / |
| Rendezvous | 120 | / | / |
| Back to Earth | 1640 | 8.07 | / |
| Inclination Change | / | (+) ² | / |
| Entry to Earth | / | / | 21.3 |
| Total | 2951 | 14.9 | / |

Table 4.1: Mission Timeline and Δv 's

4.2 - Interplanetary Trajectory Analysis

4.2.1 - Orbital Elements

The orbital elements used in the trajectory calculations of this mission are listed in table 4.2.1.1.

| | SMA | Eccentricity | Inclination | Velocity |
|-------|------|--------------|-------------|---|
| Earth | 1 AU | 0.0167 | 0 degrees | Velocity: $v_{Earth} = \sqrt{\frac{\mu_{sun}}{r_{Earth}}} = 29.8 \text{ km/s}$ |
| 311P | 2 AU | .1156 | 4.96 | Velocity: $v_{comet} = \sqrt{\frac{\mu_{sun}}{r_{comet}}} = 20.1 \text{ km/s}$ |

Table 4.2.1.1: Orbital Elements of Earth and 311P/PANSTARRS Comet

A rough estimate of the delta V for this mission is given by the following calculation:

$$\Delta v = v_{Earth} - v_{comet} = 9.7 \text{ km/s}$$

4.2.2 - Chemical Trajectory

Trajectory Plot

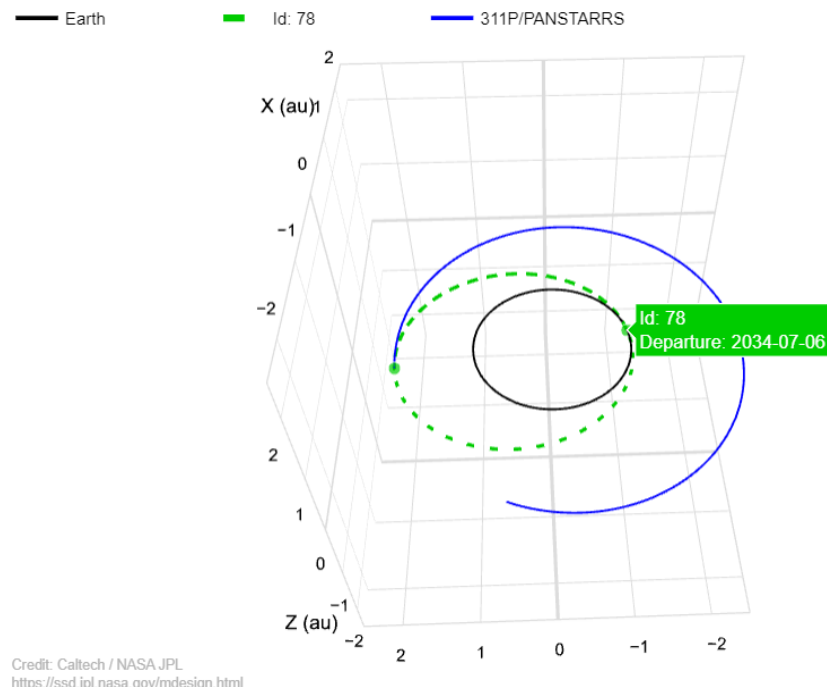


Table 4.2.1: Chemical Trajectory to 311P, by JPL Mission Design Tool (5)

Falcon heavy will launch on 7/6/2034 to place the spacecraft in a Hohmann Transfer

Orbit with a $C_3 = 22 \text{ km}^2/\text{s}^2$ and $\Delta v = 4.8 \text{ km/s}$. After completing 1.5 periods in the Hohmann Transfer Orbit (not just half a period for the purpose of phasing), the spacecraft will rendezvous with the comet on 10/9/2037. Then, a Δv of 4.9 km/s is exhibited to circularize the orbit.

Assuming a Δv of about 5 km/s to return to Earth, the total delta v implies a tremendous propellant mass. For instance, take a total Δv of 15 km/s and a highly efficient engine with an Isp value of 450s. A spacecraft of this nature with a dry mass of 1000 kg would require a wet mass of up to 30 tons, beyond the capability of any launch vehicle today. Therefore, any subsequent trajectory calculations or estimations were not performed.

4.2.3 - Solar Electric Propulsion (SEP) Trajectory

4.2.3.1 - David Oh Model

Since the semi-major axis of the comet is only about 2 AU, we employ the constant power David Oh model to analyze the trip time and corresponding Δv . Originally, we tried implementing numerical models like GMAT, however, GMAT had a steep learning curve and was hard to iterate when the relevant parameters (like the thruster model) are constantly changing.

Table 2 Model of optimum-specific-impulse circular-coplanar low-thrust transfers to Main Belt asteroids and Jupiter using SEP

| | Main Belt asteroids | Jupiter |
|---|---|--|
| Mean acceleration at $C_3 = 0$, km/s/yr | $\bar{a}_o = 17.747 t_{\text{fitt}}^{1.229}$ | $\bar{a}_o = 75.421 t_{\text{fitt}}^{-2.0363}$ |
| Burn time, yr | $t_{\text{burn}} = 1.041 t_{\text{fitt}} - 0.3571$ | $t_{\text{burn}} = 0.8984 t_{\text{fitt}} - 0.35$ |
| Adjust mean acceleration for departure C_3 , km/s/yr OR | $\bar{a} = \bar{a}_o - \frac{0.9 \sqrt{C_3^{\text{max}}}}{t_{\text{burn}}}$ <i>Note:</i> minimum allowable $\bar{a} = 2.2$ | $\bar{a} = \bar{a}_o - \frac{1.25 \sqrt{C_3^{\text{max}}}}{t_{\text{burn}}}$ <i>Note:</i> no minimum limit |
| Adjust mean acceleration for arrival C_3 , km/s/yr | $\bar{a} = \bar{a}_o - \frac{\sqrt{C_3^{\text{eff}}}}{t_{\text{burn}}}$ <i>Note:</i> minimum allowable $\bar{a} = 2.9$ | $\bar{a} = \bar{a}_o - \frac{4.7 \sqrt{C_3^{\text{eff}}}}{t_{\text{burn}}} e^{-t_{\text{fitt}}/3.5}$ <i>Note:</i> minimum allowable $\bar{a} = 4.0$ |
| ΔV , km/s | | $\Delta v = \bar{a} t_{\text{burn}}$ |
| K (from lookup table) | $K = 0.164$ to 0.706 | $K = 0.0682$ to 0.322 |
| Optimum effective exit velocity, m/s | $c^* = K \frac{2 \eta_p P_{\text{in}}}{\bar{a} m_o} + \frac{\Delta v}{2}$ | |
| Payload mass fraction | | $\frac{m_f}{m_o} = e^{-\Delta v/c^*}$ |

Table 4.2.2: David Oh's Model for circular-coplanar low-thrust transfer from Earth to Main Belt Asteroid (4)

As shown in Table 4.2.2, when using David Oh's model, we varied the trip time as input and calculated other relevant parameters, including mean acceleration and Δv , and made sure the Isps calculated matched the specifications of the thrusters chosen. Notably, we applied the constant power David Oh model, so we did not use a K constant to account for power loss. Additionally, as shown in Figure 4.2.1, assuming a wet mass of 2000 kg and Falcon Heavy as the launch vehicle, we can get over $75 \text{ km}^2/\text{s}^2$ of C3 to put into the David Oh model for reduced Δv during a trip to the comet.

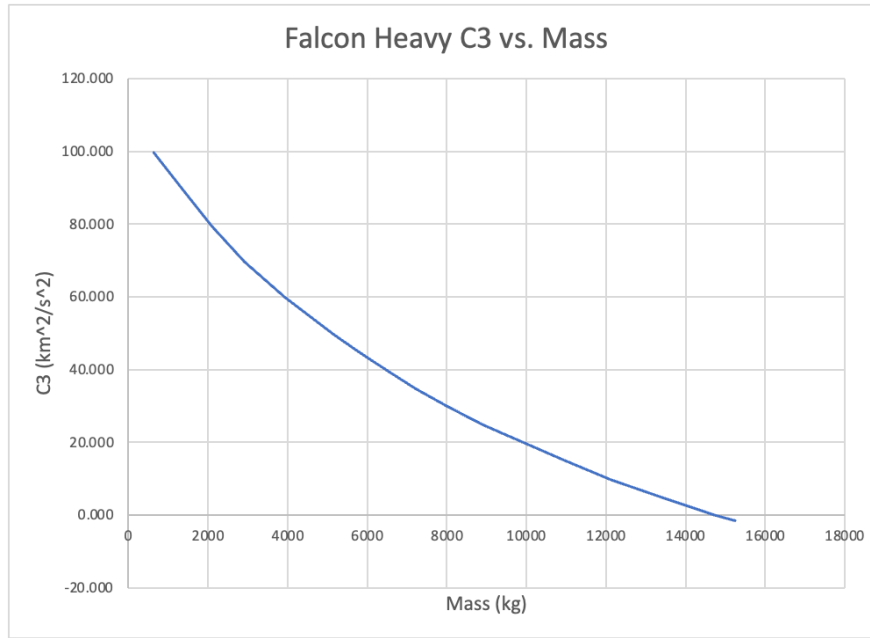


Figure 4.2.1: C3 vs Mass for Falcon Heavy Launch Vehicle

According to David Oh's model, with $C3 = 75$ from falcon heavy, and using the NEXT thruster operating at 3kW with an Isp of 4125s, it takes 3.26 years to get to comet 311P with a Δv of 4.82 km/s. The spiral orbit from Earth to 311P is shown in Figure 4.2.2. The orbit intersects Mars during the cruise from Earth to 311P; the intersection point is where the gravity assist flyby occurs.

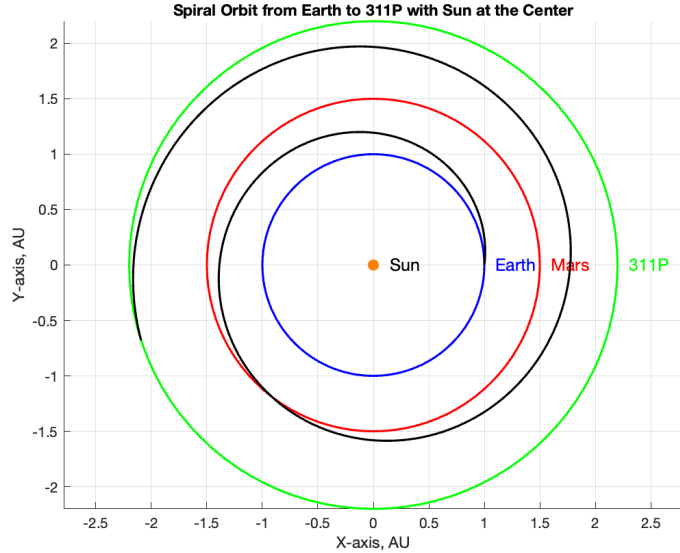


Figure 4.2.2: Approximate spiral orbit from Earth to 311P with a Mars Gravity Assist

Flyby during the journey

4.2.3.2 - Delta ν for Inclination Change

The comet 311P has an inclination of 4.96 degrees above the ecliptic plane. A simple estimation of the $\Delta\nu$ required inclination change is conducted using the formula:

$$\Delta\nu = 2v \cdot \sin\left(\frac{\Delta i}{2}\right) [1]$$

The inclination change is fixed and $\Delta\nu$ increases with a larger orbital velocity or smaller orbital radius. At Earth's, Mar's, and 311P's orbital radii, $\Delta\nu = 2.58 \text{ km/s}$, 2.11 km/s , and 1.74 km/s . As shown, the $\Delta\nu$ for inclination change is approximately 2 km/s.

4.2.3.3 - Mars Gravity Assist

311P has a low inclination of 4.96 degrees. Nevertheless, as calculated, performing an inclination change from the ecliptic plane to the comet's orbital plane still costs a $\Delta\nu$ of around 2 km/s. Since Mars lies on the spacecraft's trajectory from Earth to the main asteroid belt,

performing a Mars gravity assist flyby is ideal to compensate for the delta-v for inclination change. For a Mars gravity assist

$$\Delta v = 2v_{inf} \left(1/(1 + \frac{r_p v_{inf}^2}{\mu_{Mars}})\right) [2]$$

where v_{inf} is the hyperbolic excess velocity, r_p is the periapsis, and μ_{Mars} is the gravitational parameter of Mars. It could also be written as

$$\Delta v = 2v_{inf} \sin(\frac{\delta}{2}) [3]$$

where

$$\delta = 2 \arcsin\left(1/(1 + \frac{r_p v_{inf}^2}{\mu_{Mars}})\right) [4]$$

is the deflection angle. It is hard to estimate the hyperbolic excess velocity at Mars with the David Oh model without a numerical solution of the trajectory. Using historical data from the Rosetta mission, which conducted Mars gravity assist at $v_{inf} = 8.5$ km/s and $\delta = 24$ degrees, which gives a $\Delta v = 3.53$ km/s. The exact number will differ, but historical missions have achieved Mars gravity assists with Δv between 2 to 3 km/s, which should be enough to cover the Δv inclination change.

4.2.3.4 - Rendezvous

According to the David Oh model, and using the fact that the comet has negligible gravity, our spacecraft will arrive at 311P with an excess velocity of 0 km/s. So the spacecraft's orbit is essentially identical to that of the comet's. Therefore, we allow a sufficiently long window of 6 months for the spacecraft to orbit the comet, take sensor measurements, determine the optimal landing location, land and retrieve the sample from the comet before returning to Earth. During most of this 6-month window, Mayfly will follow the comet at a distance of about

100 km, after which it will approach the comet and retrieve surface sample. Since the comet already has a self rotation, there will be minimal effort needed to orbit the comet and take measurements.

4.2.3.5 - Patched Conics

The return trajectory will consist of two phases. The interplanetary phase where the SEP continuously supplies thrust and gradually lowers the orbit and the phase where the spacecraft enters the Earth's sphere of influence. The interplanetary phase consists of a similar trajectory as the trip from Earth to the comet, except that it is spiraling inward now. It will also have a much higher Δv because there's no departure C3 from the launch vehicle.

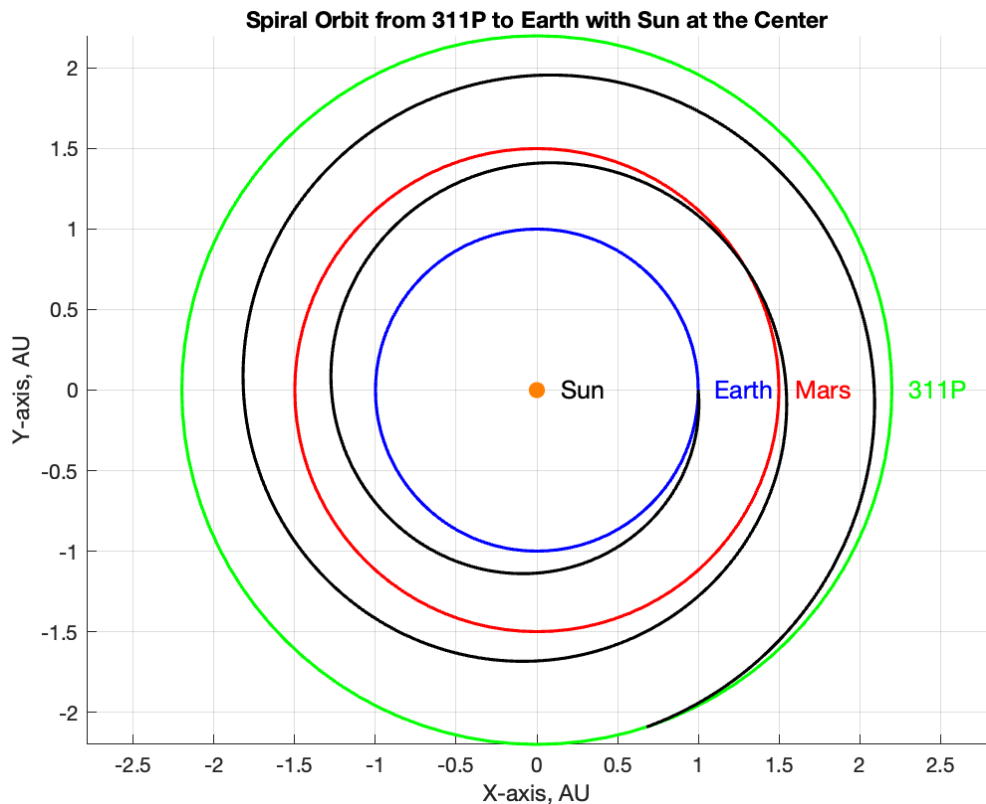


Figure 4.2.3: Approximate spiral orbit from 311P back to Earth

Note that an additionally 2 km/s will be added to the Δv to account for inclination change during return flight. The return trajectory from the comet back to Earth is shown in Figure 4.2.3.

4.2.3.6 - Hyperbolic Trajectory for Sample Return

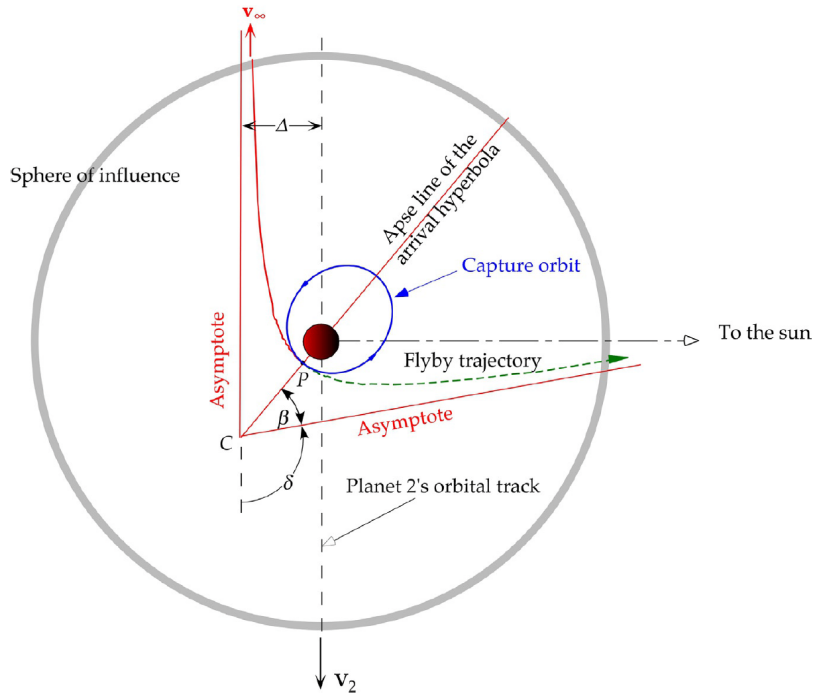


FIG. 8.14

Spacecraft approach trajectory for a Hohmann transfer to an inner planet from an outer one. P is the perihelion of the approach hyperbola.

Figure 4.2.4: Hyperbolic Flyby Illustration (2)

Figure 4.2.4 above depicts the schematic of a hyperbolic trajectory from an outer planet (comet 311P in our case) to an inner planet (Earth in our case). Although the figure says Hohmann transfer, the orbital parameters are equally relevant for a SEP trajectory. The return trajectory is different from the rendezvous trajectory because the Earth has significant gravity with a sphere of influence of up to one million kilometers. Thus Mayfly will result in a

hyperbolic trajectory entering Earth's sphere of influence moving away from the heliocentric frame of reference. With the aim of impacting Earth's atmosphere, the aiming radius must be controlled so that the periapsis intersects with Earth's atmosphere. From historical missions, the altitude h is usually taken to be 120 km. Therefore, $r_p = R_{Earth} + h = 6378 + 120 = 6498$ km.

Then, the velocity at periapsis can be calculated from the hyperbolic excess velocity,

$$v_p = \sqrt{v_{inf}^2 + \frac{2\mu_{Earth}}{r_p}} [5]$$

In our case, we want to ensure that v_p does not exceed 12 km/s. Therefore, we can rewrite the formula in terms of v_p

$$v_{inf} = \sqrt{v_p^2 - \frac{2\mu_{Earth}}{r_p}} [6]$$

Substituting $v_p = 12$ km/s and $r_p = 6498$ km, we get $v_{inf} = 4.62$ km/s. Equivalently,

$$c_3 = v_{inf}^2 = 21.3 \text{ km}^2/\text{s}^2 [7]$$

This C3 can then be input into the David Oh model as an arrival C3 when calculating the trip time for the return from Comet 311P to Earth.

With the C3 as input, David Oh model gives a trip time of 4.49 years and a Δv of 8.07 km/s for return.

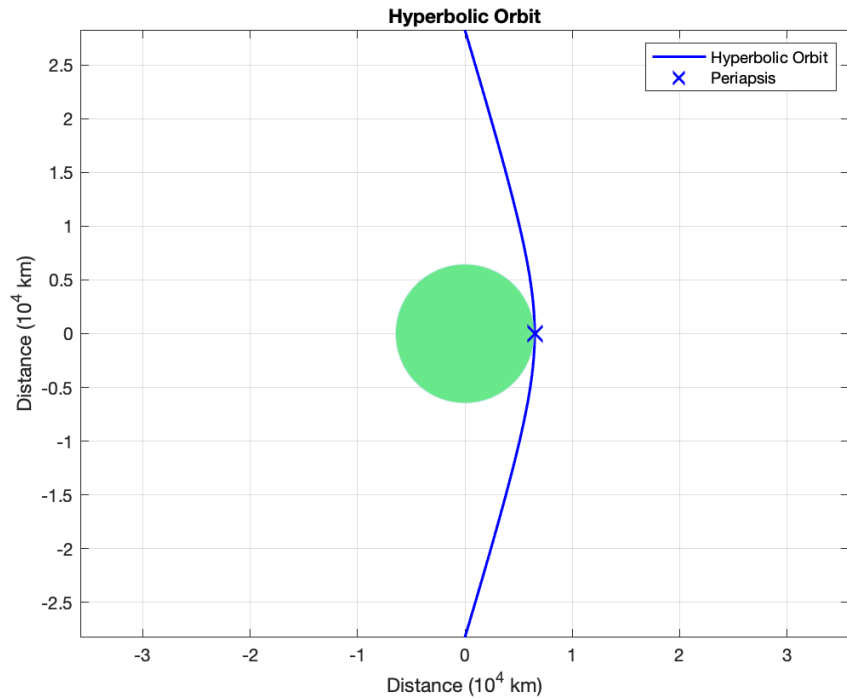


Figure 4.2.5: Hyperbolic Flyby of Earth Illustration

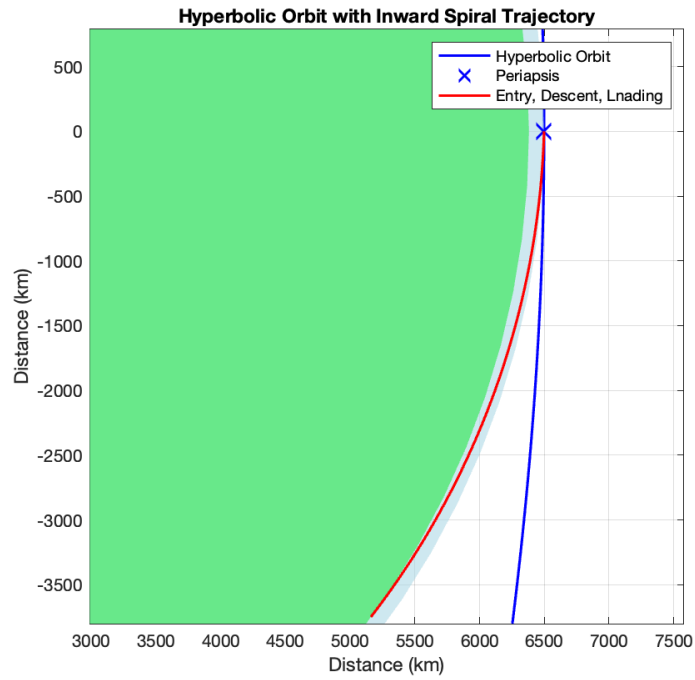


Figure 4.2.6: Hyperbolic flyby trajectory (blue), as well as Entry Descent and Landing (EDL) trajectory (red) for the sample return capsule. The Earth's atmosphere is shown in light blue.

Figure 4.2.5 and 4.2.6 depicts the hyperbolic trajectory of Earth. The Earth is the green circle drawn to scale. Figure 4.2.6 also shows an atmosphere of about 120 km in a light blue band. If there is no atmosphere, Mayfly will simply fly by Earth at the periapsis. However, in reality, the Earth atmosphere will provide air resistance to sufficiently slow the sample return capsule down and lead to a ballistic reentry of Earth, shown as the red trajectory.

5 - Design Models

5.1 - GMAT vs. David Oh Model

The General Mission Analysis Tool (GMAT) is developed by NASA to allow for complex space mission design (3). It makes use of force models and numerical solvers to propagate trajectories and allows for trajectory visualization. Compared to analytic models such as the David Oh Model (4), tools like GMAT are advantageous in that they can accurately simulate the entire mission sequence. GMAT can be as accurate as the implementation requires. Not only can it calculate and optimize for impulsive transfers and solar electric propulsion, it can also simulate multi-body problems and even solar radiation pressure.

Nevertheless, GMAT has a steep learning curve. It takes a long time to get familiar with its interface. It is time consuming to adjust the orbital parameters and optimize the trajectories. Also, as the other subsystems change over time, it is not versatile enough to follow along with changes and iterate. For instance, the entire trajectory propagation requires a specific thruster with a given Isp and thrust profile. However, if the propulsion system decides on a different thruster, the entire trajectory has to be calculated and optimized again.

On the contrary, analytic models are not as accurate and exact as numerical solvers, but they are versatile enough to aid in the process of initial mission design, as required for this project. Namely, the David Oh Model synthesizes a database of optimized low-thrust trajectories and derives empirical equations by interpolation. The results are simple equations that can be put into a spreadsheet and iterated over different initial conditions such as wet mass and thruster powers. In this project, given different wet mass and powers, a constant power David Oh Model calculates the required trip time to match the Isp of this specific thruster. The trip time is then used to calculate other useful parameters such as burn time, mean acceleration, and Δv 's.

Although the David Oh Model does not provide an exact trajectory from Earth to Comet 311P, it estimates key parameters of trip time and Δv for trajectory calculation, and it easily allows for a trade study of different thrusters (see section 7.3).

6 - Baseline Design and Vehicle Structure

The baseline vehicle design for Mayfly is inspired by several successful missions for the primary structural components, including Hayabusa2 for the main cube-like structure, which encompasses every component required for the mission including the xenon propellant tanks, the hydrazine propellant tank, two PPUs, a PDU, batteries, and four reaction wheels. Because of its frailty and critical importance, the xenon tanks required an additional central thrust cylinder housing, which recently flew on DAWN. The specific placement of the remaining payload, power, ACS, and communications components utilized the mission layout of even more flown space crafts, ranging from Europa Clipper, OSIRIS-REx, New Horizons, and even the International Space Station, which ensured all components were effectively, reliably, and efficiently being used throughout the mission.

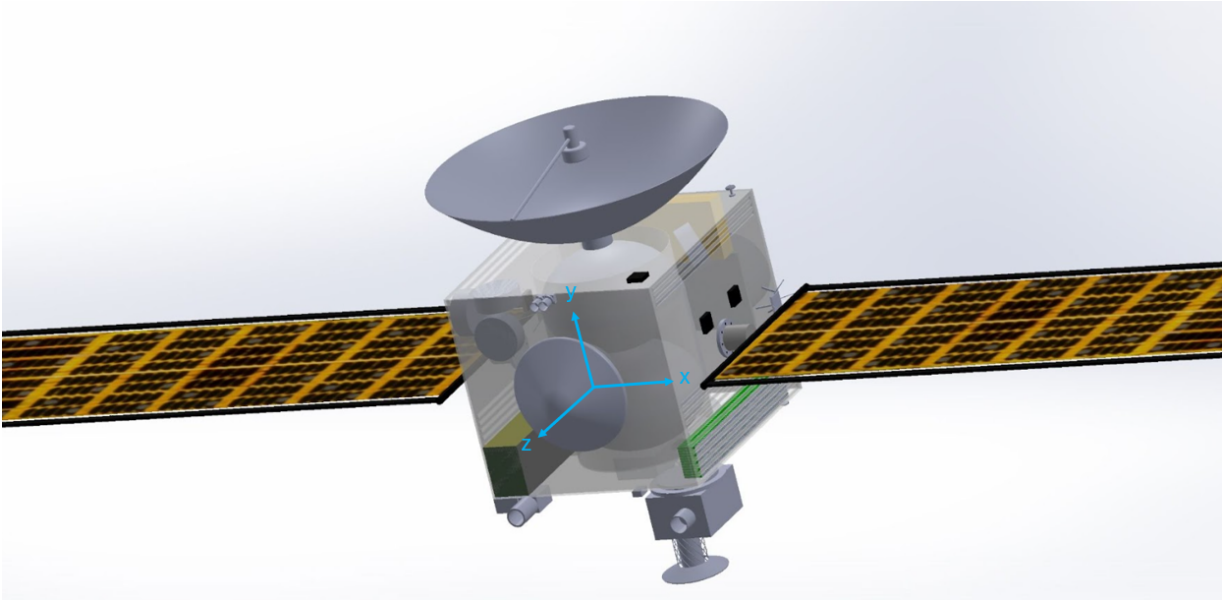


Figure 6.1: Global coordinate system for Mayfly

In terms of the spacecraft layout, and taking the reference coordinate system to be at the center of the primary cube-like structure, the ROSA solar arrays roll out in the x-axis, the xenon tank housing cylinder extends along the y-axis, and the z-axis is the axis in which the NEXT 9a ion thrusters propel the spacecraft along. More specifically, traveling from the negative x-axis to the positive x-axis, on the outside of the left face, there are two sun sensors and an ACS thruster set that contains four Monarc-1 monopropellant thrusters. These attitude determination and control thrusters are set at a small angle to improve maneuverability in multiple axes at once. On the inside bottom left face, the Power Distribution Unit (PDU) supplies electrical power to all subsystems. On the inside top left face, there are three reaction wheels, one along each axis. As you can see in Figure 6.1, the reaction wheels are aligned directly with each axis; however, in reality, they should be going through the center of mass, which is located at the coordinate (1.32 mm, -104.25 mm, -24.73 mm) from the global coordinate system. There is a fourth reaction wheel along the imaginary diagonal axis from the front bottom left vertex to the back top right vertex. On the inside bottom right face, the batteries reside and on the outside right face, two

more sun sensors and another ACS thruster set can be seen. More obvious are the two large ROSA solar arrays on the left and right sides of the primary structure.

Along the y-axis, moving from negative to positive, several of the payload components on the bottom face can be seen. Towards the front of bottom face, from left to right, the components are as followed: Hayabusa Spectrometer (NIRS3), the Hayabusa Thermal Infrared Camera (TIR), Hayabusa Sampler Horn, which is used to collect the comet sample, the Hayabusa Laser Altimeter (LIDAR), and the New Horizon Imaging Camera (Ralph). In the middle of the bottom face are two more sun sensors and on the back side of the bottom face resides the Surface Dust Analyzer (SUDA) from Europa Clipper as well as one of the low gain antennas. As one can see, the payload instruments used for this mission incorporate several components of previous missions, and thus, our mission has plenty of heritage. Inside the primary cube-like structure made of carbon fiber-aluminum honeycomb are the two Carleton xenon tanks encased in the carbon fiber cylinder as well as the ACS hydrazine tank. Moving to the top face, the high gain antenna takes up the majority of the surface area while also including two more sun sensors and the second low gain antenna. Having multiple sun sensors on each side results in sufficient redundancy to ensure the position and direction relative to the sun in relation to the spacecraft is not severed.

Lastly, moving from the negative z-axis to the positive z-axis, on the outside of the back face resides two NEXT ion thrusters and on the inside of the back face are the two Power Processing Units (PPUs) designed as a part of the electric propulsion system. On the top front face, there are two star trackers and in the middle of the front face resides Hayabusa Reentry Capsule, which is used to stow the comet sample and return it back to Earth. The below figures display multiple views of the spacecraft as well as labels to visualize the previous descriptions.

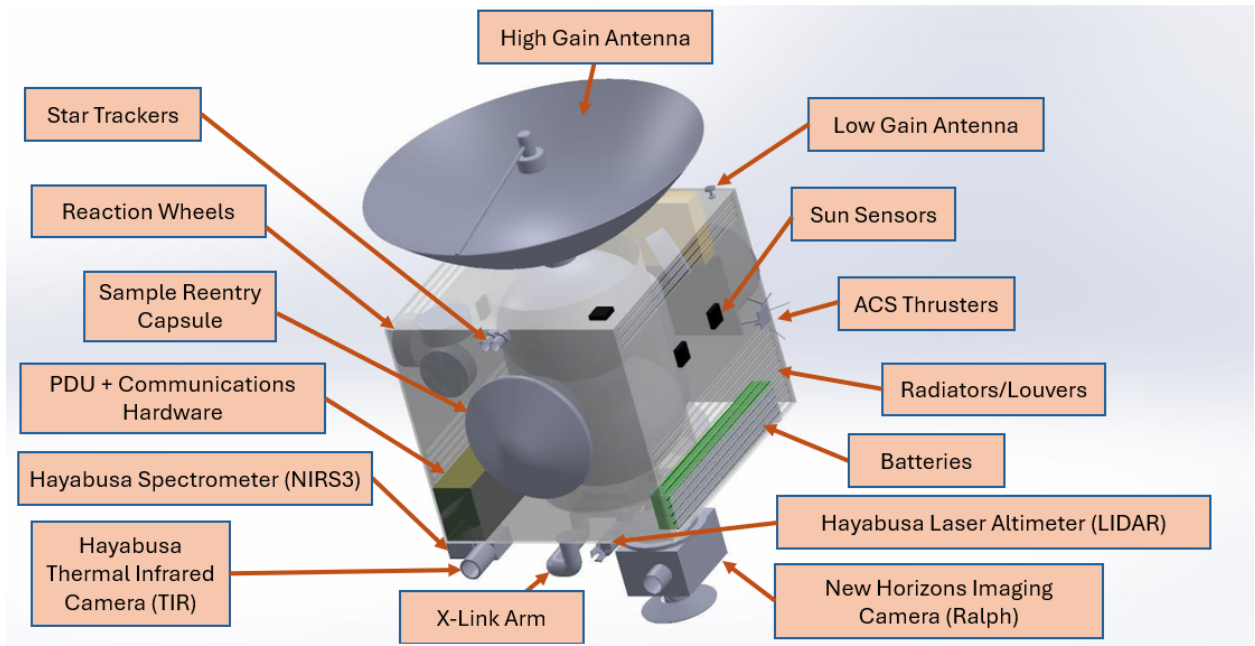


Figure 6.2: Iso front view of Mayfly with labeled components

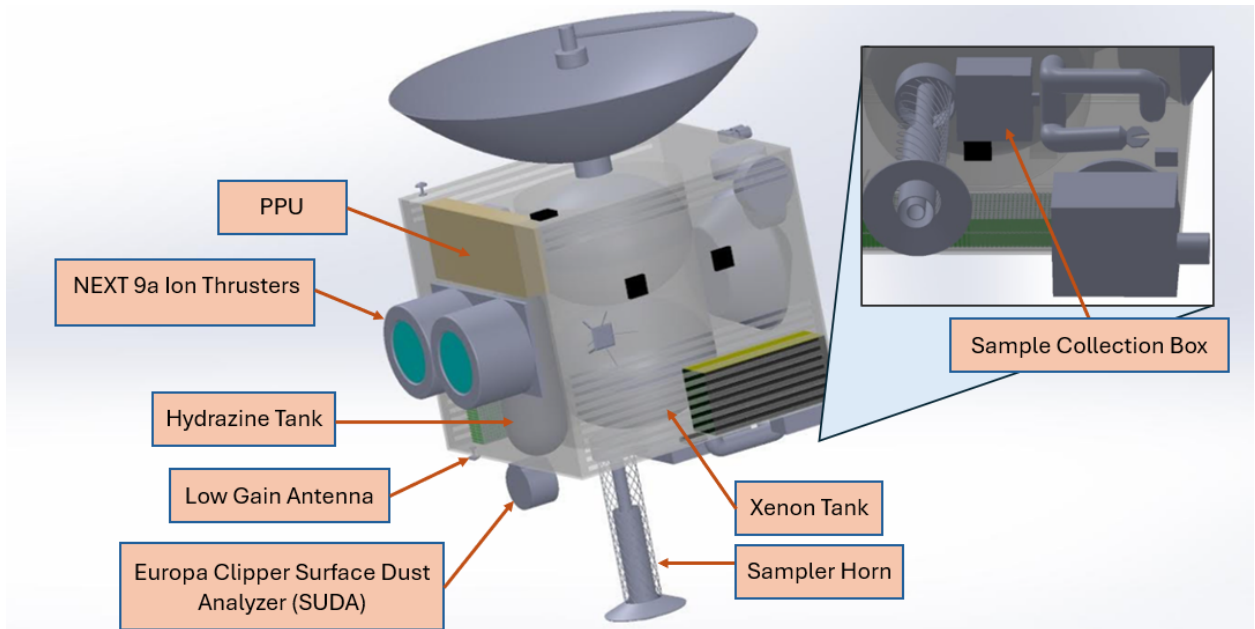


Figure 6.2: Iso back view of Mayfly with labeled components

7 - Subsystem Design

7.1 - Payload Description

The science payload for the mission to comet 311/P has been carefully chosen to ensure the efficient fulfillment of mission requirements. This selection aims to return extensive data on the comet's surface and composition, as well as to map its terrain comprehensively to identify potential sampling sites. To understand the comet's physical and chemical properties and determine if it contains volatile materials or subsurface structures, the spacecraft must gather detailed data on both the surface and the interior of 311/P.

To maximize the acquisition of new and valuable scientific data, the payload includes the Hayabusa Near-Infrared Spectrometer (NIRS3), the Hayabusa Thermal Infrared Camera (TIR), the Hayabusa Laser Altimeter (LIDAR), the Surface Dust Analyzer (SUDA), and the New Horizons Imaging Camera (Ralph). These instruments were designed to operate in concert, leveraging their unique capabilities to provide a comprehensive understanding of the comet.

The Hayabusa NIRS3 will analyze the surface composition by detecting various minerals and ices, while the Hayabusa TIR will measure thermal emissions to understand surface temperature variations and thermal properties. The Hayabusa LIDAR will map the comet's topography with high precision, helping to identify potential landing and sampling sites. The SUDA will analyze the composition of dust particles in the comet's coma, providing insights into its material makeup. Meanwhile, Ralph will capture high-resolution images of the comet's surface, aiding in the detailed mapping and analysis of its geological features.

7.1.1.1 Hayabusa Spectrometer (NIRS3)

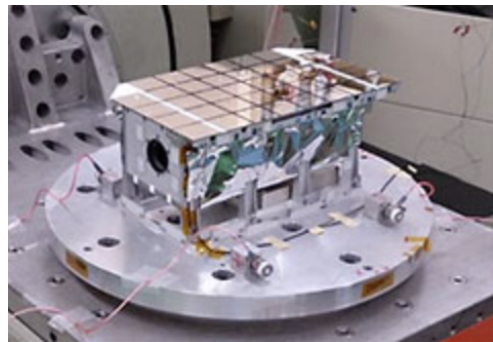


Figure 7.1.1.1: NIRS3

| | |
|-----------|--------------|
| Mass (kg) | 4.46 |
| Power (W) | 14.90 |
| Size (cm) | 35 x 17 x 10 |

Table 7.1.1.1: NIRS3 Specs

7.1.1.1 - NIRS3 Description

The Near-Infrared Spectrometer (NIRS3) on the Hayabusa spacecraft was selected to analyze the mineral composition of comet 311/P's surface, providing crucial data on its chemical makeup. NIRS3 is an advanced spectroscopic instrument consisting of an Electro-Optical Subsystem, a Solid-State Recorder Unit, and an Image Transmission Unit. The Electro-Optical Subsystem features a spectrometer with a grating system, an array of photodiodes sensitive to near-infrared light, and a calibration system to ensure accurate measurements.

NIRS3 operates in the near-infrared range (1.8-3.2 μm), providing high spectral resolution capable of distinguishing between different minerals and organic compounds. By measuring the reflected sunlight from the comet's surface, NIRS3 identifies specific minerals and organic compounds based on their spectral signatures. The instrument is designed to detect absorption features in the spectra, allowing it to determine the presence of water ice, silicates, carbonates, and organic molecules.

Extensive pre-flight calibrations ensure the accuracy and reliability of NIRS3 measurements. NIRS3 meets and exceeds our spectral resolution requirements, offering flexibility in its implementation to produce optimal data rates for various mission phases.

Target coordinates for spectroscopic measurements will be uplinked to the spacecraft, translating these coordinates into specific times during the mission when the measurements will be taken. A sequence of commands will be executed for set-up and initialization, including the alignment of the spectrometer and calibration of the photodiode array. At the correct moment, the spectrometer captures reflected sunlight data from the comet's surface. The collected data is stored in the solid-state recorder for downlink and subsequent data interpretation, enabling a detailed analysis of the comet's composition and the processes that have altered it over time.

7.1.1.2 Hayabusa Thermal Infrared Camera (TIR)

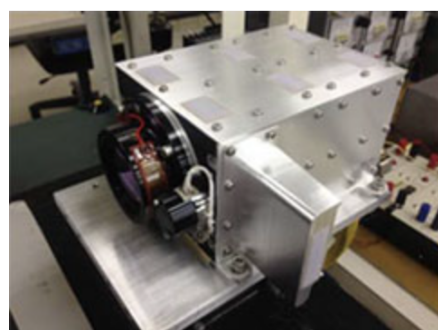


Figure 7.1.1.2: TIR

| | |
|-----------|--------------|
| Mass (kg) | 3.5 |
| Power (W) | 29.00 |
| Size (cm) | 20 x 13 x 11 |

Table 7.1.1.2: TIR Specs

7.1.1.2 - TIR Description

The Hayabusa Thermal Infrared Camera (TIR) was selected to measure the temperature distribution on the surface of comet 311/P and to gather detailed thermal information crucial for understanding the comet's physical conditions. TIR is a sophisticated imaging system that consists of an Infrared Optical Subsystem, a Thermal Imaging Unit, and a Data Processing Unit. The Infrared Optical Subsystem features a lens system optimized for the thermal infrared spectrum, a microbolometer array sensitive to thermal radiation, and a cooling system to maintain optimal sensor performance.

The TIR system operates in the thermal infrared spectrum (8-12 μm) and provides high thermal resolution to detect temperature variations across the comet's surface. The imaging unit captures thermal emission data, which is then processed to create temperature distribution maps. These maps reveal the thermal properties of the comet, such as conductivity, specific heat, and emissivity, and identify active regions with sublimation or outgassing.

Extensive pre-flight calibrations ensure the accuracy and reliability of the TIR measurements. TIR meets and exceeds our resolution requirements, offering flexibility in its implementation to produce optimal data rates for various mission phases.

Target coordinates for thermal imaging will be uplinked to the spacecraft, translating these coordinates into specific times during the mission when the measurements will be taken. A sequence of commands will be executed for set-up and initialization, including sensor calibration and system alignment. At the correct moment, the TIR captures thermal emission data from the comet's surface. The collected data is stored in the solid-state recorder for downlink and subsequent data interpretation, enabling a comprehensive analysis of the comet's thermal properties and processes.

7.1.1.3 Hayabusa Laser Altimeter (LIDAR)



Figure 7.1.1.3: LIDAR

| | |
|-----------|-------|
| Mass (kg) | 3.5 |
| Power (W) | 18.00 |

| | |
|-----------|-------------|
| Size (cm) | 6.6 x 9 x 4 |
|-----------|-------------|

Table 7.1.1.3: LIDAR Specs

7.1.1.3 - LIDAR Description

The Hayabusa Laser Altimeter (LIDAR) was selected to accurately map the topography of comet 311/P and assist in navigation and landing site selection. LIDAR is a sophisticated ranging instrument consisting of a Transmitter Subsystem, a Receiver Subsystem, and a Data Processing Unit. The Transmitter Subsystem features a diode-pumped solid-state laser that emits short pulses of light. The Receiver Subsystem includes a telescope, photodetectors, and timing electronics to measure the time it takes for the laser pulses to reflect off the comet's surface and return. The Data Processing Unit handles the conversion of raw ranging data into topographical maps.

The LIDAR system operates by emitting laser pulses towards the comet's surface and measuring the time interval for the reflected pulses to return. This process allows for precise distance measurements, with a vertical resolution of a few centimeters and a horizontal resolution dependent on the spacecraft's altitude and speed. The swath width of the LIDAR measurements varies but is optimized for comprehensive surface mapping.

Extensive pre-flight calibrations ensure the accuracy and reliability of the LIDAR measurements. The LIDAR meets and exceeds our resolution requirements, providing flexibility in its implementation to produce optimal data rates for various mission phases.

Target coordinates for the LIDAR measurements will be uplinked to the spacecraft, translating these coordinates into specific times during the mission when the measurements will be taken. A sequence of commands will be executed for set-up and initialization, including the alignment of the laser and the calibration of the timing electronics. At the correct moment, the laser emits pulses, and the reflected signals are detected and processed. The collected data is stored in the solid-state recorder for downlink and subsequent data interpretation, enabling detailed topographical analysis of comet 311/P.

7.1.1.4 - Surface Dust Analyzer (SUDA)



Figure 7.1.1.4: SUDA

| | |
|-----------|------------------|
| Mass (kg) | 5.0 |
| Power (W) | 20.40 |
| Size (cm) | 26.8 x 25 x 17.1 |

Table 7.1.1.4: SUDA Specs

7.1.1.4 - SUDA Description

The Surface Dust Analyzer (SUDA) on the Hayabusa spacecraft was selected to analyze the composition of dust particles in the coma of comet 311/P, providing critical insights into the material makeup of the comet. SUDA is a sophisticated dust detection instrument consisting of a Dust Collection Subsystem, an Analysis Unit, and a Data Processing Unit. The Dust Collection Subsystem features a capture mechanism designed to collect dust particles as the spacecraft traverses the comet's coma. The Analysis Unit includes a time-of-flight mass spectrometer that ionizes and analyzes the collected dust particles.

SUDA operates by capturing dust particles from the comet's coma and measuring their composition using the mass spectrometer. The instrument provides high-resolution mass spectra, allowing the identification of various elements and compounds present in the dust particles. This data is crucial for understanding the chemical composition of the comet and the processes that have influenced its evolution.

Extensive pre-flight calibrations ensure the accuracy and reliability of SUDA's measurements. SUDA meets and exceeds our resolution requirements, offering flexibility in its implementation to produce optimal data rates for various mission phases.

Target coordinates for dust collection will be uplinked to the spacecraft, translating these coordinates into specific times during the mission when the measurements will be taken. A sequence of commands will be executed for set-up and initialization, including the alignment of the dust collection mechanism and calibration of the mass spectrometer. At the correct moment, SUDA captures dust particles from the comet's coma, ionizes them, and analyzes their mass spectra. The collected data is stored in the solid-state recorder for downlink and subsequent data

interpretation, enabling a detailed analysis of the comet's dust composition and the processes that have shaped it.

7.1.1.5 - New Horizon Imaging Camera (Ralph)

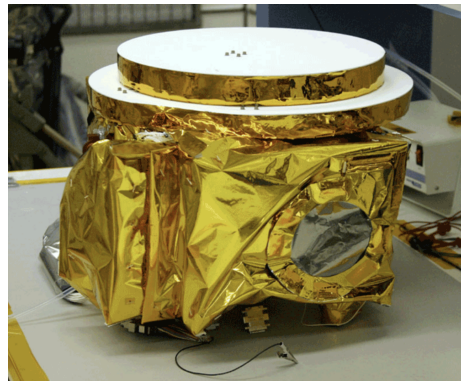


Figure 7.1.1.5: Ralph

| | |
|-----------|----------------|
| Mass (kg) | 10.5 |
| Power (W) | 7.10 |
| Size (cm) | 11 x 6.5 x 3.6 |

Table 7.1.1.5: Ralph Specs

7.1.1.5 - Ralph Description

The New Horizons Imaging Camera (Ralph) was selected to capture high-resolution images of comet 311/P's surface, providing detailed visual information crucial for mapping and analysis. Ralph is an advanced imaging system consisting of an Electro-Optical Subsystem, a

Solid-State Recorder Unit, and an Image Transmission Unit. The Electro-Optical Subsystem features a multi-spectral imager with a Korsch telescope, a set of filters for different wavelength bands, and a CCD (Charge-Coupled Device) detector array.

Ralph operates across a wide spectral range, capturing images in visible, near-infrared, and infrared wavelengths. The instrument provides high-resolution imagery with a ground sampling distance that enables detailed mapping of the comet's surface features. By capturing multi-spectral images, Ralph can help identify different materials and analyze the comet's geological and compositional properties.

Extensive pre-flight calibrations ensure the accuracy and reliability of Ralph's measurements. Ralph meets and exceeds our resolution requirements, offering flexibility in its implementation to produce optimal data rates for various mission phases.

Target coordinates for imaging will be uplinked to the spacecraft, translating these coordinates into specific times during the mission when the images will be taken. A sequence of commands will be executed for set-up and initialization, including the alignment of the telescope and calibration of the CCD detector. At the correct moment, Ralph captures images of the comet's surface across multiple spectral bands. The collected data is stored in the solid-state recorder for downlink and subsequent data interpretation, enabling a detailed visual analysis of the comet's surface and contributing to the selection of landing and sampling sites.

7.1.2 - Sample Collection and ERV Payload

The primary goal of the MAYFLY mission is to acquire and return a sample from the main belt comet 311P/PanSTARRS. In order to accomplish this, the MAYFLY has been equipped with the following three payloads: the Hayabusa Sampler Horn to acquire the physical sample, the OSIRIS-REx SRC to store and return the sample to Earth, and the xLink robotic arm system in order to transfer the sample between the previous two payloads.

7.1.2.1 - Hayabusa Sampler Horn



Figure 7.1.2.1: Hayabusa Sampler Horn

| | |
|-----------|---------------------|
| Mass (kg) | 15 |
| Size (m) | 0.2(diameter) x 1.0 |

| | |
|--|----------|
| | (length) |
|--|----------|

Table 7.1.2.1: Hayabusa Sampler Horn Description

The Hayabusa Sampler Horn was utilized on both the Hayabusa I and Hayabusa II missions to successfully acquire samples from the asteroids Itokawa and Ryugu. The sampler horn consists of a 1 meter long, 20 cm diameter cylinder that sticks out from the bottom of the spacecraft which is connected to a collection capsule. The end of this cylinder is designed to make contact with the target asteroid (or comet in this case) which then generates a touchdown signal, initiating the sample acquisition sequence [1]. The center section of the sampler horn is made from a compressible fabric which allows for some of the impact from the comet to be absorbed.

The sample acquisition sequence itself causes a high-speed tantalum bullet to be fired out of the sampler horn through use of a powder cartridge. The bullet itself is 10 mm in diameter, has a mass of 5 grams, and will travel at 300 meters per second [1]. The impact of this bullet results in small sample grains being ejected from the comet. Then as a result of the low gravity environment of comet 311P/PanSTARRS, the sample grains will travel up the horn to be gathered within the collection capsule on their own [1]. One second after the bullet is ejected, the spacecraft will fire its thrusters and begin ascending from the comet. The sample acquisition sequence is depicted below in Figure 7.1.2.2..

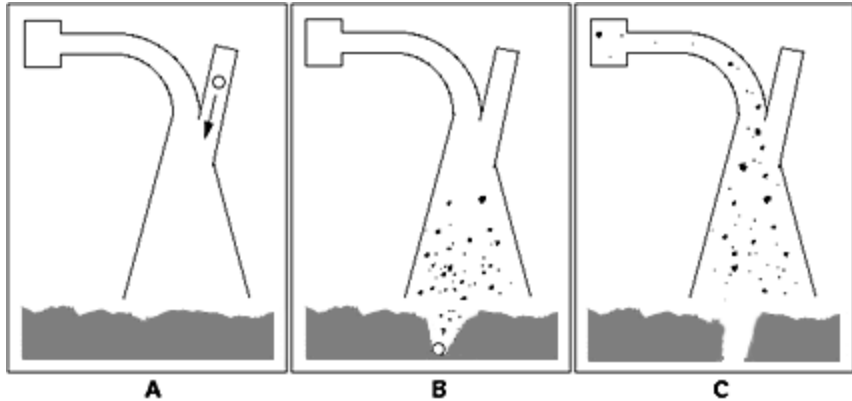


Figure 7.1.2.2: Hayabusa Sample Horn Acquisition Sequence. (A) Tantalum bullet is fired (B) Ejecta is released (C) Sample is collected within the collection capsule

There are a large number of benefits to this method of sample collection for our mission in particular. First, due to the low gravity environment present, many other sampling techniques, such as drilling, face the added challenge of somehow tethering the spacecraft to the comet during sample acquisition. The touch-and-go methodology which the sampler horn employs manages to avoid this complication by instead performing the entire sample acquisition sequence within a very short time frame before ascending from the surface of the comet. In our case, the sample acquisition sequence only lasts one second which removes the need for a tethering device. A slight downside to this methodology is that the exact quantity of the acquired sample is relatively unpredictable; however, we still expect to obtain approximately 15-30 grams of material.

Another major benefit of this system is that the projectile/impact design enables the collection of samples regardless of surface conditions. Whether the surface of the comet is powdery, hard, or anywhere in between, the tantalum bullet will be able to create ejecta which can be collected [2]. This not only varies the kinds of samples that can be obtained but also

reduces the potential number of failure cases we might encounter. Additionally, the use of tantalum as the material is beneficial as since it is a rare metal, it can be accounted for in case the samples are contaminated during the acquisition process.

Having been flight proven on two previous missions, the Hayabusa Sampler Horn has successfully demonstrated its reliability in sample retrieval. However, the sampler horn did introduce a slight issue during the Hayabusa I mission wherein the spacecraft tipped over on its side while on the asteroid Itokawa [3]. This occurred in part because the sampler horn was mounted on the edge of the spacecraft which resulted in a moment being induced when the sampler horn maintained contact with the surface of the asteroid for an extended period [2]. In order to address this potential issue, we have ensured that the sampler horn is aligned with the center of mass of our spacecraft, the MAYFLY.

7.1.2.2 - OSIRIS-REx SRC

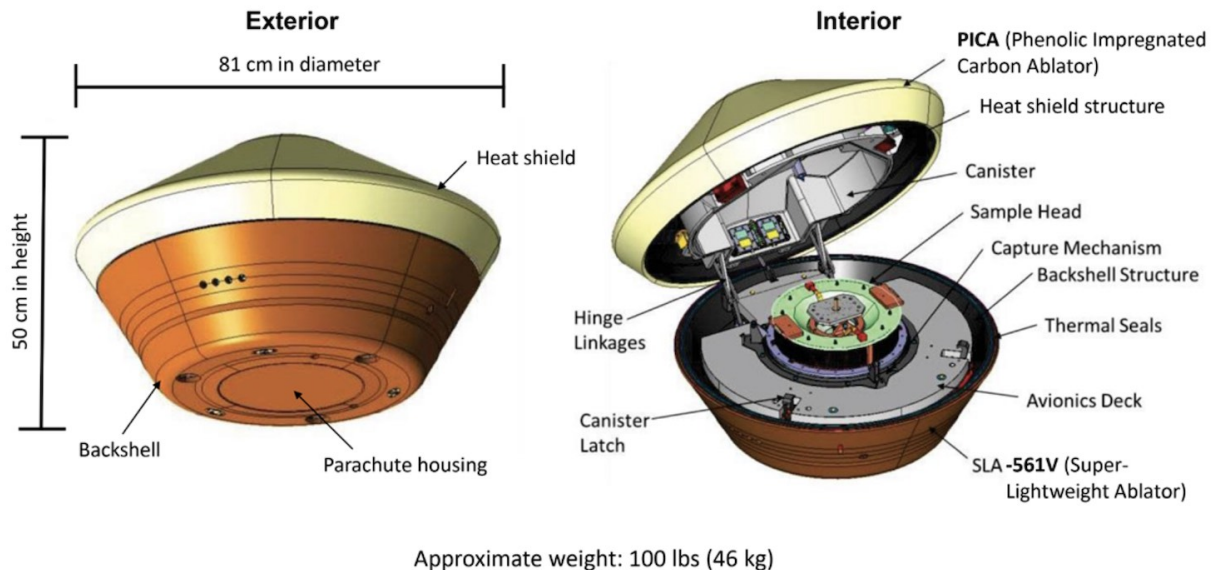


Image credit: Lockheed Martin

Figure 7.1.2.3: OSIRIS-REx SRC

| | |
|-----------|------------------------------------|
| Mass (kg) | 46 |
| Size (m) | 0.81 (diameter) x 0.50 (height) |

Table 7.1.2.2: OSIRIS-REx SRC Description

The OSIRIS-REx SRC is responsible for delivering the acquired sample from comet 311P/PanSTARRS through a high-speed reentry into the Earth's atmosphere. This sample return capsule has successfully flown on two missions previously, being OSIRIS-REx and Stardust. The forebody of the SRC is a 60° half-angle sphere cone which hinges with the afterbody, a 30° truncated cone [4]. This allows for the SRC to open during the mission such that the sampler horn collection capsule may be placed inside. It has achieved the highest reentry speed of any man made object at 12.9 kilometers per second [4]. The incredible reentry speed of the OSIRIS-REx SRC results in similarly incredible heating rates, achieving temperatures up to 2900 °C, which are accounted for with a Phenolic Impregnated Carbon Ablator (PICA) heatshield [4]. This enables the sample to be maintained below 75 °C throughout the course of the reentry sequence.

The SRC itself does not possess any guidance or control systems which reduces the total number of failure modes, but in return it is wholly reliant on its inherent aerodynamic stability to reduce any angle of attack disturbances that might occur. The entry sequence begins with the SRC being released from the main spacecraft with an additional rotation of 13.5 rpm. This further improves its aerodynamic stability and allows for the SRC to maintain a 0 degree angle of attack during coast [4]. Then, upon sensing 3 g of deceleration, a gravity-switch sensor activates

a 15 second timer which will deploy a drogue parachute at approximately Mach 1.4 through use of a mortar-tube [5]. This serves to bring the SRC to subsonic speeds and initiates a main timer of 350 seconds after which point the 8.2 meter main parachute will be deployed. The main parachute deployment occurs at approximately Mach 0.14 and 1.8 km above the ground [4]. The remaining descent is expected to take 6 minutes and upon landing, a pyrotechnic cutter will sever connection to the parachute in order to prevent the SRC from being dragged about [5]. The entry sequence and parachute recovery system are depicted in Figure 7.1.2.4 below.

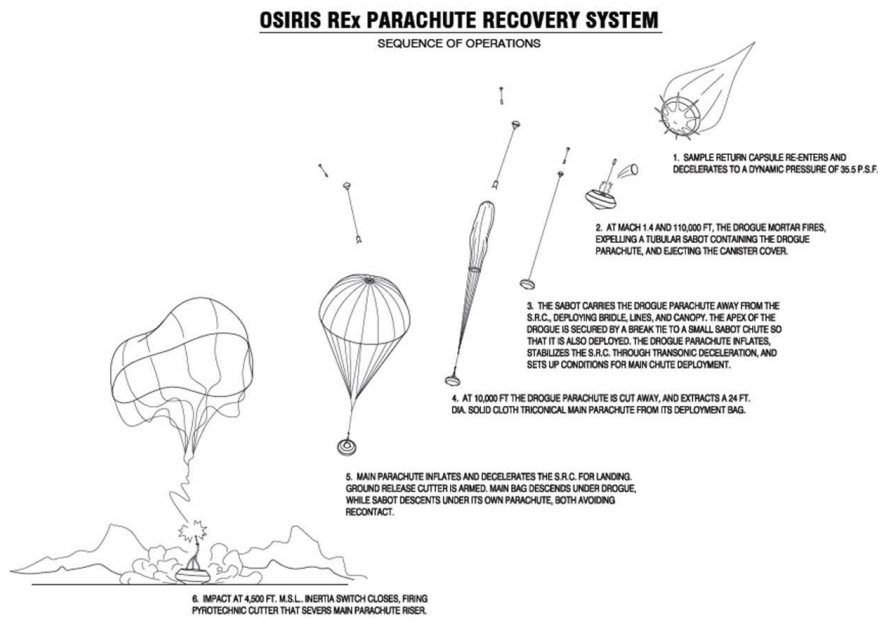


Figure 7.1.2.4: OSIRIS REx Parachute Recovery System

We will be following in the footsteps of both the Stardust and OSIRIS-REx missions by aiming for the Utah Test and Training Range (UTTR) as our landing site. This provides us with an 80 by 20 kilometer wide ellipse within which we can land and the UTTR is capable of tracking the location of the SRC within 10 meters through use of radar. As an added security

measure however, the SRC is also equipped with an on board radio locator beacon that is able to last for 20 hours [5].

7.1.2.3 - xLink Space-Rated Modular Robotic Arm System

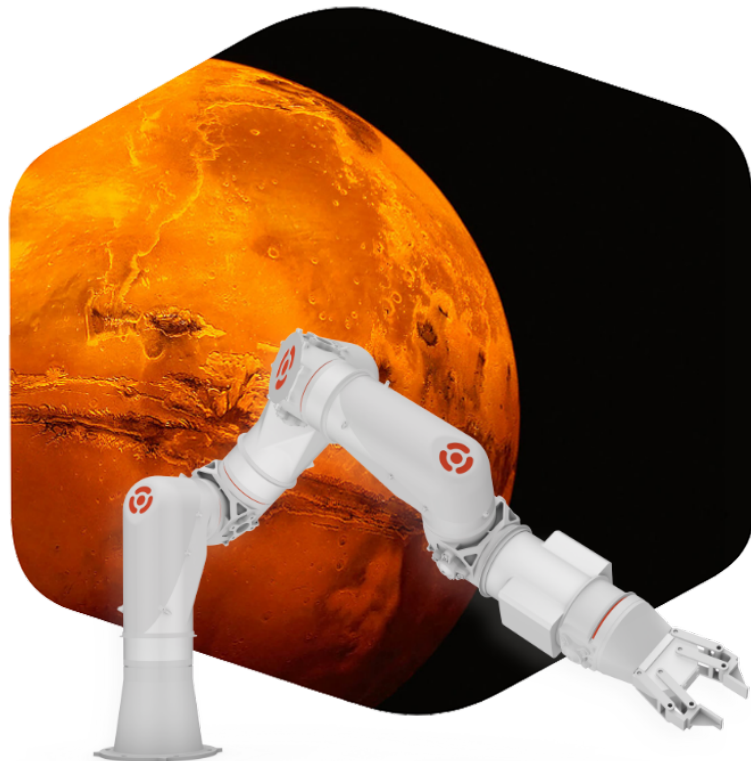


Figure 7.1.2.5: xLink Robotic Arm

| | |
|-----------|---------------------------------------|
| Mass (kg) | 50 |
| Power (W) | 100 |
| Size (m) | 1.0 (length) x 0.1 (diameter) x 6-DOF |

Table 7.1.2.3: xLink Robotic Arm Description

In order to interface between the Hayabusa Sampler Horn and the OSIRIS-REx SRC, the xLink Space-Rated Modular Robotic Arm System, developed by Motiv Space Systems, was selected. This robotic arm is onboard NASA's OSAM-2 mission where it will perform a variety of assembly and manufacturing tasks [6]. The role of this robotic arm in our mission is to transfer the collection capsule of the sampler horn to the OSIRIS-REx SRC and it will be mounted on the outside of the spacecraft between the two. A mock-up of this transfer is depicted below in Figure 7.1.2.6 on a simplified model of the MAYFLY.

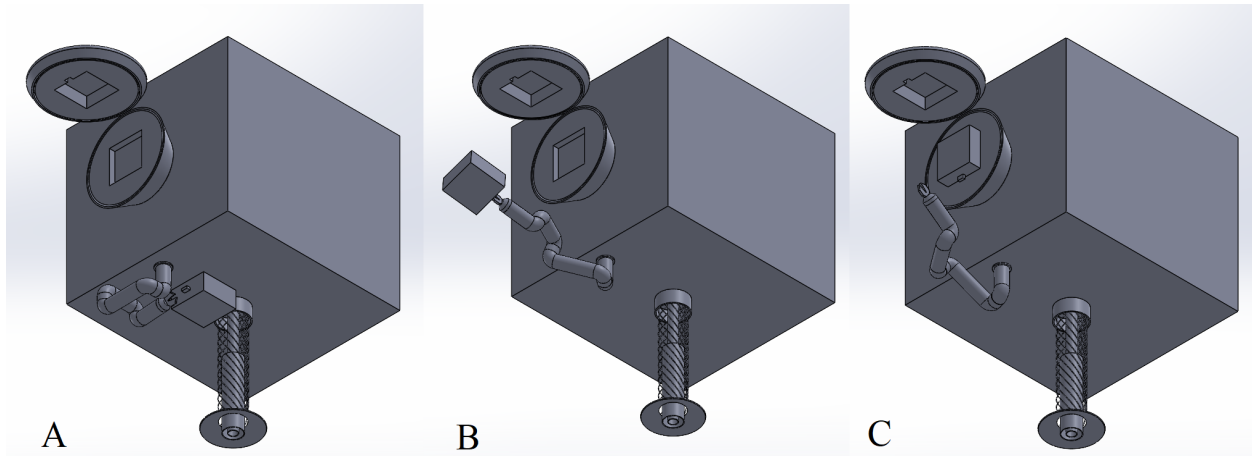


Figure 7.1.2.6: Sample Transfer Mock-Up (A) Idle (B) xLink transferring collection capsule (C)

Collection Capsule placed within SRC

Once all the samples have been acquired and the MAYFLY has successfully ascended from comet 311P/PanSTARRS, the OSIRIS-REx SRC will open using a clamshell mechanism. The xLink robotic arm will then grasp onto and separate the collection capsule from the body of the spacecraft. The robotic arm itself is 1 meter long and possesses 6 degrees of freedom,

enabling it to reach around the side of the MAYFLY and place the collection capsule within the SRC. Once this is completed, the arm will return to its original stored configuration and the SRC will shut.

Created by the same team who developed the robotic arm of the Perseverance rover, the primary advantage of the xLink robotic arm in particular comes from its modular design which enables us to customize the length and degrees of freedom of the robotic arm to suit our specific mission requirements. Rather than being beholden to a previous mission's robotic arm design which might include unnecessary components or need to be designed around, this system reduces design complexity and ultimately allows for the contributed mass to be as low as possible [6]. Furthermore, while some robotic arms are centered around functions such as repair or docking, the xLink is designed for a wide range of manipulation tasks, including positioning and connecting modules which is the precise use case we require it for [6].

7.2 - Launch Vehicle

This section studies and compares launch vehicles considered for the Mayfly mission. In this analysis, we consider a variety of parameters from deliverable C3, to fairing size, to age, to cost for the Falcon Heavy, Delta IV Heavy, and the Falcon 9. Though the Delta IV Heavy has similar capabilities to the Falcon Heavy, the Falcon Heavy seems to edge it out in every category. Therefore, in concluding this analysis, we ultimately find that the Falcon Heavy is the launch vehicle best suited for the Mayfly mission.

7.2.1 - Launch Vehicle Trade Study

The main job of the launch vehicle is to deliver the spacecraft to space, imparting a C3 that helps the spacecraft make it to its destination. In finding the optimal launch vehicle for the Mayfly mission, we conducted a trade study on the Falcon 9, Delta IV Heavy, and Falcon Heavy. In the following analysis, we examine a variety of factors that help us determine the best launch vehicle for the Mayfly mission. In determining the optimal launch vehicle, we first consider the C3 each launch vehicle is capable of imparting on our spacecraft. Displayed in the figure below is each launch vehicle's deliverable C3 as a function of spacecraft launch mass.

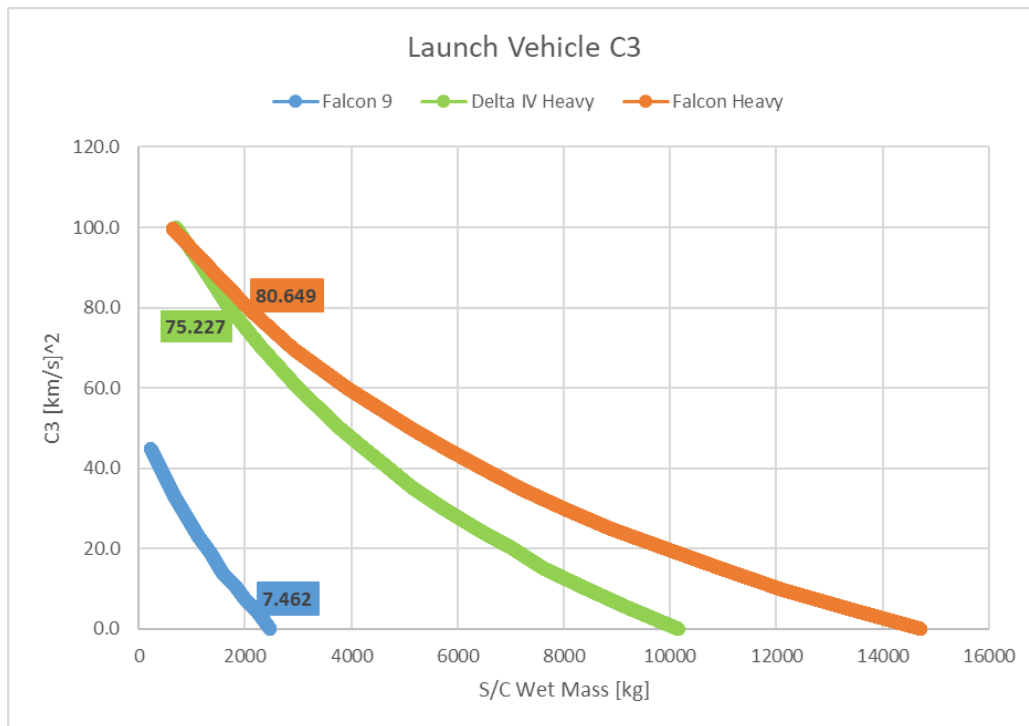


Figure 7.2.1: Launch Vehicle C3 at Varying S/C Masses

As shown across all wet masses, the Falcon 9 delivers the lowest C3 to the spacecraft while the Falcon Heavy delivers the most. From rough calculations, we determine that our spacecraft will have a wet mass in the ballpark of 2000 kg. Analyzing the launch vehicle data at 2000 kg, we observe that the Falcon 9 only delivers about $7.5 \frac{\text{km}^2}{\text{s}^2}$ while the Falcon Heavy delivers a C3 of about $80 \frac{\text{km}^2}{\text{s}^2}$. After conducting some rough trajectory calculations, we eliminate the Falcon 9 due to its lack of C3.

Comparing the C3 of the Falcon Heavy and the Delta IV Heavy, we see the Falcon Heavy delivers a C3 of about $80 \frac{\text{km}^2}{\text{s}^2}$ while the Delta IV Heavy delivers a C3 of about $75 \frac{\text{km}^2}{\text{s}^2}$. Therefore, because each vehicle delivers a comparable amount of C3, we begin to consider the payload fairing size, the availability, and the cost of each vehicle.

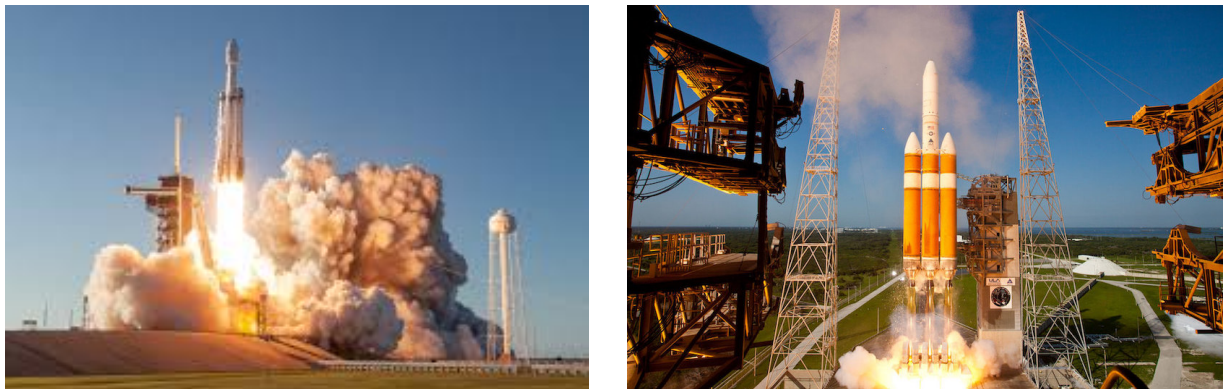


Figure 7.2.2: Falcon Heavy (left) and Delta IV Heavy (right) at launch

First, we examine the payload fairing size of each launch vehicle. From SpaceX's website, we see that the Falcon Heavy has a payload fairing height of 13 m and a diameter of 5

m. From ULA's website, the Delta IV Heavy has two fairings with a 5 m diameter: one with about a 14 m height, and another with about a 19 m height. Because our spacecraft is only 1 or 2 meters tall, both launch vehicles provide adequate volume to store our spacecraft. However, the excess height associated with the Delta IV Heavy is unnecessary.

Next, we consider the age of each launch vehicle. The Falcon Heavy is a relatively new launch vehicle, having completed 9 launches with its first launch in February 2018. Conversely, the Delta IV Heavy is in its later years, with 16 launches and its final launch being conducted in April 2024. Therefore, from this analysis, we begin to heavily focus on the Falcon Heavy.

Lastly, though cost does not play a large role in this mission design, it is still good to consider. After conducting some research we find that according to *Space.com*, the launch cost of the Falcon Heavy is only about \$90 million while the Delta IV Heavy is around \$350 million.

Therefore, we select the Falcon Heavy as the launch vehicle for the Mayfly mission. This is because it is capable of delivering a higher C3 at a given spacecraft wet mass, its payload fairing fits our spacecraft, and it is newer, all while being significantly cheaper than the Delta IV Heavy.

7.3 - On-Board Propulsion

This section analyzes and compares a variety of chemical and solar electric propulsion systems considered for the Mayfly mission. Trade studies were conducted for both propulsion system categories and ultimately, because of the required propellant masses, the chemical systems were eliminated. Within the solar electric propulsion system trade study, we dive into the specifics of each engine and compare the maximum thrusts, input powers, specific impulses, efficiencies, trip times, and propellant masses at various wet masses. From this trade study, we

select the high-Isp NEXT 9a ion thruster for its high efficiency, high specific impulse, low propellant mass, and adequate total trip time.

7.3.1 - Chemical Propulsion Trade Study

In finding the right propulsion system for the Mayfly mission, a chemical propulsion trade study was conducted. Both bipropellant and monopropellant thrusters were analyzed in this study, with Aerojet Rocketdyne's R-40, R-40B, AJ10-190, and MR-80B thrusters being the main contenders. These thrusters were considered for their high thrust values and their flight heritage.

Using a simple Hohmann transfer trajectory from Earth (1 AU) to the 311P/PANSTARRS comet (~2 AU), a total Δv of approximately $8.47 \frac{km}{s}$ was calculated. With this Δv , and assuming an initial dry mass of 2000 kg, the total propellant mass can be calculated using the rocket equation displayed below.

$$m_{propellant} = m_{initial} \left(1 - \exp\left(\frac{-\Delta v}{gIsp}\right)\right) \quad (7)$$

The calculated propellant mass along with thrust, specific impulse, and engine mass are displayed in the table below.

| Engine (Aerojet Rocketdyne) | Max. Thrust [N] | Isp [s] | Engine Mass [kg] | Total Propellant Mass [kg] |
|-----------------------------|-----------------|---------|------------------|----------------------------|
| R-40 | 3870 | 281 | 10.5 | 41,000 |
| R-40B | 4000 | 293 | 10.5 | 36,000 |
| AJ10-190 | 26,700 | 316 | 118 | 28,000 |
| MR-80B | 3100 | 225 | 168 | 91,000 |

Table 7.3.1: Chemical Thruster Trade Study

As shown, if we assume an overall wet mass of 2000 kg, the amount of propellant required to complete the mission with a chemical propulsion system is quite large. The figure below compares the Aerojet Rocketdyne AJ10-190 to the high-Isp NEXT 9a ion thruster, with both systems having the highest specific impulses in each of their respective categories. As can be seen, the solar electric propulsion system requires significantly less propellant mass than the chemical system.

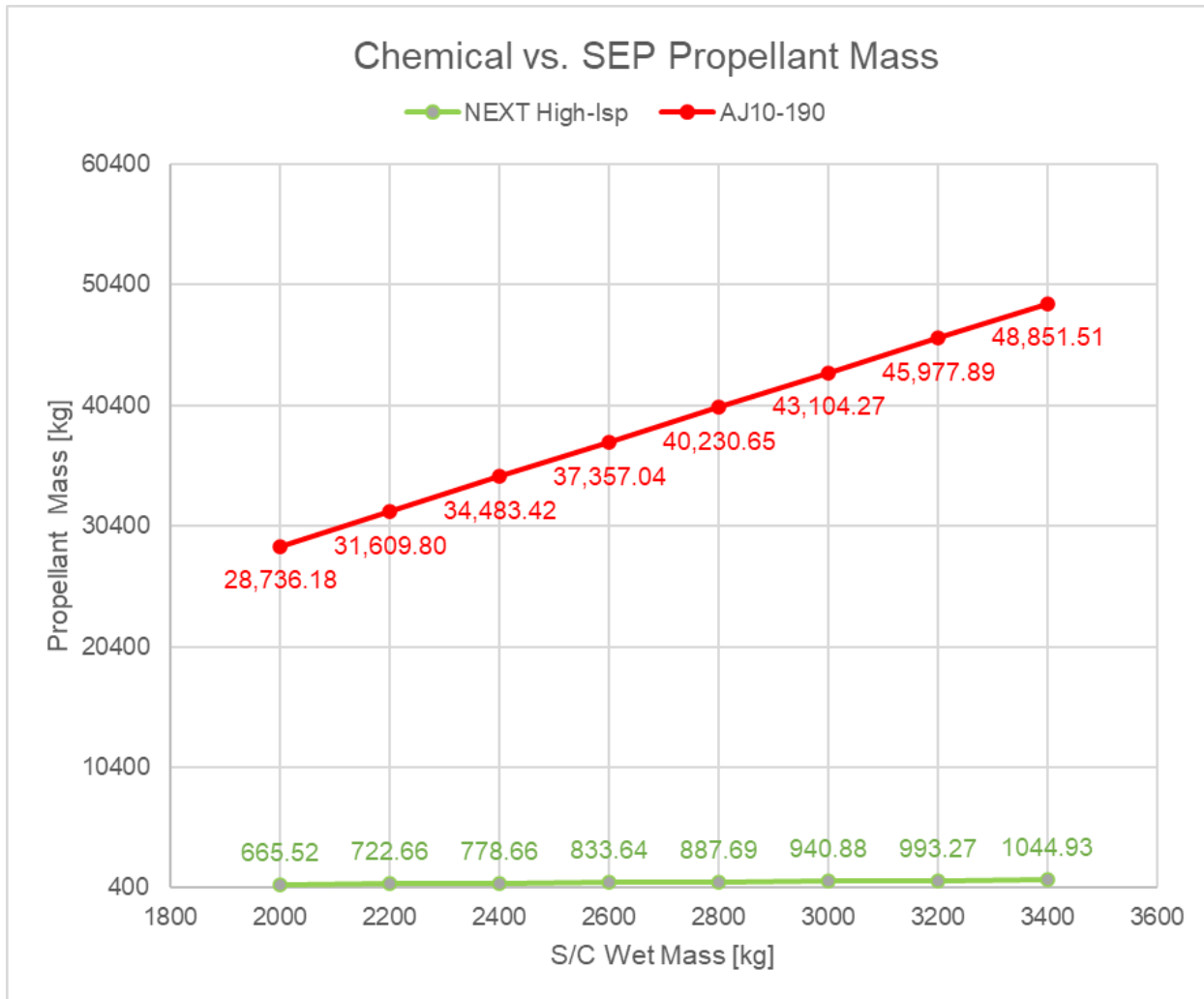


Figure 7.3.1: Chemical and Electric Propulsion System Propellant Masses

7.3.2 - Solar Electric Propulsion Trade Study

As discussed above, because the required propellant mass for a chemical system was so high, we conducted a solar electric propulsion trade study. Included in this study are both hall-effect and ion thrusters: the BPT-4000 Hall-effect thruster, the high-Isp NEXT 9a ion thruster, the high-thrust NEXT 9a ion thruster, and the XIPS 7d ion thruster. These engines were selected because of their high specific impulses and because each of them is flight-proven, with

NEXT recently successfully flying on the DART mission. The maximum input power, thrust, specific impulse, and engine mass are compared in the table below.

| <u>Engine</u> | <u>Max. Input Power [kW]</u> | <u>Max. Thrust [mN]</u> | <u>Isp [s]</u> | <u>Engine & PPU Mass [kg]</u> |
|------------------------|------------------------------|-------------------------|----------------|-----------------------------------|
| BPT-4000 | 4.5 | 235 | 2041 | 27.3 |
| High-Isp NEXT 9a | 6.9 | 226 | 4152 | 36.4 |
| High-Thrust NEXT 9a | 6.9 | 230 | 4085 | 36.4 |
| XIPS 7d | 4.5 | 157 | 3487 | 36 |

Table 7.3.2: SEP Input Power, Thrust, Specific Impulse, and Mass Comparison

It is also worth investigating how varying each engine's input power affects each system's specific impulse, thrust, and efficiency. Because each engine can be throttled, these values vary with input power. The curves associated with these parameters are displayed in the figures below.

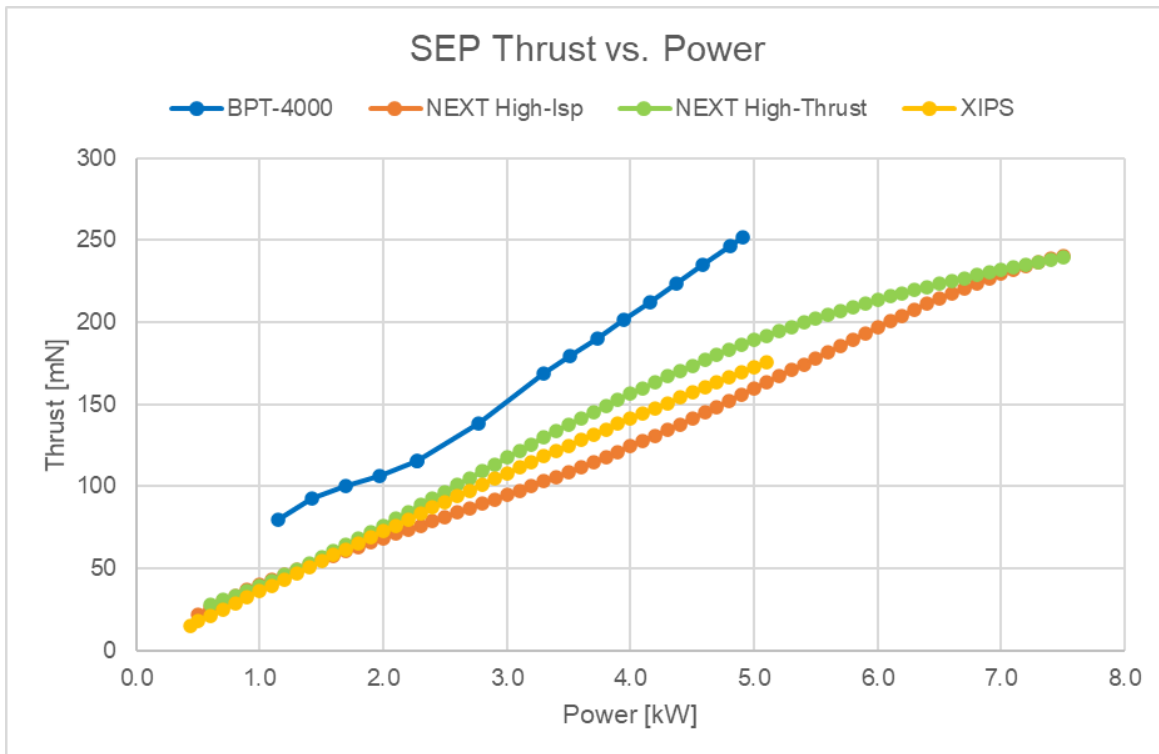


Figure 7.3.2: SEP Thrusts at Varying Power

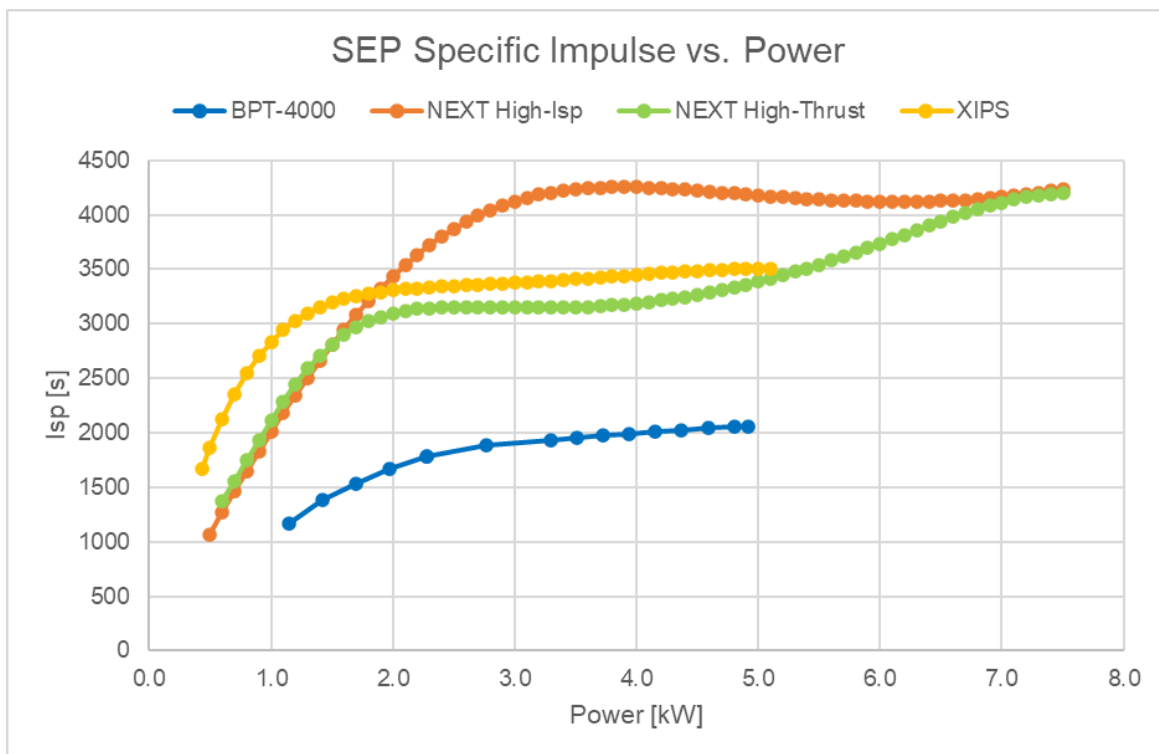


Figure 7.3.3: SEP Specific Impulse at Varying Power

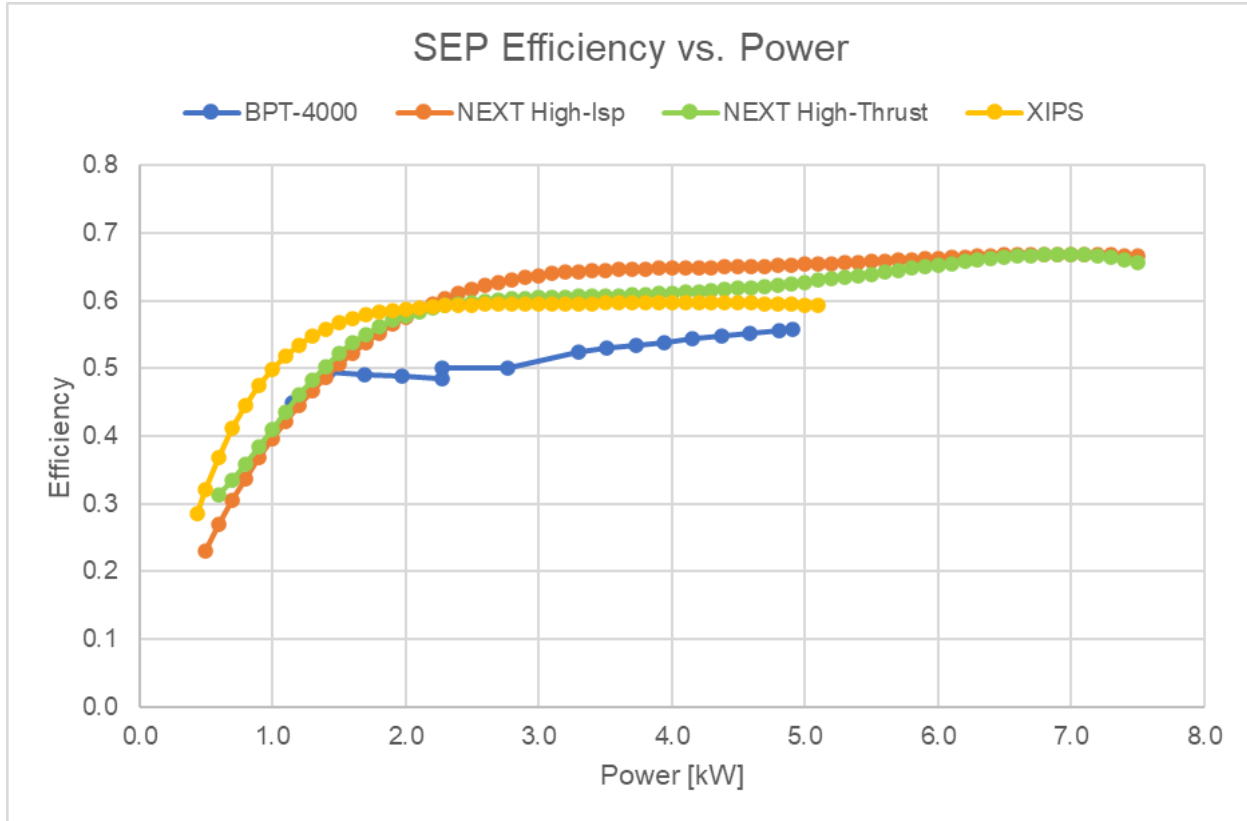


Figure 7.3.4: SEP Engine Efficiency at Varying Power

Notice that from about 2.0-5.0 kW, the specific impulse and efficiency of each engine curve are relatively stable and flat. Additionally, in this range, the thrust for each engine has close to a constant slope upward. This is good because this means that though we will be producing less thrust, we can create thrust at about the same efficiency as we would at high input powers. This results in smaller overall solar array sizes.

Regarding each engine individually, the BPT-4000 Hall-effect thruster produces the highest amount of thrust, however, it also has the lowest efficiency and specific impulse across input powers. This effectively results in more propellant mass and thus less payload space aboard the spacecraft.

Conversely, the high-Isp NEXT 9a ion thruster produces the lowest thrust with the highest efficiency and specific impulse across input powers. While this might not seem great, this engine will allow us to maximize our payload size and minimize our propellant mass. If the overall trip time is small enough, this engine is the optimal solution for this mission. However, if the overall trip time is too large, the high-thrust NEXT 9a and the XIPS ion thrusters are also great options. These engines are not as efficient as the high-Isp NEXT 9a thruster, but they would still allow us to decrease the propellant mass and increase our payload size.

Analyzing each of the ion engines at an input power of 3.0 kW, and the Hall-effect thruster at an input power of 4.5 kW, we calculate the deliverable mass of each engine using the David Oh model. This is displayed in the figure below.

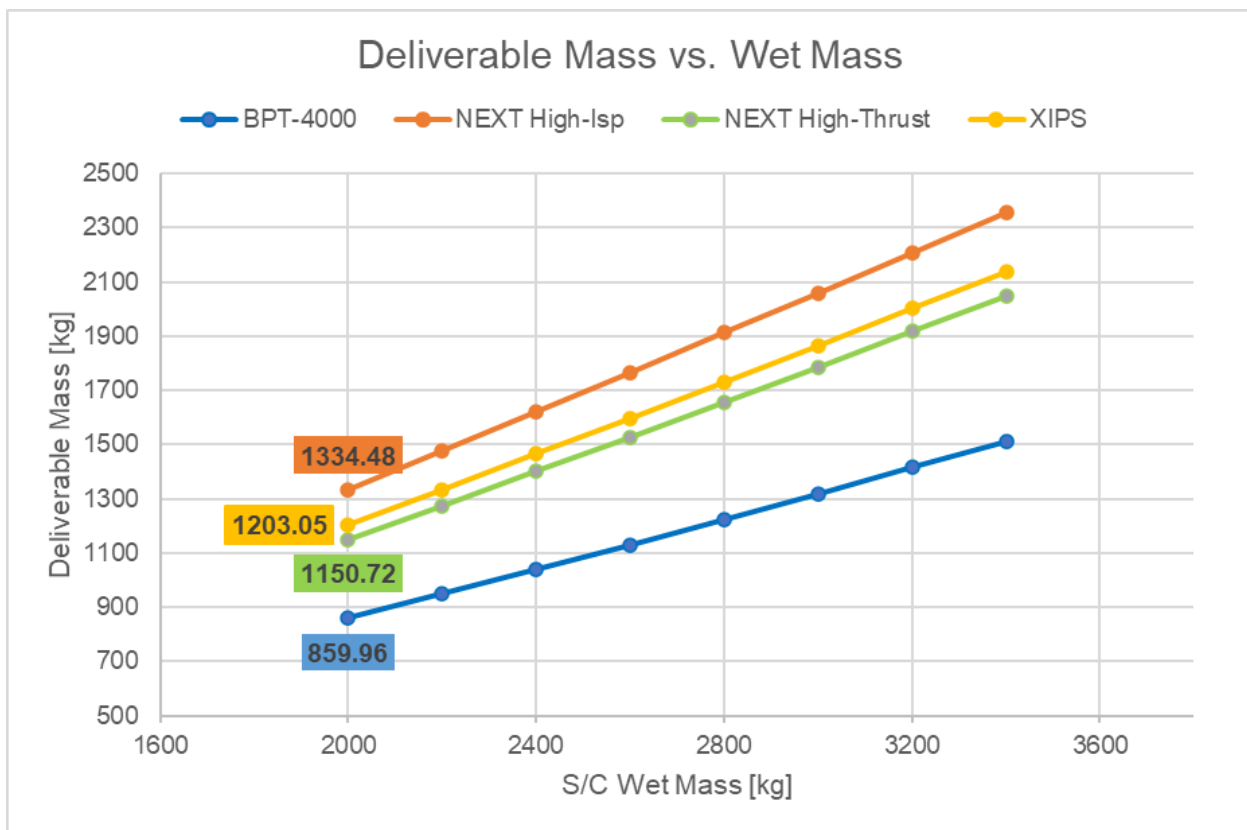


Figure 7.3.5: Engine Deliverable Masses

As expected from figures 7.3.2, 7.3.3, and 7.3.4 above, across all wet masses the total deliverable mass of the ion thrusters is higher compared to the Hall-effect thruster. With the high-Isp NEXT 9a ion thruster capable of delivering the most payload at 1334.48 kg at a wet mass of 2000 kg, it is beginning to look like the best thruster for this mission. Next, we analyzed the trip times of these thrusters at the same input power using the same David Oh model. These can be seen in the plot below.

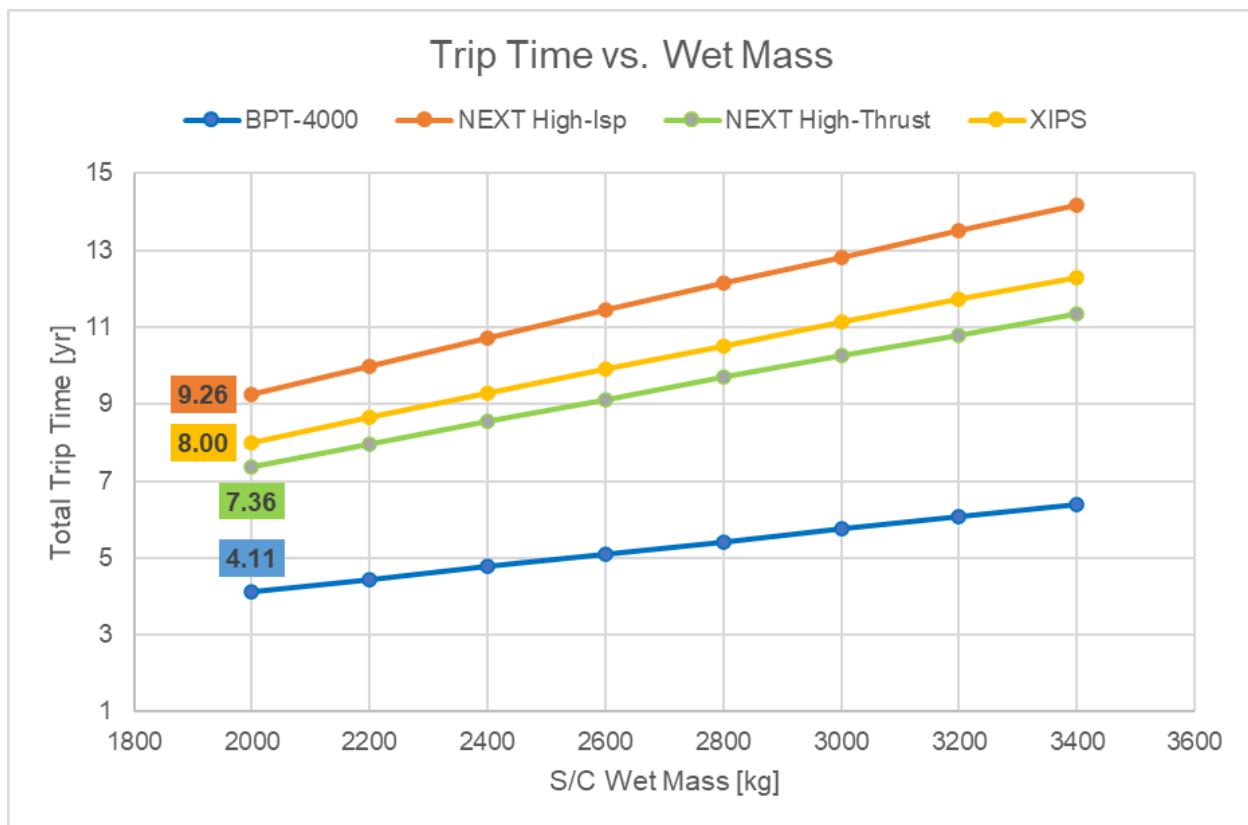


Figure 7.3.6: Engine Deliverable Masses

As shown, the overall trip time for each engine satisfies the 10-year mission timeline. After analyzing each engine and because the efficiency, specific impulse, and deliverable

payload mass are the highest, and the overall trip time still fits within the mission timeline, we select the high-Isp NEXT 9a ion thruster as our propulsion system for the Mayfly mission.

7.3.3 - High-Isp NEXT 9a Ion Thruster Analysis

After selecting our propulsion system, we determined the best trajectory for the mission and conducted further analysis on the high-Isp NEXT 9a ion thruster. As previously mentioned, we are running the high-Isp NEXT 9a ion thruster at an input power of 3.0 kW to minimize the solar array size. At this input power, the engine has a specific impulse of 4125s, a maximum thrust of 94.57 mN, and an efficiency of about 0.64. Using the David Oh model with these values and all the equations corrected for our actual trajectory, we determined the total trip time of the mission to be 7.52 yr, with a total Δv of $12.39 \frac{km}{s}$, a total propellant mass of 527.49 kg (580.24 kg with 10% contingency), and a deliverable mass of 1472.51 kg (1419.76 kg with 10% propellant mass contingency).

With an engine throughput of 600 kg, our mission only requires one NEXT 9a ion thruster. However, for redundancy, we will bring one additional thruster aboard the spacecraft. Displayed in the tables below are the quantities and masses of each subcomponent of the propulsion system.

| <u>Component</u> | <u>Mass [kg]</u> | <u>Quantity</u> | <u>Total Mass [kg]</u> |
|--|------------------|-----------------|------------------------|
| NEXT 9a Thruster | 12.70 | 2 | 25.40 |
| PPU | 33.90 | 2 | 67.80 |
| Misc. Subcomponents (Gimbals, Cables, etc.) | 15.00 | 2 | 30.00 |
| Carleton Xenon Tank | 45.00 | 2 | 90.00 |
| <u>Total Dry Mass [kg]</u> | | | 213.20 |

| | |
|--|--------|
| Propulsion System Dry Mass [kg] | 213.20 |
| Xenon Propellant [kg] | 580.24 |
| <u>Total System Wet Mass</u> <u>[kg]</u> | 793.44 |

Table 7.3.3: NEXT 9a System Component Masses

Shown in the images below are the NEXT 9a ion thruster in its thrusting configuration, a PPU, and a xenon fuel tank to be used with the thruster. Additionally, below these images is a schematic depicting a proposed configuration of the NEXT 9a ion thruster and its subcomponents.



Figure 7.3.7: NEXT 9a Ion Thruster (left), PPU (middle), & Xe Propellant Tank (right)

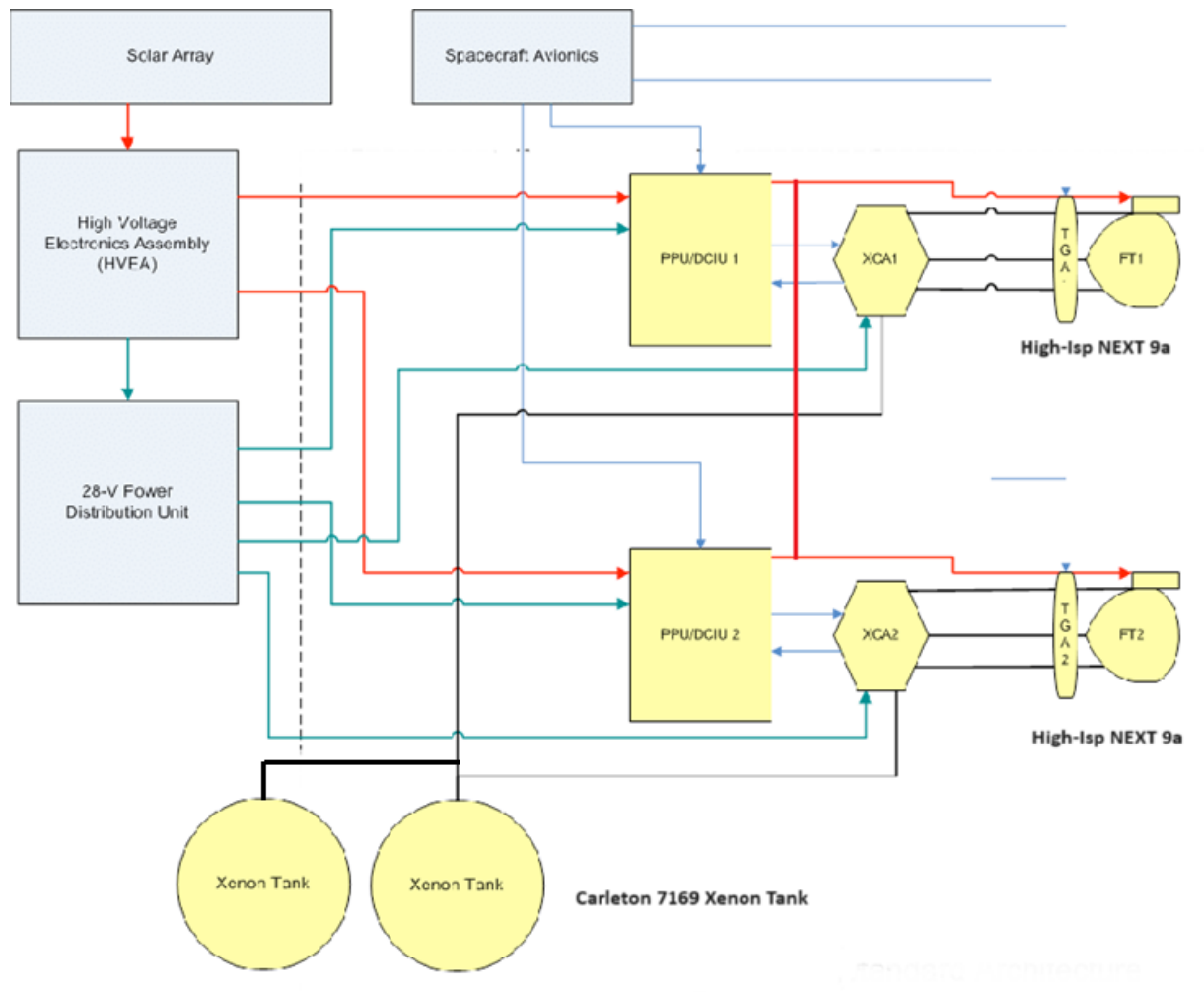


Figure 7.3.8: Proposed Propulsion System Configuration

7.3.4 - Risk Assessment

The NEXT 9a ion thruster recently achieved a TRL of 9 with the DART (Double Asteroid Redirection Test) mission, launched in late 2021 and executed in late 2022. Because this system is just recently flight-proven, to account for any unknown or unaccounted-for errors within the propulsion system, one additional NEXT 9a ion thruster and PPU are added to this spacecraft for redundancy. Additionally, having flown on the DAWN mission, the Carleton 7169 xenon fuel tank has a TRL of 9. These tanks coupled with a propellant contingency of 10% provide the MAYFLY mission with plenty of excess fuel to account for any trajectory or deep space adjustments throughout the mission.

7.4 - Power

7.4.1 - Power Summary

The Mayfly's power system is designed to operate for the duration of the mission, with power generation starting when the solar array is rolled out, just after separation from the launch vehicle, until the payload is released back to Earth. Several options for power production are available for spacecraft, including Radioisotope Thermoelectric Generators (RTGs), solar arrays, fission reactors, or hybrid systems.

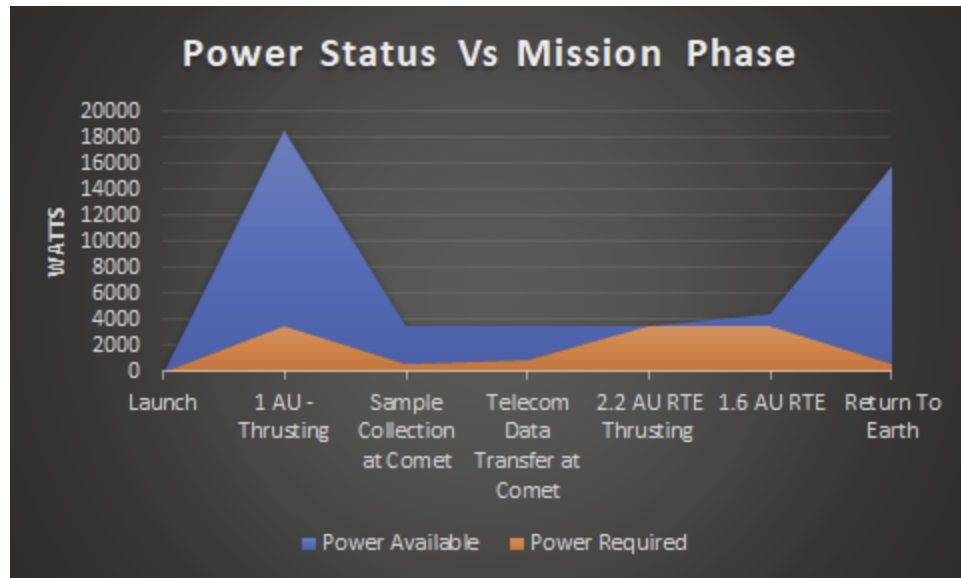


Figure 7.4.1: Mission Phase Power Requirements

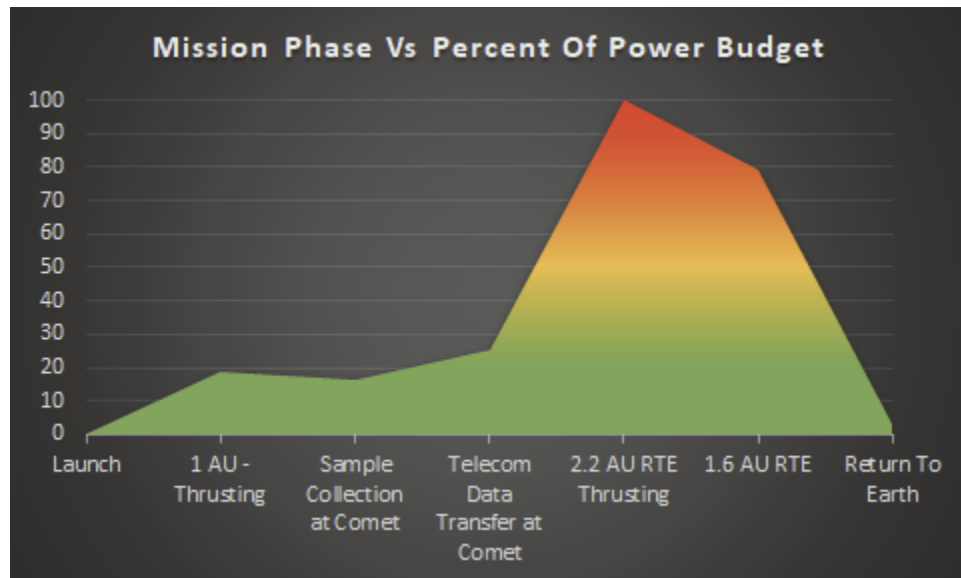


Figure 7.4.2: Power Budget Timeline

7.4.2 - Power Trade Study

An initial trade study was done to determine baseline characteristics of the different power generation options and is presented below.

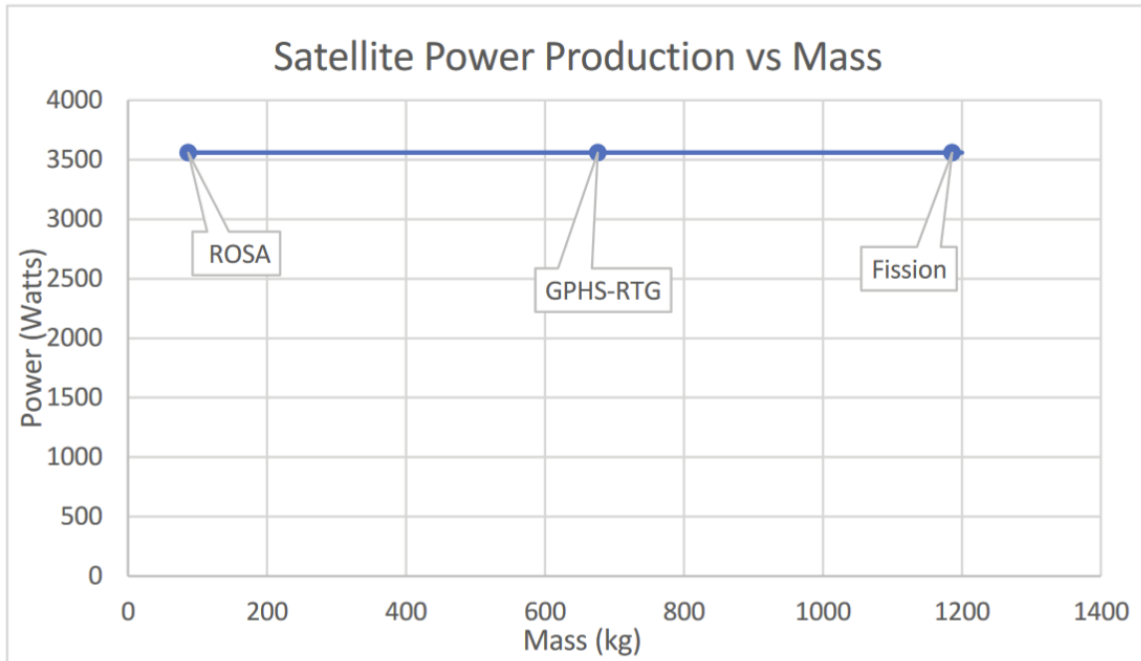


Figure 7.4.3: Power Generation Trade Study

For the Mayfly's relatively short-duration mission with an apogee at 2.2 AU, solar arrays are the best-suited power generation method. Other mission factors also narrow down the power generation method to solar arrays, including the Mayfly's compact size and small weight constraints. Additionally, the wattage required to power electric propulsion systems would necessitate increased complexity with RTG power, as 12 RTGs would be required to produce enough power for the spacecraft. Fission reactors were quickly excluded because their mass exceeds the total mass target of the spacecraft, and the heat they produce would require excessive cooling infrastructure.

7.4.3 - Solar Array

Originally, Rocket Lab Z4J+ cells were specified for the solar array due to their class-leading power efficiency. However, it was discovered that there were issues with this cell in

flight, so the alternative Roll Out Solar Array manufactured by Redwire Space was chosen as a replacement. Primary considerations for the choice in solar array were configurability, stowability, and power density. Configurability was important to closely match the power demands of the spacecraft without adding excessive weight. Stowability was crucial to achieve a compact volume that fits under the fairing of the launch vehicle. Finally, power density was crucial to achieving the 1000 kg weight goal of the spacecraft since the array must be oversized to produce enough power, as the solar irradiance at apogee is only about 22% of the irradiance at Earth. The Roll Out Solar Array has been in use on the International Space Station since 2021.

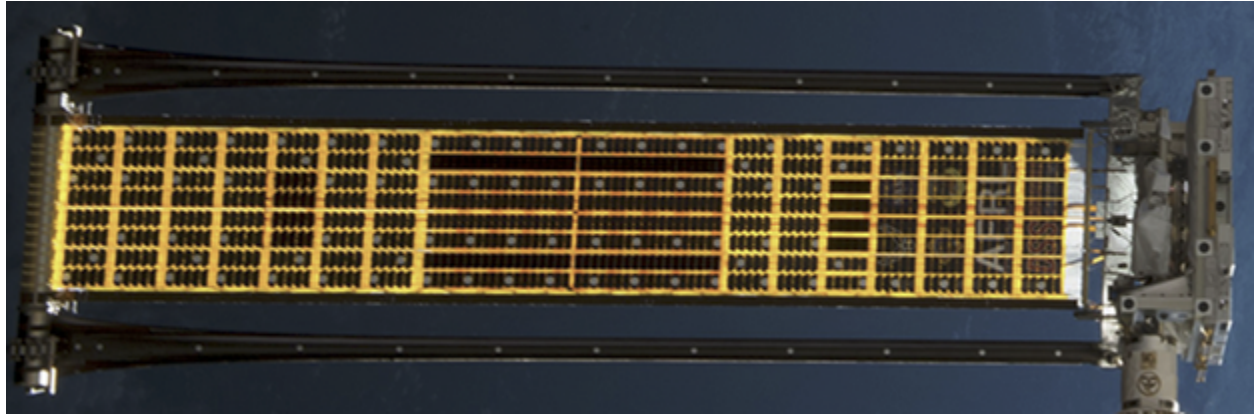


Figure 7.4.4: Rosa Array

Array sizing was determined with the formulas:

$$PI_{Apogee} = \frac{S_{flux} * \eta_{array} * \eta_{conversion}}{R^2} * Degradation^{Yrs Elapsed} \quad (2)$$

$$Area = \frac{P_{Safe\ Mode}}{PI_{Apogee}} \quad (3)$$

$$Mass_{Array} = \frac{PI_{Perigee}}{E_{specific}} \quad (4)$$

7.4.4 - Battery

The backup battery is configured for a safe mode that powers communications, attitude control, and electric heaters. Initially designed for 24 hours of safe mode operation without any power generation from the solar array—an unlikely case as there is no expected eclipse time during the mission—it would provide ample troubleshooting time if a problem arose. The batteries chosen were the LG Chemical MJ1 Lithium-Ion 18650-sized cells for their modularity, high specific energy, and efficiency. Lithium-ion batteries have become the standard power storage chemistry across most industries and are now becoming more prevalent in aerospace. The individual cells are rated for a maximum discharge current of 10 amps and a capacity of 3500 milliamp hours. Independent testing has shown 11-12 watt-hours of capacity, so a conservative 10 watt-hours per cell was considered for capacity design. The lightweight cells weigh 45 grams each.



Figure 7.4.5: LG MJ1 cells

| Item | Condition / Note | Specification |
|--|--|--|
| 2.1 Energy | Std. charge / discharge | Nominal 3500 mAh Minimum 3400 mAh |
| 2.2 Nominal Voltage | Average | 3.635V |
| 2.3 Standard Charge (Refer to 4.1.1) | Constant current Constant voltage End current(Cut off) | 0.5C (1700mA) 4.2V 50mA |
| 2.4 Max. Charge Voltage | | 4.2 ± 0.05V |
| 2.5 Max. Charge Current | | 1.0 C (3400mA) |
| 2.6 Standard Discharge (Refer to 4.1.2) | Constant current End voltage(Cut off) | 0.2C (680mA) 2.5V |
| 2.7 Max. Discharge Current | | 10A |
| 2.8 Weight | Approx. | Max. 49.0 g |
| 2.9 Operating Temperature | Charge Discharge | 0 ~ 45°C -20 ~ 60°C |
| 2.10 Storage Temperature (for shipping state) | 1 month 3 month 1 year | -20 ~ 60°C -20 ~ 45°C -20 ~ 20°C |

Table 7.4.6: MJ1 Specifications

A 2-module battery pack was designed, with each module configured as 12 x 73 cells, for a total of 1752 cells with a capacity of 17,024 watt-hours. As some thermal design factors changed, requiring more power for the electric heaters, the decision was made to stick with the battery pack that was initially sized to optimize safe mode time without adding any additional mass to the bus. This thermal power draw change resulted in 17 hours of safe mode operation, limiting the depth of discharge to 80 percent. In the event that more safe mode operation was necessary, an additional 2 hours of capacity can be utilized with 100 percent depth of discharge. Because the power draw of electric propulsion is so high, primary propulsion thrusting is not allowable during safe mode. The cells chosen have been evaluated for use on NASA's PACE mission, and to the best of our knowledge, were launched on the spacecraft on 8 February 2024.

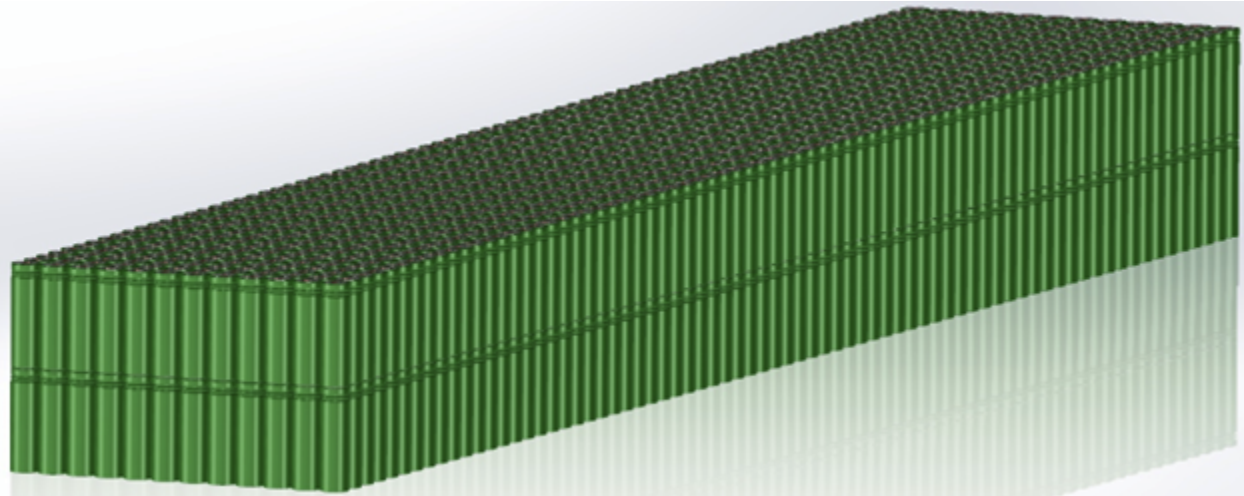


Figure 7.4.7: 18650 Battery Pack

| | |
|------------------------|---------------------|
| Solar Array Area | 83 m ² |
| Solar Array Mass | 86.87 kg |
| Battery Cells Required | 1752 |
| Battery Volume | 0.03 m ³ |
| Battery Mass | 76.61 kg |

Table 7.4.8: Component Specifications

Battery sizing was determined with the equations:

$$E_{req} = \frac{P_{emgcy} * Usage\ Hours}{\eta DOD} \quad (5)$$

$$N_{cells} = \frac{E_{req}}{Capacity_{cell}} \quad (6)$$

with a conservative transmission efficiency (of 0.85. The depth of discharge was specified to be 80%, with the expectation that the batteries are not anticipated to undergo many cycles, and they would retain a reserve capacity of 20% if the need arose.

7.4.5 – Power Distribution and Conditioning Unit

The Power Distribution and Conditioning Unit (PDCU) had several constraints that dictated unit selection. The primary concern was finding a unit that could support 3 kilowatts of constant power on the main bus for the electric propulsion system while retaining the capacity to supply power to secondary buses for the onboard computer, science instruments, payload, and electric heaters. The Airbus PSR 100V MkII PDCU was chosen for Mayfly's application. The

unit is 2-fault tolerant on the secondary power buses, has extensive flight heritage with 30 units being placed in spaceflight and 30 years in orbit around Earth. The PDCU also offers the benefits of dual voltage secondary buses and a power distribution capacity that is nearly twice Mayfly's mission requirements. Additionally, the PDCU boasts a 98.8% solar conversion rate and can manage 2 batteries, charging them at 20 amps. Finally, the PDCU is relatively lightweight at 31 kg, contributing to the goal of keeping Mayfly's dry mass under 1000 kg.



Figure 7.4.9: Airbus PSR 100V MkII

7.5 - Communications

7.5.1 Communications Overview

The communications subsystem is vital for maintaining a two-way communication link for transmitting and receiving information from the Earth ground stations and the spacecraft. It

acts as a bridge between Earth and the spacecraft for sending commands to the spacecraft while also offloading data collected from the mission back down to Earth.

While the ultimate goal is to establish a functioning two-way communication link, it is important to consider the design requirements and constraints imposed by the mission and spacecraft. First, it is a mission requirement to communicate with the 34 meter Deep Space Network (DSN) antenna network. Second, there is an upper bound on the bit error rate (BER) of one in one million to ensure that all of the data from one pass can be downlinked before the next pass. In addition to these requirements, the size of the components are also constrained by the size of the spacecraft. For example, the diameter of the high gain antenna must not exceed the length of the spacecraft. Also, the power consumption of the communication must be within the power production of the power subsystem. All of these factors play a vital role in determining the size, performance, and sustainability of the communication subsystem.

7.5.2 Hardware

The spacecraft is equipped with a 2.5 meter high gain antenna (HGA) for communication during normal operations. This design choice is to preserve heritage due to its technology readiness level (TRL) of TRL9 as proven on the JUNO mission. The spacecraft is also equipped with two 0.24 meter low gain antennas positioned on opposite sides of the spacecraft to maintain communication capabilities in all directions. Using these antennas, the communication will be conducted on the X-band radio frequency, which corresponds to a downlink frequency of 8420 MHz (spacecraft to Earth) and a uplink frequency of 7145 MHz (Earth to spacecraft).

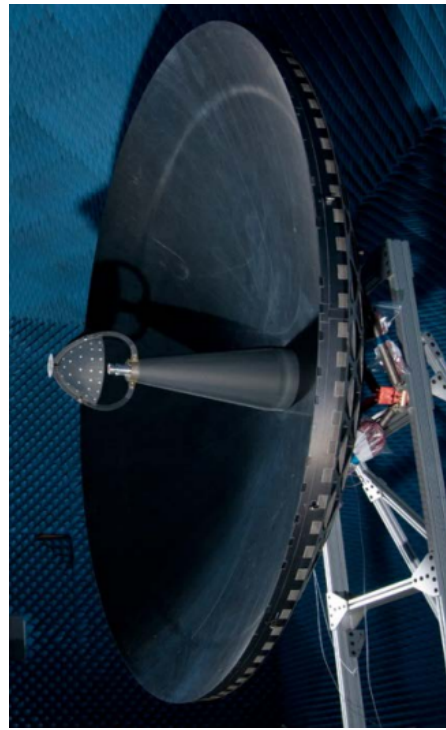


Figure 7.5.1. Juno 2.5 meter High Gain Antenna (Source: IEEE)



Figure 7.5.2. Juno Low Gain Antenna (Source: NASA)

On board the spacecraft, Mayfly has two small deep space transponders (SDST), which handles the transmitting and receiving of communications. The SDST that will be used on this mission will be sourced from the JUNO mission, which also has a TRL9 and demonstrated its mission capabilities. This SDST has the command rate capability of 4000 bps, but only 2000 bps when used operationally. It is also important to note that this SDST is capable of turbo encoding, which is essential for noise reduction in the safe mode downlink.



Figure 7.5.3. Juno Small Deep Space Transponder (SDST)

To amplify the output signal from Mayfly, two L3 X-band Traveling Wave Tube Amplifiers (TWTA) will be equipped on the spacecraft. Under the conditions of the mission, the TWTA will be operating at 165 W at 65% efficiency, which is the upper bound for the L3 X-band Traveling Wave Tube Amplifier. For this specific model, there are over 118 units in orbit currently, which have survived over 1.9 million on-orbit hours collectively. Due to its reliability and abundance in other spacecraft, it is safe to assume that the L3 X-band Traveling Wave Tube Amplifier has TRL9. For uplink communications from Earth, a Low Noise Amplifier (LNA) will be used to amplify those signals.



Figure 7.5.4. L3 X-band Traveling Wave Tube Amplifier

Besides the main critical components for the communication subsystem, components such as, the waveguide transfer switch, coax transfer switch, X-band diplexer, X-band isolator, hybrid coupler, coax cable, and WR-112 WG, unite the entire communication subsystem ensuring reliable two-way communication for this mission. The dippers ensure that the signals being transmitted or received are distinguished properly and relayed to the correct components. The waveguide switches serve as a three-way pathway at junction points to allow for redundancy and link multiple antennas to the same signal pathway. The cables ensure that the signals are routed to the necessary components in the communication subsystem, while minimizing the loss.

7.5.3 Band Choice

The two primary communication bands that will be considered for this mission are the X-band and Ka-band offered by the Deep Space Network (DSN) 34 meter antennas, located in California, Spain, and Australia. These strategic locations of the antenna ensure that at least one of them will be facing the spacecraft. The X-band frequency ranges between 8-12 GHz, while the 7.145-8 GHz frequency band is used for deep space communications. The advantages of the

X-band is that it has been extensively used for decades in deep space communications in missions such as JUNO, making it a well-understood and reliable option. The X-band signals also experience less attenuation due to the Earth's atmosphere and weather conditions compared to higher frequency bands. Given that the X-band has been used extensively for decades, there exists a vast infrastructure and equipment optimized for X-band communication. Some of the disadvantages are limited bandwidth and congestion. The lower frequency range offers less bandwidth, which can limit data transmission rates. In addition, X-band is more crowded with other users and applications, which could lead to potential interference issues.

The Ka-band frequency band ranges between 26.5-40 GHz, the 31.8-32.3 GHz frequency band is used for uplink and the 34.2-34.7 GHz is used for downlink in deep space communications. The advantages of the Ka-band include higher bandwidth and less congestion. Ka-band provides significantly more bandwidth compared to X-band, allowing for higher data transmission rates, which is crucial for missions requiring high-resolution data, such as imaging and scientific measurements. The Ka-band is also less crowded, reducing the likelihood of interference with other users and applications. The disadvantages of the Ka-band are higher atmospheric attenuation and less mature infrastructure. Ka-band signals are more susceptible to attenuation due to the Earth's atmosphere, especially under adverse weather conditions. Also, Ka-band technology is newer, and the infrastructure and equipment are not as mature or widespread as those for X-band.

Given this information on X-band and Ka-band and flight heritage data from missions like JUNO, the Mayfly mission will opt to use only the X-band for communication. The first reason for this choice is flight heritage. The X-band has proven and demonstrated flight reliability in deep space missions, like the JUNO mission. The second reason is that the DSN-34

architecture only uplinks to spacecraft on the X-band, which implies that X-band hardware will be necessary on the spacecraft. To limit confusion and extra design, it is wise to communicate strictly on the X-band. The third reason is that the total data rate of the instruments on board is around 83 kbps and with a data rate of 100 kbps, the spacecraft is able to offload data when it is facing the Earth. The Attitude and Control Subsystem has also optimized the spacecraft position so that it is able to offload 250 Gb (gigabit) of data in around 4 hours. Given the feasibility of this and the reasons above, the X-band is the best choice for the frequency band.

7.5.4 Simplified Block Diagram

The simplified block diagram for the spacecraft communication subsystem is shown below.

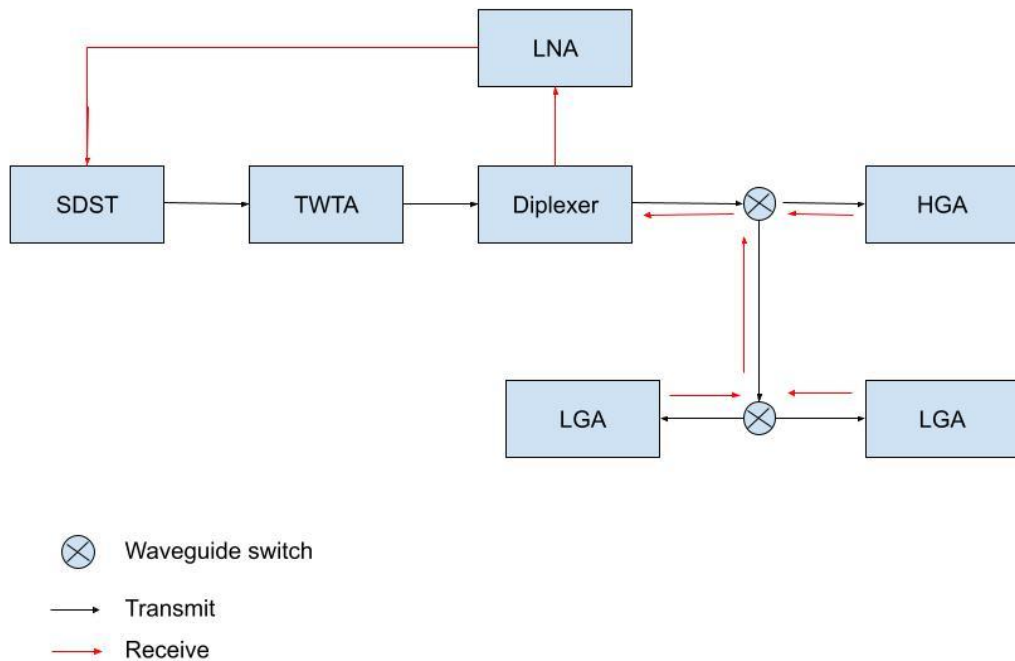


Figure 7.5.5. Simplified Communication Block Diagram

From the figure, it is important to note that this is half of the communication system. The purpose of the simplified block diagram is to help visualize the transmit and receive pathways. In

the actual communication system, there are redundant components, such as two TWTA, diplexers, low noise amplifiers (LNA), and small deep space transponders (SDST). During the transmitting process, the SDST first sends the data to the TWTA, where the signal is amplified. Next, the signal is sent to the diplexer, where it is routed to the appropriate antenna and broadcasted back to the DSN on Earth. During the receiving process, the signal is picked up by the antenna(s), and sent to the diplexer. From there, the signal is sent to the low noise amplifier, where the signal is amplified to a reasonable level. Finally, the signal is sent to the SDST, which interprets the message.

7.5.5 Noise Figures

Losses will naturally occur when the signal travels through a wire or passes one of the critical components mentioned before. Using these losses, a noise figure can be generated in order to determine the uplink values for the spacecraft communication with the DSN. From the spreadsheet, a total noise figure of 1.27 is calculated. Using the equation.

$$T_{eff} = T_o(F - 1) \quad (1)$$

the effective temperature is 78 K.

7.5.6 Link Performance

The detailed link performance calculations are shown in the linked sheet. The goal of the link performance analysis is to ensure that the gain of the necessary components exceed the losses from the components and mostly the free space propagation, which is related to the distance between the comet and Earth.

The downlink through the high gain antenna results in a gain of 45.3 dB on the 2.5 meter high gain antenna. The DSN-34 antenna has a gain of 68.1 dB overall. When downlinking data from the spacecraft to Earth, the majority of the loss comes from the free space propagation of the signal, which is around -283.5 dB. The system noise temperature is about 14.8 K, resulting in a signal to noise ratio of 22.7.

The uplink through the DSN to the high gain antenna results in a gain of 66.5 dB on the DSN antennas and has a similar free space propagation loss as the downlink. The signal to noise ratio for the uplink is around 3660.

The calculations for the safe mode communication link through the low gain antennas are the same as the calculations for the downlink and uplink through the high gain antennas with some exceptions. The most notable difference is that the data rate is reduced to 10 bps for both uplink and downlink. The second difference is that the low-gain antenna is much smaller than the high gain antenna with a diameter of 0.24 m compared to the 2.5 meter high gain antenna. The signal to noise ratio for downlink through the safe mode is 1380 and the signal to noise ratio for the uplink is 3890. The data rate, signal to noise ratio (SNR), energy per bit to noise power spectral density ratio (Eb/N0), and bit error rate (BER) are tabulated below.

Table 7.5.1. Communication Performance

| | Data Rate (bps) | SNR | Eb/N0 | BER |
|-----------------------|-----------------|------|-------|-----------|
| Downlink | 100000 | 22.7 | 11.3 | 9.86e-07 |
| Uplink | 1000 | 2700 | 1350 | 0 |
| Safe Mode Downlink | 10 | 1380 | 688 | 2.57e-301 |
| Safe Mode Uplink | 10 | 3890 | 1940 | 0 |

As shown in the table above, the BER condition of less than 1e-6 is satisfied as all the values are below this upper bound. Under normal conditions, the data is downlinked with a data rate of 100000 bps with a BER of 9.87e-07 which is below the upper bound of 1e-6. Under the same normal conditions, the data is uplinked with a data rate of 1000 bps with a BER of 0, which is below the upper bound of 1e-6. Under the safe mode conditions, the data is downlinked with 10 bps, resulting in a BER of 2.57e-301. Under the safe mode conditions, the data is uplinked with 10 bps, resulting in a BER of 0. In both safe mode and normal conditions, the TWTA is assumed to be operating at 165 W.

The power required by the communication subsystem will vary throughout the journey of the mission. When the spacecraft is at launch, at 1 AU from the Earth, and during sample collection at the comet, the power required by the spacecraft is 10 W. While the spacecraft is at the comet performing telecom data transfer and during safe mode operations, the power required by the spacecraft is 282.25 W, which comes from the 65% efficiency of the 165 W TWTA plus an additional 10 W.

7.6 - Attitude Control System (ACS)

For this mission, we assume that the disturbances acting on the spacecraft occur in 3 main phases. The first is when the spacecraft is around the Earth or 1 AU from the sun. The second phase occurs in the midpoint of the line between Earth and the asteroid we are aiming to probe. The asteroid is around 2.2 AU away from the sun so we can assume that the spacecraft is at around 1.6 AU for this phase. Finally our final phase is at the asteroid which is at a distance 2.2 AU from the sun. We note that solar pressure affects our spacecraft at all distances in our mission, but gravity gradient only plays a role at 1 AU or when the spacecraft is around the sun.

Here are some metrics for the physical properties of our spacecraft that were used in our ACS design.

Table 7.6.1:

| Properties | magnitude | units |
|----------------------------|-----------|------------------------------|
| Solar arrays' Frontal Area | 1.25 | m^2 |
| I_x | 556 | $\text{kg} \cdot \text{m}^2$ |
| I_y | 4842 | $\text{kg} \cdot \text{m}^2$ |
| I_z | 4829 | $\text{kg} \cdot \text{m}^2$ |
| Reflectance factor, q | .9 | |
| μ | 3.99E+14 | m^3/s^2 |
| r | 6300000 | m |
| Solar Intensity at Earth | 1380 | W/m^2 |

Table 1: Physical Constants

Through these values we can calculate the disturbances on our spacecraft at 3 distinct locations on our journey. We only care about the gravity gradient in the first case when our spacecraft is near Earth, and the rest of the disturbances are from solar pressure. We can find the magnitude of solar pressure at a given location by dividing the solar intensity by the speed of light. Solar intensity at variable distance is a function of the inverse square law which can be found quickly by dividing the solar intensity at Earth by the distance from the sun in AU squared. The formulas to calculate solar pressure and gravity gradient are given to be Eq 1 and Eq 2 respectively.

$$Ts = (1 + q) * Ps * Asc * \cos(\theta) * L \quad (1)$$

Where Ts is the solar torque, q is the reflectance factor, Ps is the solar pressure, Asc is the frontal area of the spacecraft, theta is the angle between the incoming light rays and the normal vector of the area, and L is the moment arm found by the difference between center of gravity and center of pressure.

$$Tg = ((3 * \mu) * |Iz - Iy| * \sin(2\theta)) / (2r^3) \quad (2)$$

Where Tg is the gravity gradient torque, μ is the gravitational constant of Earth equal to GM, r is the radial distance from the center of the Earth to the COM of the spacecraft, Iz and Iy are moments of inertia in the z and y directions respectively and theta is Euler angle.

Table 7.6.2:

| Disturbances | Magnitude | Units |
|--------------------------|-----------|-------|
| Solar Torque at 1 AU | 1.84E-06 | Nm |
| Gravity Gradient at 1 AU | 3.11E-05 | Nm |
| Solar Torque at 1.6 AU | 1.15E-06 | Nm |
| Solar Torque at 2.2 AU | 4.59E-07 | Nm |

Table 7.6.2: Disturbance Torques

Angular Momentum of the disturbance depends on the duration of the disturbance and the magnitude of the disturbance.

$$\text{Angular Momentum} = \text{Torque} * \text{Time}$$

Table 7.6.3

| Disturbance | Time | Angular Momentum (Nms) |
|-------------|---------------------------------|------------------------|
| At 1 AU | 2 weeks or 1209600 seconds | 39.8 |
| At 1.6 AU | 9.75 years or 307476000 seconds | 353 |
| At 2.2 AU | 2 months or 5184000 seconds | 2.38 |

Table 7.6.3: Angular momentum of the disturbance

During our mission, we need to orient the spacecraft to Earth in order to do data uplink and downlink for parameters such as spacecraft condition, data collection, and trajectory analysis. We also need to orient the spacecraft at our comet so that our instruments can collect data from the surface of the comet. The term for this reorientation is “slew”. We can find the torque necessary for a slew and the momentum that is built from the following formulas.

$$Tslew = (4 * Iy * \Delta\theta) / (\Delta t)^2 \quad (3)$$

Where $Tslew$ is the amount of torque needed for a slew. Iy is the moment of inertia in the y axis. $\Delta\Theta$ is the change in angle orientation associated with a slew and Δt is the time needed for the slew.

$$Mslew = Tslew * \Delta t \quad (4)$$

Where M_{slew} is the momentum built up from slew, T_{slew} is the amount of torque needed for a slew and Δt is the time needed for the slew.

For a single slew during cruise, we can assume the following

$$\Delta\Theta = 90 \text{ degrees or } \pi/2 \text{ radians}, \quad I_y = 4842 \text{ kgm}^2, \quad \Delta t = 10 \text{ mins or } 600 \text{ seconds}$$

This gives us a momentum build up of 101 Nms through Eq 3 and 4.

Note: This number is doubled due to the fact that we reorientate our spacecraft back to the original direction it was pointing.

The momentum build up of 101 Nms is valid for pointing our spacecraft back to the direction of Earth during both cruise and while at the comet.

We use the 101 Nms momentum to determine our overall momentum generated both during cruise and while at the comet. 101 Nms is the momentum generated for one slew so we must know how many times we slewed during the course of our mission. Since our mission timeline is 10 years, around 9 years and 10 months is spent on cruise, which can be equated to being 508 weeks. If we assume we slew once a week that gives 508 slews during cruise. Finally at the comet we need to send more data which increases the frequency of our slews. Even though we spend only 60 days at the comet, I chose to downlink 3 times a day so 180 slews which should provide ample time to send the data.

Finally at the comet, we must use our instruments to gather the necessary data. Assuming that we obtain 250 Gb of data from the surface of the comet, we can obtain a time needed from the slew by dividing 250 Gb by the bit rate and number of slews. For this data collection portion of the mission, we have a

$$\Delta t = 250Gb/(100kbs * 180) = 3.85 \text{ hrs or } 13860 \text{ seconds}$$

So for a slew for data collection:

$$\Delta\Theta=360 \text{ degrees or } 2\pi \text{ radians}, \quad I_y=4842 \text{ kg*m}^2, \quad \Delta t=3.85 \text{ hrs or } 13860 \text{ seconds}$$

The momentum build up is approximately: 8.8 NM through Eq 3 and 4

The calculated momentum build up at different portions of our trip are as follows:. We found this by taking our slew momentum and multiplying it by number of slews

Table 7.6.4

| Variety of Slew | Magnitude | Units |
|--------------------------|-----------|-------|
| Earth Downlink at Cruise | 51515 | Nms |
| Data Collection at Comet | 18253 | Nms |
| Earth Downlink at Comet | 1580 | Nms |

Table 7.6.4: Angular Momentum build up

Now we will cover what is needed from our momentum wheels and hydrazine thrusters to ensure that the mission goes smoothly. For this mission we chose the Goodrich, Ithaco TW-45C250, 45 Nms @ 4500 rpm. This means that we have momentum storage capability of around 45 Nms. From figure 4 we have the total momentum accumulation. From this we can calculate the number of momentum dumps needed as well as the momentum accumulation time.

$$MAT = Mrw/Tslew \tag{5}$$

Here MAT is the momentum accumulation time and Mrw and Tslew are the momentum of the reaction wheel and torque of the slew respectively.

$$\# \text{ dumps} = M_{\text{slew}} / M_{\text{rw}} \quad (6)$$

here # dumps indicate how many times the reaction wheel must accumulate its maximum angular momentum to effectively point our spacecraft in the right direction.

Table 7.6.5

| Type of Slew | Number of Dumps | Momentum Accumulation Time |
|----------------------------------|-----------------|----------------------------|
| Total Disturbances on Spacecraft | 9 | 15.1 days |
| Downlink at Cruise | 1145 | .15 hours |
| Downlink at Comet | 406 | .15 hours |
| Data Collection at Comet | 36 | .82 days |

Table 7.6.5: Number of Dumps and Momentum Accumulation Time

Note the momentum accumulation time at the comet is for 180 downlinks in order to ensure that we get all the necessary data out.

In order to negate the momentum built up in our reaction wheels, we must use the thrusters associated with the ACS system on the probe. The main problem we have is that we must determine how much of our propellant we must bring in order to satisfy all of our mission requirements. In the first part of this section regarding the ACS thrusters, we will find how much propellant mass we need for reorientation and rotational changes. The duty of moving the spacecraft with its sample retrieval apparatus onto the surface of the comet from our parking orbit and back off of the comet also falls on the ACS thrusters. To find this needed propellant

mass ratio we can use the rocket equation given a particular delta v for landing on the comet, and also for another delta v to escape the comet. Using these two mass ratios found from the rocket equation, and accounting for the propellant mass needed to do reorientation/rotational changes during both the cruise to and back from the comet we can find the overall propellant mass necessary.

$$t_{burn} = Mrw / (T_{thruster} - T_{slew}) \quad (7)$$

Where t_{burn} is the time the thruster must be on to desaturate the reaction wheel, MRW is the angular momentum stored on the reaction wheel and $T_{thruster}$, T_{slew} are the torques of the thruster and the slew torques for each variety of slew. After calculating total burn time we get a value of 143 seconds. We can break this value up into 72 seconds of burn for reorientations going to the comet and 72 seconds for orienting on the way back to Earth

Finally, the mass of hydrazine needed to rotational changes can be given by

$$m_{hydrazine} = 2 * flowrate * t_{burn} * \#dumps \quad (8)$$

Where $m_{hydrazine}$ is the mass of hydrazine needed to point the spacecraft in the right direction. Flowrate, is the mass flow rate of the thruster which can be calculated from Isp. t_{burn} is the time the thruster must be on to desaturate the reaction wheel. Finally # dumps is how many times the reaction wheel has to store its maximum angular momentum. We assume an equal number of dumps on the way to and from the comet. When we do the calculations we get a mass of hydrazine for reorientations of 50.7 kg on the way to the comet and 50.7 kg on the way back

In order to calculate the overall propellant we need we must consider 2 different delta v rocket equations. The first is for landing the spacecraft on the surface of the comet which has a delta v

of approximately 5 m/s. The second is for allowing the spacecraft to escape the comet's gravity and this has a delta v value of .25 m/s.

$$\Delta v = Isp * g * \ln(m_i/m_f) \quad (9)$$

Where delta v is the needed speed to perform an orbit change, Isp is the specific impulse, g is the gravitational constant of earth or 9.8 m/s/s. Finally m initial is the mass of the spacecraft before the maneuver and mfinal is the mass of the spacecraft after the maneuver. For this calculation we will label 3 different mass values. The first is the mass of the spacecraft with its propellant before it does the orbit maneuver of landing or m1. The second is the mass of the spacecraft on the surface of the comet or m2. Finally we have the weight of the comet as it leaves the comet or m3. M3 is the amalgamation of the dry mass added with the propellant needed to reorientate the spacecraft on the way back to Earth. M3 then is 1210 kg+50.7 kg or 1260 kg. From the equation above we get a m2 of around 1260 kg. Finally we use the equation above again to find m1. When we do the calculation we get a value of 1260 kg wet when the spacecraft is about to do its landing maneuver. We subtract the dry mass from the wet mass to get to total fuel needed for orbital maneuvers or 53.6 kg. Finally we add the mass of propellant needed for reorientation for the cruise to the comet which is 50.7 kg. We get a needed propellant mass of 104 kg.

Table 7.6.6

| | Wet mass | Propellant mass |
|----|----------|-----------------|
| m3 | 1260 | 50 |
| m2 | 1260 | 50 |

| | | |
|----|--------|------|
| m1 | 1263.6 | 53.6 |
| m0 | 1314 | 104 |

Table 7.6.6: Propellant Mass Values

Finally we need a method to figure out the current location and orientation of the spacecraft at any given time during our mission. To do this, we use Kearfott IMU, VST-68M star trackers and Coarse sun sensor. The IMU uses accelerometers and gyroscopes to figure out the linear and angular acceleration of the spacecraft and uses kinematics to solve for the current position or orientation. The problem is that the device can only be precise up to a certain threshold. Since the IMU does not take any data input the resultant location and orientation will grow more and more inaccurate as time goes on. The IMU has a mass of 3.5 kg and we use 2 for redundancy. The other devices, the star tracker and sun sensor, use solar rays from the sun and stars with a known location to figure out orientation and location. Since there is a data input we can use these devices to ensure good results for our location and orientation determination. We use 2 star trackers with a weight of .47 kg each and 8 sun sensors with a weight of .215 kg each. Overall we have a mass of around 12 kg to determine orientation and location. Finally, we have a power draw of 54 Watts for the entire ACS subsystem.

Note: All of equations 1-9 were found in SMAD, cited in bibliography at the end

7.7 - Structures

7.7.1 - Structures Summary

There are several aspects and goals that the structures subsystem must meet, including minimizing the structural mass and ensuring the structural reliability while integrating all components for a successful mission. A trade study was conducted to determine the material used for the primary structure where we eventually decided to use a honeycomb structure with aluminum core and carbon fiber facesheet. A majority of our structural components have a TRL 9 since they have been utilized on previous missions, and if they had to be manufactured, as is the case with the primary cube-like structure of our spacecraft, they were modeled to take a similar form to previously successful spacecrafts for the highest probability of success. In terms of structural analysis, a first order frequency study in Solidworks was analyzed to ensure the primary structure could handle the vibrations experienced during a Falcon 9 launch.

7.7.2 - Spacecraft Bus Design

The spacecraft bus design gained inspiration from several spacecrafts, namely Hayabusa2 for the cube-like primary structure and DAWN for the cylindrical xenon propellant tank housing. The first task was to determine what material the primary structure walls would be made of. Considering the most common metals for aerospace systems, that is, tungsten, titanium, and aluminum [1], we came to the conclusion that because of aluminum's high strength-to-weight ratio the goal of minimizing weight while ensuring structural integrity could be met. In terms of the specific alloy, 6061, 2024, and 7075 aluminum alloy are commonly used for different aerospace structures; however, because the main concern of the primary structure is not breaking

under the severe loads during launch, 7075 aluminum alloy was chosen for its higher hardness and strength.

| Aluminum Alloy | Density (kg/m ³) | Ultimate Tensile Strength (psi) |
|----------------|------------------------------|---------------------------------|
| 7075 | 2810 | 76,000 |
| 2024 | 2780 | 64,000 |
| 6061 | 2700 | 42,000 |

Table 7.7.1: Comparison of Common Aluminum Alloy Densities [2], [3], [4]

As seen in Table 7.7.1, although 7075 aluminum alloy has the largest density, and thus, weighs the most, the ultimate tensile strength is also much larger. Fortunately, since aluminum has relatively the same properties in tension and compression, 7075 aluminum alloy will also be strong in compression, which is important to sustain the loads the spacecraft will experience during launch.

Despite the positives in terms of strength, determining the weight required for a 1.4 m x 1.5 m x 1.6 m spacecraft with 0.1 m thick walls comes out to be 757.6 kg, which is clearly undesirable. That said, honeycomb panels are particularly attractive for the high strength to weight ratio as well as the stiffness to weight ratio.

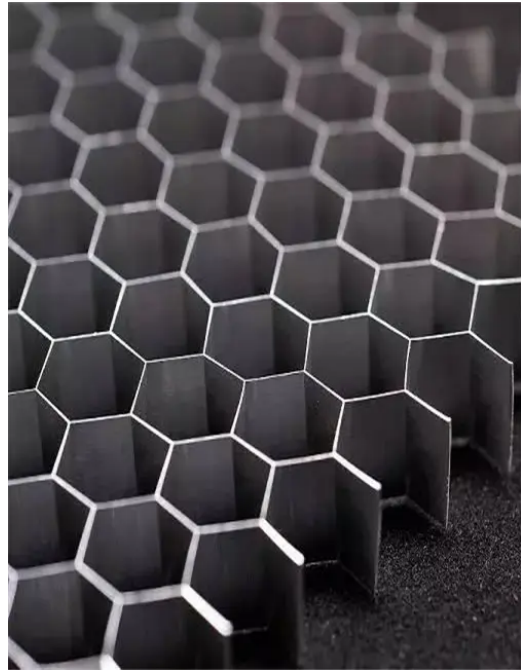


Figure 7.7.1: Aluminum honeycomb core [9]

While there are other types of core materials for a honeycomb structure, such as Nomex, we decided to stick with aluminum for its high strength and rigidity compared to Nomex's core ability to be deformable and lightweight. With this decision solidified, totally primary structural weight can be calculated starting with the dimensions of the primary cube-like structure, the density of aluminum 7075, which was 2810 kg/m^3 , the density of t800 carbon fiber, which was 1800 kg/m^3 [6], the core thickness of 0.005 m, core wall thickness of 0.001 m, and the facesheet thickness of 0.0025 m, which there are two.

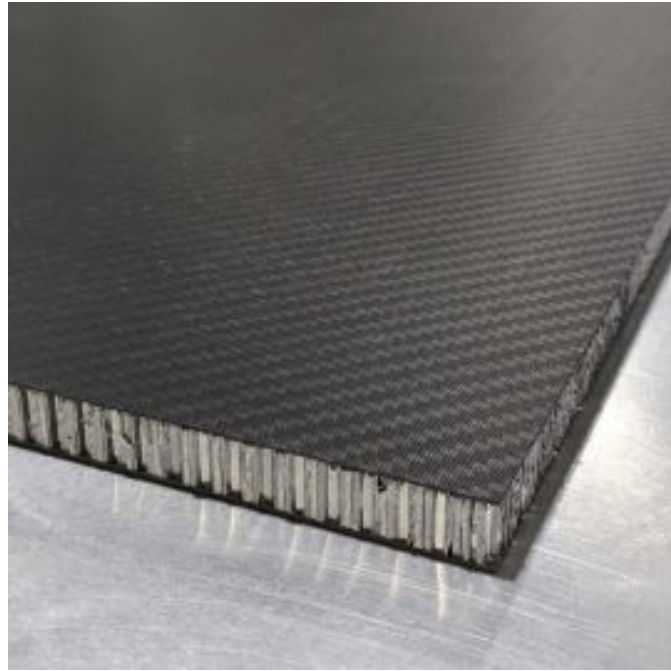


Figure 7.7.2: Complete honeycomb structure [10]

To begin, the area of a solid 2D honeycomb was calculated through the following equation:

$$A_{c,p} = \frac{3\sqrt{3}}{3} * h_{c,p}^2 \quad (1)$$

where h is the core wall length, which was defined to be the same dimension as the core thickness. Thus, the calculated area was:

$$A_{c,p} = \frac{3\sqrt{3}}{3} * (0.005 m)^2 \quad (2)$$

$$A_{c,p} = 4.3 \times 10^{-5} m^2 \quad (3)$$

Then, based on the total surface area of the cube-like primary structure, the total number of honeycombs can be calculated:

$$A_p = 2(l * w) + 2(w * h) + 2(h * l) \quad (4)$$

$$A_p = 13.48 m^2 \quad (5)$$

$$\# \text{ of honeycomb} = \frac{A_p}{A} = 313488 \quad (6)$$

From here, the equation for the core wall area for a single honeycomb was found and computed through the following:

$$A_{w,p} = 0.866 t_{cw,p}^2 + 1.861 \sqrt{A} * t_{cw,p} \quad (7)$$

where $t_{cw,p}$ is the honeycomb wall thickness and $A_{c,p}$ is the area of a solid honeycomb. Then,

$$A_{w,p} = 0.866(0.001 m)^2 + 1.861 \sqrt{4.3 * 10^{-5} m^2} * 0.001 m \quad (8)$$

$$A_{w,p} = 1.307 * 10^{-5} m^2 \quad (9)$$

Then the total core area, $A_{tc,p}$, the total core volume, $V_{tc,p}$, and the total core mass, $m_{tc,p}$, can be calculated:

$$A_{tc,p} = A_{w,p} * \# \text{ of honeycomb} \quad (10)$$

$$A_{tc,p} = 1.307 * 10^{-5} m^2 * 313488 \quad (11)$$

$$A_{tc,p} = 4.0973 m^2 \quad (12)$$

$$V_{tc,p} = A_{tc,p} * t_{c,p} \quad (13)$$

$$V_{tc,p} = 4.0973 m^2 * 0.005 m \quad (14)$$

$$V_{tc,p} = 0.02049 m^3 \quad (15)$$

$$m_{tc,p} = V_{tc,p} * \rho_{Al} \quad (16)$$

where ρ_{Al} is the density of aluminum. Thus,

$$m_{tc,p} = 0.02049 m^3 * 2810 \frac{kg}{m^3} \quad (17)$$

$$m_{tc,p} = 57.58 kg \quad (18)$$

The total facesheet volume, $V_{tf,p}$, and the total facesheet mass, $m_{tf,p}$ can be calculated using a similar process.

$$V_{tf,p} = 2 * A_s * t_f \quad (19)$$

where t_f is the facesheet thickness for the cube-like primary structure.

$$V_{tf,p} = 2 * 13.48 m^2 * 0.0025 m \quad (20)$$

$$V_{tf,p} = 0.0674 m^3 \quad (21)$$

$$m_{tf,p} = V_{tf,p} * \rho_{CF} \quad (22)$$

$$m_{tf,p} = 0.0674 m^3 * 1800 \frac{kg}{m^3} \quad (23)$$

$$m_{tf,p} = 80.88 kg \quad (24)$$

Summing these two material weight, we get a total weight for the primary structure:

$$m_{t,p} = m_{tf,p} + m_{tc,p} \quad (25)$$

$$m_{t,p} = 80.88 kg + 57.58 kg \quad (26)$$

$$m_t = 138.5 kg \quad (27)$$

Moreover, because the decision was made to manufacture the cylindrical xenon propellant tank housing with carbon fiber - aluminum honeycomb, a similar process can be carried out to determine the structural weight. A concept that was previously flown on DAWN, this structure helps maintain the center of mass while providing protection for one of the most fragile and critical components to the mission.



Figure 7.7.3: DAWN spacecraft's core graphite cylinder

Because the total thickness was 0.01 m where the core thickness was 0.005 m and the facesheets were 0.0025 m each, the inner, d_i , and outer, d_o , diameters were 0.904 m and 0.924 m, respectively, to account for the diameter of the xenon propellant tanks and the height, h_c , was 1.3462 m to account for the two xenon propellant tanks stacked on top of each other. That said, the total area, A_c , can be calculated through the following:

$$A_c = 2\pi h_c \left(\left(\frac{d_o}{2} \right) + \left(\frac{d_i}{2} \right) \right) + 2\pi * \left(\left(\frac{d_o}{2} \right)^2 - \left(\frac{d_i}{2} \right)^2 \right) \quad (28)$$

$$A_c = 2\pi(1.3462 \text{ m}) \left(\left(\frac{0.924 \text{ m}}{2} \right) + \left(\frac{0.904 \text{ m}}{2} \right) \right) + 2\pi * \left(\left(\frac{0.924 \text{ m}}{2} \right)^2 - \left(\frac{0.904 \text{ m}}{2} \right)^2 \right) \quad (29)$$

$$A_c = 5.25 \text{ m}^2 \quad (30)$$

From here, you can calculate the area of a solid honeycomb:

$$A_{c,c} = \frac{3\sqrt{3}}{3} * h_{c,c}^2 \quad (31)$$

$$A_{c,c} = \frac{3\sqrt{3}}{3} * (1.3462 m)^2 \quad (32)$$

$$A_{c,c} = 4.3 * 10^{-5} m^2 \quad (33)$$

Then, based on the total area of the cylindrical housing, the total number of honeycombs can be calculated:

$$\# \text{ of honeycomb} = \frac{A_c}{A} = 122133 \quad (34)$$

From here, the equation for the core wall area for a single honeycomb was found and computed through the following:

$$A_{w,c} = 0.866 t_{cw,c}^2 + 1.861 \sqrt{A_c} * t_{cw,c} \quad (35)$$

where $t_{cw,c}$ is the honeycomb wall thickness for the cylindrical housing and $A_{w,c}$ is the area of a solid honeycomb. Then,

$$A_{w,c} = 0.866(0.001 m)^2 + 1.861 \sqrt{4.3 * 10^{-5} m^2} * 0.001 m \quad (36)$$

$$A_{w,c} = 1.307 * 10^{-5} \quad (37)$$

Then the total core area, $A_{tc,c}$, the total core volume, $V_{tc,c}$, and the total core mass, $m_{tc,c}$, can be calculated:

$$A_{tc,c} = A_{w,c} * \# \text{ of honeycomb} \quad (38)$$

$$A_{tc,c} = 1.307 * 10^{-5} m^2 * 122133 \quad (39)$$

$$A_{tc,c} = 1.5963 m^2 \quad (40)$$

$$V_{tc,c} = A_{tc,c} * t_{c,c} \quad (41)$$

where $t_{c,c}$ is the core thickness. Therefore,

$$V_{tc,c} = 1.5963 m^2 * 0.005 m \quad (42)$$

$$V_{tc,c} = 7.98 * 10^{-3} m^2 \quad (43)$$

$$m_{tc,c} = V_{tc,c} * \rho_{Al} \quad (44)$$

where ρ_{Al} is the density of aluminum. Thus,

$$m_{tc,c} = 7.98 * 10^{-3} m^2 * 2810 \frac{kg}{m^3} \quad (45)$$

$$m_{tc,c} = 22.43 kg \quad (46)$$

The total facesheet volume, $V_{tf,c}$, and the total facesheet mass, $m_{tf,c}$ can be calculated using a similar process.

$$V_{tf,c} = 2 * A_s * t_{f,c} \quad (47)$$

where $t_{f,c}$ is the facesheet thickness for the cylindrical housing.

$$V_{tf,c} = 2 * 5.25 m^2 * 0.0025 m \quad (48)$$

$$V_{tf,c} = 0.0263 m^3 \quad (49)$$

$$m_{tf,c} = V_{tf,c} * \rho_{CF} \quad (50)$$

$$m_{tf,c} = 0.0263 m^3 * 1800 \frac{kg}{m^3} \quad (51)$$

$$m_{tf,c} = 31.51 kg \quad (52)$$

Summing these two material weight, we get a total weight for the primary structure:

$$m_t = m_{tf,c} + m_{tc,c} \quad (53)$$

$$m_{t,c} = 31.51 kg + 22.43 kg \quad (54)$$

$$m_{t,c} = 53.9 \text{ kg} \quad (55)$$

Two additional components that are integral to the spacecraft are the solar array booms and the payload fairing adapter. The Roll Out Solar Array (ROSA) Innovative Composite Booms produce significant deployment force to become ROSA's primary structure; thus, no motors or mechanisms are required. Moreover, the Falcon Heavy payload fairing adapter provided by SpaceX to ensure the spacecraft remains properly aligned and stable through launch is necessary to secure the spacecraft to the payload fairing.

7.7.3 - Spacecraft Structural Properties

One important structural property for the spacecraft is understanding the moment of inertia in the x, y, and z axis. First, the axes of rotation must be defined.

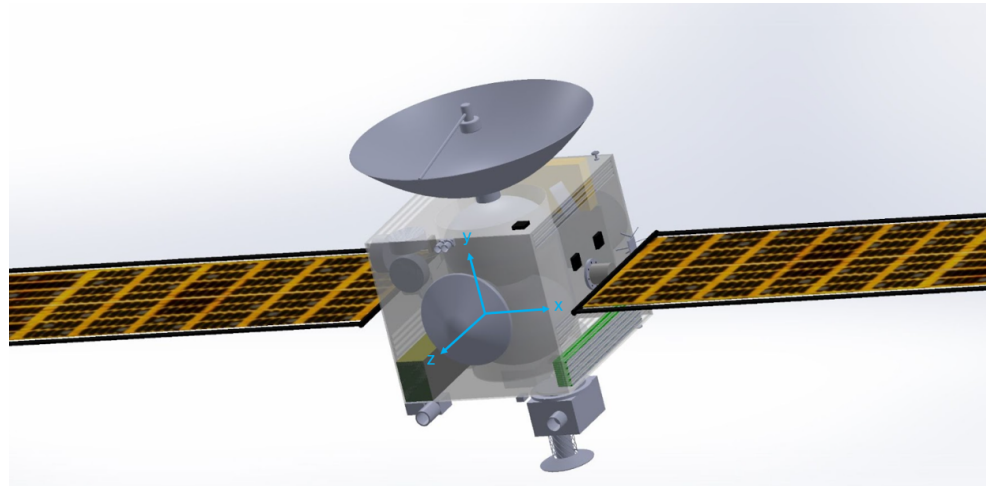


Figure 7.7.4: CAD model displaying Cartesian coordinates

As seen in Figure 7.7.4, the Cartesian system we use was labeled as followed: x is in the direction of the solar arrays, y is in the direction parallel to the centerline of the cylindrical housing, connecting the scientific instruments to the HGA, and z is in the direction of motion.

This coordinate system was defined to be at the center of the cube-like primary structure because it was the most logical starting point. Next, by using the parallel axis theorem, that is:

$$I = I_{cm} + md^2 \quad (56)$$

where I_{cm} is the moment of inertia about the center of mass axis, m is the mass of the component, and d is the distance from the components center of mass and the rotational axis, the total moment of inertia about each rotational axis can be calculated and verified using Solidworks where the software utilizes finite mass elements rather than entire components. Because the Solidworks CAD model has more accurate locations, and thus, would produce a more accurate analysis, the results are as followed:

| | |
|---|--|
| Center of Mass | x-coordinate: 1.32 mm y-coordinate: -104.25 mm z-coordinate: -24.73 mm |
| Moment of Inertia - I_x | 556.15 kg · m ² |
| Moment of Inertia - I_y | 4,842.06 kg · m ² |
| Moment of Inertia - I_z | 4,829.13 kg · m ² |

Table 7.7.2: Results summary from Solidworks

Another important structural property is the first order frequency, which can be assumed to be the fundamental frequency such that it is the natural frequency of the first order. Because our spacecraft is launching on a Falcon Heavy, the Falcon User's Guide from SpaceX lists the primary lateral and axial frequencies.

| | |
|--------------------------------|-------|
| Minimum Axial Frequency | 25 Hz |
|--------------------------------|-------|

| | |
|----------------------------------|-------|
| Minimum Lateral Frequency | 10 Hz |
|----------------------------------|-------|

Table 7.7.3: Primary frequencies produced by Falcon Heavy

Ideally, our spacecraft would want to maintain a frequency above the frequencies listed in Table 7.7.3 to ensure the structure does not fail. To calculate the fundamental frequencies of our spacecraft, a Solidworks frequency analysis was conducted; however, the resulting first order frequency of 0.827 Hz did not seem reasonable. Thus, a new method was carried out using the Euler-Bernoulli Beam Theory where the aluminum-carbon fiber honeycomb cube-like primary structure was modeled such that each dimension was considered as three different beams.

Assuming material properties for aluminum 7075 of $\rho_{Al} = 2810 \text{ kg/m}^3$ and an elastic modulus of 71.7 GPa, I first calculated the cross-sectional area and moment of inertia for each side. Take, for example, the 1.5 m width dimension, W, of the primary structure where the cross sectional area, A_W , is computed:

$$A_W = H * D \quad (57)$$

where H is the height and D is the depth of the primary structure. Thus,

$$A_W = 1.4 \text{ m} * 1.6 \text{ m} \quad (58)$$

$$A_W = 2.24 \text{ m}^2 \quad (59)$$

Next, the moment of inertia is computed for the beam along the width:

$$I_W = \frac{1}{12} D H^3 \quad (60)$$

$$I_W = \frac{1}{12} * 1.6 \text{ m} * (1.4 \text{ m})^3 \quad (61)$$

$$I_W = 0.3659 \text{ m}^4 \quad (62)$$

Now, using the fundamental frequency of a cantilever beam equation [8], assuming that our primary structure has a fixed end and a free end, with a β value of 1.875 since we are determining the first mode, the following calculation for the beam along the width can be made:

$$\omega_{W1} = \left(\frac{\beta_n^2}{L^2}\right) \sqrt{\frac{EI}{\rho A}} \quad (63)$$

where n represents the mode we solve for. Thus,

$$\omega_{W1} = \left(\frac{1.875^2}{1.5^2}\right) \sqrt{\frac{(71.1 \text{ GPa})(0.3659 \text{ m}^4)}{(2810 \frac{\text{kg}}{\text{m}^3})(2.24 \text{ m}^2)}} \quad (64)$$

$$\omega_{W1} = 505.2 \text{ Hz} \quad (65)$$

This process can be followed for the beam along the height and the beam along the depth to get the following results:

| | First Order / Fundamental Frequency (Hz) |
|--------------------------|---|
| Beam Along Width | 505.2 |
| Beam Along Height | 621.4 |
| Beam Along Depth | 475.8 |

Table 7.7.4: First order frequencies along primary structure dimensions modeled as beams

If we consider the frequency experienced for the beam along the height equivalent to the axial frequency and the frequency experienced for the beams along the width and depth equivalent to the lateral frequency, the trend holds true that the axial frequency is much larger than the lateral frequency. Additionally, after reviewing these results and understanding that we are only modeling the primary structure, these frequencies are bound to be lower if all components are considered. This is because a heavier mass would result in a lower frequency through the following natural frequency equation:

$$f = \frac{1}{2\pi} \sqrt{\frac{k}{m}} \quad (66)$$

As the stiffness stays the same since the same material is being used, increasing the mass would clearly decrease the fundamental frequency, resulting in a more reasonable result that can be compared to the Falcon Heavy frequency specs. Despite this, I can reason that our spacecraft will survive the launch with several factors of safety above the recommended frequencies.

7.8 - Thermal

The purpose of the thermal control subsystem is to maintain operational temperatures for all components of the spacecraft. This includes identifying the operational requirements of various parts of the spacecraft, and then making design choices to balance the thermal state of the bus during the entire mission in order to keep those parts functional. The easiest way to accomplish this is by identifying the most challenging environments the spacecraft will experience, which tends to be the hottest and coldest points it will go through along its journey and then building a thermal system to withstand these conditions. Once the spacecraft can handle these extreme cases, balances can be made across the journey of the mission in order to plan for working temperatures and a successful mission.

7.8.1 - Temperature Requirements

For this mission, the temperature requirements for our equipment were the main reasons for our thermal design. Those temperatures are given in the table below:

| Operational Temperature Ranges (°C) | | |
|-------------------------------------|--------------|--------------|
| System | Minimum Temp | Maximum Temp |
| | | |

| | | |
|--------------|------|-----|
| Batteries | -20 | 60 |
| Antennas | -140 | 90 |
| Solar Arrays | -150 | 110 |
| Instruments | -40 | 90 |
| Structure | -78 | 107 |
| ADCH | -54 | 93 |

Table 7.8.1: Operational Temperature Ranges for Mayfly Components

The batteries have the highest minimum operational temperature, and the lowest maximum temperature, so it is important to maintain the temperature of the spacecraft body within that range and design it to be between -20°C-60°C so our batteries can have a successful journey. For the most part of our design the temperature was kept well within the range of this value of -20°C. Though it can withstand this low of a temperature in order to keep the mission safe and not have too much risk the temperature was kept at about -9.58°C in order to have some leniency on the tolerance of the battery for which we need for our entire mission timeline.

7.8.2 - Iterative Thermal Design Process

The design of the spacecraft thermal system involves trying to balance thermal controls for the cold case and hot case during the mission. Some of the first passive controls that were implemented in the design of this mission were surface properties which in this case involves absorptivity in the visible spectrum and emissivity in the IR spectrum in order to balance the both of these extreme cases. After attempting to balance the temperatures using constant passive

controls, active controls such as louvers, heaters, and radiators were considered to allow the spacecraft to adapt to the extreme thermal environments that it'll undergo.

So, in order to ensure that our design was functioning properly we go through an iterative process of adjusting passive and active thermal controls to allow for both the hot and cold case which eventually led to the thermal design of our spacecraft. This in turn calls for heaters, a set of louvers, and multi-layer insulation (MLI). The louvers allow the spacecraft to change its emissivity to a value of 0.75, and the heaters allow for internal heating while further away from the sun with a maximum of _____. The MLI has a surface absorptivity of 0.1, and emissivity of 0.3. The use of passive and active thermal controls is important to take note of because of the thermal system it allows for thermal balancing of our spacecraft.

7.8.3 - Thermal balance at Earth

The largest source of heat throughout the entire mission is the sun. Primarily due to this the hottest expected for the mission is when the spacecraft detaches from the launch vehicle near earth and around 1AU. For this reason the hot cases was identified to be on our mission trajectory near earth at 1 AU from the sun.

The relationship which was used to find the steady-state temperature of the spacecraft is the from of the conservation of energy shown below:

$$Q_{in} = Q_{out}$$

The difficulty in completing the thermal balance comes with identifying all sources of heat flux in and out of the spacecraft. The above equation was expanded to the following which includes all expected fluxes:

$$Q_{sun} + Q_{planet\ to\ S/C} + Q_{albedo} + Q_{in} = Q_{S/C\ to\ space} + Q_{S/C\ to\ Earth}$$

So going through the equation we can identify the heat fluxes from most of the sources we have and calculate them using their respective equations like so:

$$Q_{\text{sun}} = aA_{\text{sun}} I_{\text{earth}} \quad (1)$$

Where

a = absorptivity in visible spectrum, given by the surface properties of MLI = 0.3

A_{sun} = Projected area of spacecraft facing the sun = 10.34m²

I_{earth} = Solar Irradiance at Earth = 1371 W/m²

$$Q_{\text{planet to S/C}} = 0 \quad (2)$$

It should equal 0 because the spacecraft is now hotter than the earth and therefore should be radiating heat towards the earth

$$Q_{\text{albedo}} = aA_{\text{earth}} a_{\text{earth}} F_{\text{earth}} I_{\text{earth}} \quad (3)$$

Where

a_{earth} = albedo of earth = 0.31

$$Q_{\text{int}} = \text{Heat of S/C} \quad (4)$$

This heat flux comes from the spacecraft and is the total heat generation of all of our systems that are using power.

$$Q_{\text{out to space}} = A_{\text{space}} \sigma \epsilon_{S/C} (T_{S/C}^4) F_{S/C \text{ to space}} \quad (5)$$

Where

σ = Boltzmann constant

A_{space} = Projected area facing space = 11.48m² for MLI & and 2m² for Louver

F_{space} = View factor of spacecraft to space = 1

$\epsilon_{s/c}$ = emissivity of louvers and MLI insulation: 0.75 & 0.3

$T_{S/C}$ = what were solving for

$T_{space} = 0 \text{ K}$

$$Q_{S/C \text{ to planet}} = \sigma F_{S/C \text{ to earth}} \epsilon_{earth} \epsilon_{S/C} A_{planet-facing} (T_{S/C}^4 - T_{earth}^4) \quad (6)$$

$F_{S/C \text{ to earth}}$ = view factor of spacecraft to earth = 1

$\epsilon_{s/c}$ = emissivity of MLI insulation: 0.3

$A_{planet-facing}$ = area of insulation and projected area combined = 13.48m²

$T_{S/C}$ = temperature of Spacecraft

$T_{earth} = 293 \text{ K}$

$\epsilon_{earth} = 0.65$

Plugging in Equations (1) - (6) into conservation of equations shown above we can solve for the temperature of the spacecraft when we first enter outer space. This yields the following temperature for our hottest temperature experienced by the spacecraft which is 31.81°C.

This temperature is below the maximum desired temperature, and should allow the spacecraft to survive the expected hot case. This in fact tells us that our spacecraft will not overheat as long as it does not get closer to the sun and it or approach very close to other planetary bodies. There is an expected gravity assist from Mars during the trip of our mission, but no thermal analysis was conducted for this maneuver because Mars sits at an average orbit radius of 1.534AU from the sun, and the surface temperature of Mars is lower than Earth's. This

means the gravity assist near Mars is expected to be a colder thermal environment than near Earth.

7.8.4 - Thermal balance at Comet

For the transit between Earth and the Comet (311P), the spacecraft will largely only have three heat flux sources which are the Sun, Space, and internal spacecraft heating. The largest source of heat throughout the mission is the sun so the cold extreme cases for the mission is when the spacecraft is farthest from the Sun while on orbit to 311P. The farthest the Comet gets from the sun in its orbit is 2.2AU, and so that is where the cold case is evaluated, using a similar method to the thermal balance around Earth. The distance was evaluated to be 329100000 km, with a view factor of 1, and a corresponding view factor of 1 to space.

$$Q_{\text{sun}} + Q_{\text{planet to S/C}} + Q_{\text{albedo}} + Q_{\text{in}} = Q_{\text{S/C to space}} + Q_{\text{S/C to Earth}}$$

So going through the equation we can identify the heat fluxes from most of the sources we have and calculate them using their respective equations like so:

$$Q_{\text{sun}} = aA_{\text{sun}} I_{\text{Comet}} \quad (7)$$

Where

a = absorptivity in visible spectrum, given by the surface properties of MLI = 0.3

A_{sun} = Projected area of spacecraft facing the sun = 10.34m²

I_{comet} = Solar Irradiance at Earth = 283.62 W/m²

$$Q_{\text{planet to S/C}} = \sigma F_{\text{max distance to S/C}} \epsilon_{\text{comet}} \epsilon_{\text{S/C}} A_{\text{comet-facing}} (T_{\text{near comet}}^4 - T_{\text{S/C}}^4) \quad (8)$$

$F_{\text{S/C to earth}}$ = view factor of spacecraft to earth = 1

$\varepsilon_{s/c}$ = emissivity of MLI insulation: 0.3

$A_{planet-facing}$ = area of insulation and projected area combined

$T_{S/C}$ = temperature of Spacecraft

$T_{near comet}$ = temperature near comet = 200 K

ε_{comet} = 0

$$Q_{albedo} = aA_{comet} \alpha_{comet} F_{comet} I_{comet} \quad (9)$$

Where

α_{comet} = albedo of comet = 0

$$Q_{int} = Heat\ of\ S/C \quad (10)$$

This heat flux comes from the spacecraft and is the total heat generation of all of our systems that are using power.

$$Q_{out\ to\ space} = A_{space} \sigma \varepsilon_{S/C} (T_{S/C}^4) F_{s/c\ to\ space} \quad (11)$$

Where

σ = Boltzman constant

A_{space} = Projected area facing space = 11.48m² for MLI & and 2m² for Louver

F_{space} = View factor of spacecraft to space = 1

$\varepsilon_{s/c}$ = emissivity of louvers and MLI insulation: 0.74 & 0.3

$T_{S/C}$ = what were solving for

T_{space} = 0 K

$$Q_{S/C\ to\ planet} = 0 \quad (12)$$

It should equal 0 because the spacecraft is now cold and should be incapable of radiating heat to the comet since we're running on heater power. The comet is also too small to radiate heat towards.

This energy balance deviates from the previous energy balance because this one includes the temperature at 2.2AU and the heat created by the spacecraft, which now contains heater power in addition to internally dissipated power. The final deviation, and most important, is the change in spacecraft emissivity as the louvers are now closed, giving the spacecraft an emissivity of 0.1.

Solving for the spacecraft temperature using the same method as before, and with an internal heating power of 215W and dissipating 488.40W of heat, we are able to keep the spacecraft at a temperature -9.58°C .

The spacecraft is not expected to go any further from the sun, so there should be no case that is colder than this. So, a thermal balance has been performed on the hottest and coldest environment, and a set of thermal control solutions have been generated for the transfer period, so the thermal system should prove capable of handling all expected thermal conditions throughout the course of the mission.

7.8.5 - Thermal Controls

The thermal controls available were used to achieve operational temperatures for the spacecraft through the duration of its mission. The available tools were in passive instruments such as MLI and active instruments such as louvers, radiators, and heaters. The overall spacecraft design calls for all of these components for a successful journey.

The two practical restraints on the thermal system were the mass and power consumption. Surface controls such as MLI and louvers are relatively heavy but require no power, and heaters

are lightweight but require a relatively large power budget. For this reason both power and mass had to be considered in order to build a system which is both lightweight and low power.

7.8.6 - Surface Property Controls

In designing the controls, a target of surface properties were made for both the hot and cold case considering the heat fluxes at both points. For the absorptivity of the spacecraft It is held constant, while the emissivity could change in early design to try to find an optimal temperature for both the cold and hot case.

This resulted in the emissivity being chosen for the MLI to be 0.30 which is composed of Aluminized Beta Cloth. The MLI was chosen to have this emissivity in order to help the louvers high emissivity of 0.75 also emit more heat as well. The other design property that was chosen for the MLI was a desired absorptivity of 0.1. This value was chosen for the MLI in order to help keep some heat inside the spacecraft.

Louvers were necessary to alter the emissivity during the mission, as the range of environmental temperatures is too much for the MLI to handle alone. The louvers have the emissivity values of 0.75 when open and 0.1 when closed. The absorptivity of the spacecraft was 0.1 because that is the side that will face the Sun. The current design of the spacecraft calls for 2 sets of thermal and about $10-13.48\text{m}^2$ of MLI for a corresponding side of the spacecraft.

7.8.7 - Heaters

Balancing the temperatures at the extreme thermal environments was not possible only using surface properties though. The louvers help with the emissivity and it would not be desirable to have an extremely low emissivity because it leaves no room for error. However, they are required in our hot case to help cool the spacecraft when we are closer to the Sun. In contrast

to this for this reason it was decided that heaters should be added in order to keep the temperature during the cold part of the mission acceptable.

The power budget of the spacecraft at the comet where the heaters will be used since they are farthest away from the sun was kept to a minimum in order to save power. So, the final design for the thermal system requires 215W of power for the heaters. For contingency we are also capable of loading more heaters onto the spacecraft since the mass is almost negligible for the patch heaters we choose in case we need more heater power on our spacecraft.

8 - Mass, Power, TRL, and Summary Tables

| | Margin | Mode 1 Launch | Mode 1 Total (W) | Mode 2 1 AU Thrusting | Mode 2 Total (W) | Mode 3 Comet Sample Collection | Mode 3 Total (W) | Mode 4 Comet Telecom Data Transfer | Mode 4 Total (W) | Mode 5 Safe Mode | Mode 5 Total (W) | Max Power All On | Max Total (W) |
|-----------------------------------|--------|------------------|---------------------|-----------------------------|---------------------|---|---------------------|---|---------------------|------------------------|---------------------|------------------------|------------------|
| <i>Power Mode Duration (Days)</i> | | | | | | | | | | | | | |
| <i>Payload on this Element</i> | | | | | | | | | | | | | |
| Instruments | 30% | 0 | 0.00 | 0.00 | 0.00 | 89.40 | 116.22 | 75.00 | 97.50 | 0.00 | 0.00 | 89 | 116.22 |
| <i>Spacecraft Bus</i> | | | | | | | | | | | | | |
| Attitude Control | 30% | 0 | 0.00 | 54.00 | 70.20 | 54.00 | 70.20 | 54.00 | 70.20 | 54.00 | 70.20 | 54 | 70.20 |
| Payload | 30% | 0 | 0.00 | 0.00 | 0.00 | 10.00 | 13.00 | 0.00 | 0.00 | 0.00 | 0.00 | 39 | 50.18 |
| Power | 30% | 20 | 26.00 | 20.00 | 26.00 | 20.00 | 26.00 | 20.00 | 26.00 | 20.00 | 26.00 | 20 | 26.00 |
| Electric Propulsion | 15% | 0 | 0.00 | 3000.00 | 3450.00 | 0.00 | 0.00 | 0.00 | 0.00 | 0.00 | 0.00 | 3000 | 3450.00 |
| Structures | 0% | 0 | 0.00 | 0.00 | 0.00 | 0.00 | 0.00 | 0.00 | 0.00 | 0.00 | 0.00 | 0 | 0.00 |
| Communications | 30% | 10 | 13.00 | 10.00 | 13.00 | 10.00 | 13.00 | 282.25 | 366.93 | 282.25 | 366.93 | 282 | 366.93 |
| Thermal | 30% | 0 | 0.00 | 0.00 | 0.00 | 260.00 | 338.00 | 260.00 | 338.00 | 260.00 | 338.00 | 260 | 338.00 |
| Bus Total | | 30 | 39 | 84 | 109 | 354 | 460 | 616 | 801 | 616 | 801 | 655 | 851 |
| Spacecraft Power | | 30 | 39 | 3084 | 3559 | 443 | 576 | 691 | 899 | 616 | 801 | 3744 | 4418 |

Figure 8.2: MAYFLY Mission PEL

| Subsystem/Component | Revision # | | |
|--|--------------------|---------------|----------------|
| | Predicted Mass, kg | | |
| | Total | Contingency | Total Flt |
| Flight (kg) | % | w/Contingency | |
| SPACECRAFT BUS | | | |
| Power | 194.47 | 30.0% | 252.82 |
| Command & Data Handling | 7.30 | 30.0% | 9.49 |
| ACS | 155.46 | 30.0% | 202.10 |
| Telecom | 18.00 | 30.0% | 23.40 |
| Electric Propulsion | 212.80 | 30.0% | 276.64 |
| Thermal | 40 | 30.00% | 52 |
| Mechanisms | 7.90 | 30.0% | 10.27 |
| Structures | 192.74 | 30.0% | 250.56 |
| SCIENCE INSTRUMENTS | | | |
| Sample Retrieval (SMP Hayabusa Sampler Horn) | 15.00 | 10.0% | 16.50 |
| Reentry Vehicle (OSIRIS-REx SRC) | 46.00 | 15.0% | 52.90 |
| xLink Space-Rated Modular Robotic Arm | 50.00 | 10.0% | 55.00 |
| Hayabusa Spectrometer (NIRS3) | 4.70 | 10.0% | 5.17 |
| Surface Dust Analyzer (SUDA) | 5.00 | 12.00% | 5.60 |
| Hayabusa Thermal Infrared Camera (TIR) | 3.50 | 14.0% | 3.99 |
| New Horizon Imaging Camera (Ralph) | 10.50 | 20.0% | 12.60 |
| Lasar Altimeter (LIDAR) | 3.50 | 20.0% | 4.20 |
| Spacecraft Dry Mass (Earth-to-PANSTARRS): | 966.87 | 21.9% | 1233.24 |
| EXPENDABLES | | | |
| Hydrazine Usable (Nominal) | | | 93.00 |
| Spacecraft Neutral Mass: | 1326.24 | | |
| SEP Propulsion | | | |
| Xenon Usable (Nominal) | | | 527.49 |
| 6% Perf. Margin + 4% Residuals | | | 580.24 |
| Spacecraft Wet Mass at LV Separation: | 1906.5 | | |
| Falcon Heavy (C3 = 75.113 km ² /s ²): | | | 2000.0 |
| Launch Margin: | | | 4.9% |

Figure 8.1: MAYFLY Mission MEL

| Subsystem | Component | TRL |
|---------------------------|--------------------------------------|-----|
| Power | Power Distribution Unit | 9 |
| Power | ROSA Solar Arrays | 9 |
| Power | 1752 LG Chemical 10A Batteries | 9 |
| ACS | PTD-96 Hydrazine Tank | 9 |
| ACS | Monarc-1 Thrusters | 9 |
| ACS | Coarse Sun Sensor | 9 |
| ACS | VAT-68M Star Trackers | 9 |
| ACS | Goodrich Ithaco 45Nms Reaction Wheel | 9 |
| Communications | 2.5 m High Gain Antenna | 9 |
| Communications | .24 m Low Gain Antenna | 9 |
| Thermal | Radiator, Louvers | 9 |
| Payloads | Spectrometer NIRS3 | 9 |
| Payloads | Thermal Infrared Camera (TIR) | 9 |
| Payloads | Laser Altimeter (LIDAR) | 9 |
| Payloads | Surface Dust Analyzer (SUDA) | 9 |
| Payloads | Imaging Camera (Ralph) | 9 |
| Sample Collection and ERV | XLink Arm | 8 |
| Sample Collection and ERV | Sampler Horn and Collection Box | 9 |
| Sample Collection and ERV | Sample Re-Entry Capsule (SRC) | 9 |

Figure 8.3: TRL Summary

| List of Necessary Instruments | | | | | |
|--|-----------|---------------|------------------|-----------------|---------------------|
| Instrument | Mass (kg) | Max Power (W) | Dimensions (cm) | Data Rate (bps) | Temperature Range K |
| Hayabusa Spectrometer (NIRIS3) | 4.46 | 14.90 | 35 x 17 x 10 | 16 | 183 - 213 |
| Hayabusa Thermal Infrared Camera (TIR) | 3.50 | 29.00 | 20 x 13 x 11 | 32,000 | 150 - 460 |
| Hayabusa Laser Altimeter(LIDAR) | 3.50 | 18.00 | 6.6 x 9 x 4 | 9.6 | 293 - 320 |
| Surface Dust Analyzer (SUDA) | 5.00 | 20.40 | 26.8 x 25 x 17.1 | 13,000 | 350 - 430 |
| New Horizon Imaging Camera (Ralph) | 10.5 | 7.10 | 11 x 6.5 x 3.6 | 38,000 | 200 - 400 |
| Totals | 26.96 | 89.40 | | 83025.6 | |

Figure 8.4: MAYFLY List of Science Instruments

| | Total Flight (kg) |
|---|-------------------|
| Structure | |
| Primary Structure (carbon fiber - aluminum honeycomb) | 192.439649 |
| Secondary Structure (brackets / solar array) | 0.3 |
| Total Structure Mass | 192.739649 |
| Mechanisms | |
| Deployable structures (payloads, booms) | 2.9 |
| Actuators | 5 |
| Total Mechanism Mass | 7.9 |

Figure 8.5: Structures Mass Calculations

Concluding Remarks

The Mayfly mission will return a sample from Main Belt Comet 311P/PANSTARRS.

Also, we will visualize and perform measurements of the comet's surface characteristics before sample acquisition and return to Earth. Due to the high-TRL componentry and thoroughly devised objectives, we have confidence in our system to accomplish our mission goals. Every member of this design team would like to acknowledge the assistance and guidance of Dr. Dan Goebel and teaching assistant Pavel Shafirin. Thank you both for such an enjoyable quarter!

Bibliography

Trajectory

1. “311P/PANSTARRS.” *Comet 311P/PANSTARRS | Space Reference*, www.spacerefERENCE.org/comet/311p-panstARRS. Accessed 9 June 2024.
2. Curtis, Howard D. *Orbital Mechanics for Engineering Students*. Butterworth-Heinemann, An Imprint of Elsevier, 2021.
3. NASA Goddard Space Flight Center. General Mission Analysis Tool (GMAT) v.R2016a, NASA, Year, <https://gmat.gsfc.nasa.gov/>
4. Oh, David Y., and Damon Landau. “Simple semi-analytic model for optimized interplanetary low-thrust trajectories using solar electric propulsion.” *Journal of Spacecraft and Rockets*, vol. 50, no. 3, May 2013, pp. 609–619, <https://doi.org/10.2514/1.a32326>.
5. Roa, Javier, et al. “Automatic design of missions to small bodies.” *2018 Space Flight Mechanics Meeting*, 7 Jan. 2018, <https://doi.org/10.2514/6.2018-0200>.

Propulsion

1. “Falcon Heavy.” *SpaceX*, www.spacex.com/vehicles/falcon-heavy.
2. *Delta IV*, www.ulalaunch.com/rockets/delta-iv.
3. Howell, Elizabeth. “Delta IV Heavy: Powerful Launch Vehicle.” *Space.Com*, Space, 20 Apr. 2018, www.space.com/40360-delta-iv-heavy.html.

Payload

1. “Hayabusa-2 – Spacecraft & Satellites.” *Spacecraft & Satellites*, spaceflight101.com/spacecraft/hayabusa-2/. Accessed 10 June 2024.
2. Yano, Hajime. “High Hopes for Successful Sample Collection.” *JAXA*, global.jaxa.jp/article/special/hayabusa/yano_e.html. Accessed 10 June 2024.
3. O’Callaghan, Jonathan. “The Story of Hayabusa: Why Asteroid Mining Is so Last Decade.” *Space Answers*, 11 Feb. 2013, www.spaceanswers.com/space-exploration/the-story-of-hayabusa-why-asteroid-mining-is-so-last-decade/.
4. Desai, Prasun N., et al. “Entry, descent, and landing operations analysis for the Stardust entry capsule.” *Journal of Spacecraft and Rockets*, vol. 45, no. 6, Nov. 2008, pp. 1262–1268, <https://doi.org/10.2514/1.37090>.
5. “Osiris-Rex Sample Return Capsule.” *SpaceFlight101*, spaceflight101.com/osiris-rex/osiris-rex-sample-return-capsule/. Accessed 10 June 2024.
6. “Build the Future of Space with: xLink Space-Rated Modular Robotic Arm System.” *Motiv Space Systems*, 10 Jan. 2024, motivss.com/products-capabilities/robotics/xlink/.
7. Iwata, Takahiro. “Hayabusa2 NIRS3 Data Product Software Interface Specification”, 8 March 2017, sbnarchive.psi.edu/pds4/hayabusa2/hyb2_nirs3/document/hyb2_nirs3_dpsis.xml.
8. Okada, T. “Thermal-Infrared Imager Tir on Hayabusa-2 To …”, 2012, www.lpi.usra.edu/meetings/lpsc2012/pdf/1498.pdf.
9. Noda, H. “Scientific Measurements of Hayabusa-2 Laser …”, 2015, www.hou.usra.edu/meetings/astrokecon2015/pdf/6017.pdf.

10. Kempf, S. "Suda: A Dust Mass Spectrometer for Compositional ...", 2014, meetingorganizer.copernicus.org/EPSC2014/EPSC2014-229.pdf&lang=en.
11. Reuter, Dennis. "Ralph: A Visible/Infrared Imager for the New Horizons Pluto ..." www.boulder.swri.edu/pkb/ssr/ssr-ralph.pdf.

Systems

1. Wertz, James Richard, et al. Space Mission Engineering: the New SMAD . Microcosm Press, 2011.
2. NASA Rqmnts_Module_Basics_808, "Requirements Module: The Basics." bruinlearn.ucla.edu.
3. "NASA Systems Engineering Handbook," NASA/SP-2007-6105 Rev1. December 2007. bruinlearn.ucla.edu.
4. Manning, Catherine. "Technology Readiness Levels." 27 Sep. 2023. <https://www.nasa.gov/directorates/somd/space-communications-navigation-program/technology-readiness-levels/>.
5. Sorensen, George. "STARDUST: NASA's Comet Sample Return Mission." 26 Nov., 2003. <https://solarsystem.nasa.gov/stardust/home/index.html>
6. Guido, Ernesto. "The Multi-Tailed Main-Belt Comet P2013 P5." 8 Nov., 2013.

ACS:

1. Wertz, James Richard, et al. Space Mission Engineering: the New SMAD . Microcosm Press, 2011.

Structures:

1. "3 Most Common Metals for Aerospace Systems." *N&S Aero*, 4 June 2018, nsaerollc.com/3-common-metals-aerospace-systems/.

2. “7075 Aluminium Alloy.” *Ferguson Perforating*, www.fergusonperf.com/the-perforating-process/material-information/specialized-aluminum/7075-aluminium-alloy/. Accessed 2 June 2024.
3. “6061 Aluminium Alloy.” Ferguson Perforating, www.fergusonperf.com/the-perforating-process/material-information/specialized-aluminum/6061-aluminium-alloy/. Accessed 8 June 2024.
4. *Aluminum 2024-T4; 2024-T351*, www.matweb.com/search/datasheettext.aspx?matguid=67d8cd7c00a04ba29b618484f7ff7524. Accessed 6 June 2024.
5. “Toray T800S Carbon Fiber.” *MatWeb*, www.matweb.com/search/datasheettext.aspx?matguid=5df1e45601214077b674daa817cba3d3. Accessed 8 June 2024.
6. Yap, Yee Ling, and Wai Yee Yeong. “Shape Recovery Effect of 3D Printed Polymeric Honeycomb.” *ResearchGate*, Apr. 2015, www.researchgate.net/publication/281303407_Shape_recovery_effect_of_3D_printed_polymeric_honeycomb.
7. Space Exploration Technologies Corp. Staff. “Falcon User’s Guide.” *Space Exploration Technologies Corp.*, Space Exploration Technologies Corp., Sept. 2021, www.spacex.com/media/falcon-users-guide-2021-09.pdf.
8. Deshmukh, Nilaj N. “Effect of Crack on Natural Frequency for Beam Type of Structures.” *ResearchGate*, ResearchGate, July 2017, www.researchgate.net/figure/values-of-a-frequency-calculated-from-equation-1-in-rad-sec-and-frequency-in-Hz_tbl1_318578751.
9. Pentapur Staff. “Aluminium Honeycomb Core.” *Pentapur*, Pentapur, 26 Sept. 2020, www.furrental.com/product/aluminium-honeycomb-core/.

10. Rock West Composites Staff. "Honeycomb Core Sandwich Panels." *Rock West Composites*, Rock West Composites,
www.rockwestcomposites.com/shop/plates-panels-angles/sandwich-panels/honeycomb-core-sandwich-panels. Accessed 10 June 2024.

Thermal

1. "Multilayer Insulation Material Guidelines." *NASA*,
ntrs.nasa.gov/api/citations/19990047691/downloads/19990047691.pdf. Accessed 11 June 2024.
2. Thermal Louver Spec information from class website
https://bruinlearn.ucla.edu/courses/185746/files/17066014?module_item_id=6722616
https://bruinlearn.ucla.edu/courses/185746/files/17109473?module_item_id=6727673
3. *Kapton and Silicone Rubber Flexible Heaters*,
www.nph-processheaters.com/assets/uploads/pdfs/flexible-heaters/Kapton_Insulated_and_Silicone_Rubber_Flexible_Heaters.pdf. Accessed 11 June 2024.

Power

1. *Airbus Universal Registration Document 2022_0.PDF*,
www.airbus.com/sites/g/files/jlcbta136/files/2023-04/Airbus%20Universal%20Registration%20Document%202022_0.pdf. Accessed 11 June 2024.
2. *Roll out Solar Array (Rosa)*,
redwirespace.com/wp-content/uploads/2023/06/redwire-roll-out-solar-array-flysheet.pdf. Accessed 11 June 2024.

3. *Transformational Solar Array Final Report*,
<ntrs.nasa.gov/api/citations/20170010684/downloads/20170010684.pdf>. Accessed 11 June 2024.
4. *International Space Station (ISS) Roll-out Solar Array (ROSA) Spaceflight Experiment Mission and Results | IEEE Conference Publication | IEEE Xplore*,
<ieeexplore.ieee.org/document/8548030>. Accessed 11 June 2024.
5. “ROSA and Solar Cell Module Combined Environments Test Plan.” *NASA*,
<ntrs.nasa.gov/api/citations/20220006807/downloads/wright-16thSCTC-%23028-paper.pdf>. Accessed 11 June 2024.
6. *Performance of Commercial High Energy and High Power ...*,
www.nasa.gov/wp-content/uploads/2021/10/3-nasa_battery_workshop_nov_2019_high_power_li-ion_cells_final.pdf?emrc=4b6c1c. Accessed 11 June 2024.
7. *Specification INR18650MJ1 22.08.2014.PDF*,
<www.nkon.nl/sk/k/Specification%20INR18650MJ1%2022.08.2014.pdf>. Accessed 11 June 2024.
8. “New LG MJ1 18650 Battery Review (3500mAh).” *18650 Battery | BATTERY BRO*,
<batterybro.com/blogs/18650-wholesale-battery-reviews/40773059-new-lg-mj1-18650-battery-review-3500mah>. Accessed 11 June 2024.
9. *Multi-Mission Radioisotope Thermoelectric Generator (MMRTG)*,
mars.nasa.gov/internal_resources/788/. Accessed 11 June 2024.
10. *A Truly General-Purpose Space RTG*,
www.researchgate.net/profile/Gary-Bennett-2/publication/252828339_The_General-Purpose_Heat_Source_Radioisotope_Thermoelectric_Generator_A_Truly_General-Purpose_

Space _RTG/links/570978cc08aea66081358a1d/The-General-Purpose-Heat-Source-Radio
isotope-Thermoelectric-Generator-A-Truly-General-Purpose-Space-RTG.pdf. Accessed
11 June 2024.